European air quality maps for 2014

PM_{10}, $PM_{2.5}$, Ozone, NO_2 and NO_x spatial estimates and their uncertainties

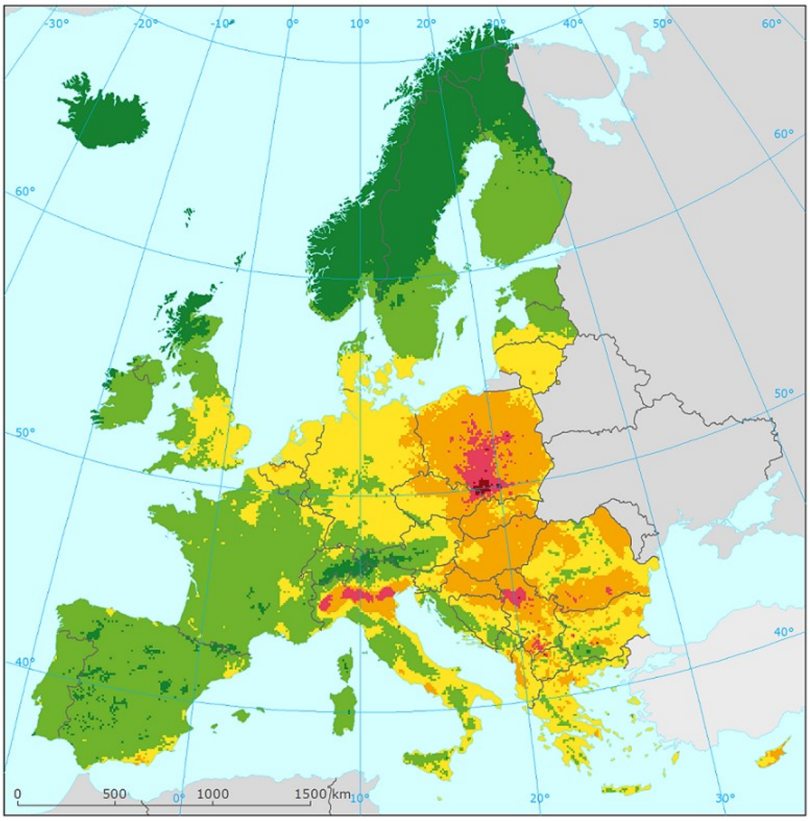

ETC/ACM Technical Paper 2016/6

December 2016

Jan Horálek, Peter de Smet, Frank de Leeuw,
Pavel Kurfürst, Nina Benešová

European Topic Centre on Air Pollution and Climate Change Mitigation

The European Topic Centre on Air Pollution and Climate Change Mitigation (ETC/ACM)
is a consortium of European institutes under contract of the European Environment Agency
RIVM Aether CHMI CSIC EMISIA INERIS NILU ÖKO-Institut ÖKO-Recherche PBL UAB UBA-V VITO 4Sfera

Front page picture:
Concentration map of $PM_{2.5}$ annual average for the year 2014. Spatially interpolated concentration field. Units: µg.m^{-3}. (Map 3.1 of this paper.)

Author affiliation:
Jan Horálek, Pavel Kurfürst, Nina Benešová: Czech Hydrometeorological Institute (CHMI), Prague, Czech Republic
Peter de Smet, Frank de Leeuw: National Institute for Public Health and the Environment (RIVM), Bilthoven, The Netherlands

Refer to this document as:
Horálek J, De Smet P, Kurfürst P, De Leeuw F, Benešová N (2017). European air quality maps for 2014. ETC/ACM Technical paper 2016/6.
http://acm.eionet.europa.eu/reports/ETCACM_TP_2016_6_AQMaps2014

DISCLAIMER

This ETC/ACM Technical Paper has not been subjected to European Environment Agency (EEA) member country review. It does not represent the formal views of the EEA.

© ETC/ACM, 2016
ETC/ACM Technical Paper 2016/6
European Topic Centre on Air Pollution and Climate Change Mitigation
PO Box 1
3720 BA Bilthoven
The Netherlands
Phone +31 30 2748562
Fax +31 30 2744433
Email etcacm@rivm.nl
Website http://acm.eionet.europa.eu/

Contents

1 Introduction

This paper provides an update of European air quality concentration maps, population exposure estimates and probabilities of exceeding relevant thresholds for 2014. The analysis is based on interpolation of annual statistics of monitoring data from 2014, reported by EEA member and cooperating countries in 2015. The paper presents mapping results and includes an uncertainty analysis of the interpolated maps, adopting the latest methodological developments (see Horálek et al. (2014) and reference citied therein),

We consider in this paper PM_{10}, $PM_{2.5}$, ozone, NO_2 and NO_x for 2014, being the most relevant pollutants for annual updating. The analysis method applied is similar to that of previous years. Another potentially relevant pollutant, benzo[a]pyrene (BaP), is not presented, as the station coverage is not dense enough for enable the regular mapping. For BaP mapping development, see Guerreiro et al. (2015) and Horálek et al. (2017).

The mapping method is based primarily on air quality measurements. It combines monitoring data, chemical transport model results and other supplementary data (such as altitude and meteorology). The method is a linear regression model followed by kriging of the residuals produced from that model ('residual kriging').

The maps of health related indicators of PM_{10}, $PM_{2.5}$, ozone, and NO_2 are created for the rural and urban (including suburban) background areas separately on a grid at 10x10 km resolution. Subsequently, the rural and urban background maps are merged into one final combined air quality indicator map using a 1x1 km population density grid, following a weighting criterion applied per grid cell. This fine resolution takes into account the smaller urbanisations in the European context that are not resolved at the 10x10 km grid resolution. The maps of vegetation related ozone and NO_x indicators are at a grid resolution of 2x2 km and based on rural background measurements; in the case of ozone they serve as input to EEA's core indicator CSI005.

Next to the annual indicator maps, we present in tables the population exposure to PM_{10}, $PM_{2.5}$, ozone, and NO_2, and the exposure of vegetation to ozone. Tables of population exposure are prepared using the final combined maps and the population density map of 1x1 km grid resolution. The tables of the vegetation exposure are prepared with a 2x2 km grid resolution based on the Corine Land Cover 2006.

Chapters 2, 3 and 4 present the concentration maps and exposure estimates for PM_{10}, $PM_{2.5}$, and ozone, respectively. Chapter 5 introduces the concentration map and exposure estimate for NO_2 and the concentration map for NO_x. Chapter 6 summarizes the trends in exposure estimates in the period 2005 – 2014 (or 2007 – 2014 for $PM_{2.5}$).

Annex 1 describes briefly the different methodological aspects. Annex 2 documents the input data applied in the 2014 mapping and exposure analysis. Annex 3 presents the technical detail of the maps and their uncertainty analysis including the cross-validation results and the maps of probability of exceedance of limit/target values. Annex 4 shows the inter-annual changes including the inter-annual difference maps between 2013 and 2014, the evolution of the population exposure in the period 2005 – 2014 for PM_{10} and ozone, resp. 2007 – 2014 for $PM_{2.5}$ and the results of the trend analysis for these relevant periods. Annex 5 presents the concentration maps including the station points, in order to provide more complete information of the air quality for 2014 across Europe.

2 PM_{10}

The Ambient Air Quality Directive (EU, 2008) sets limit values for long-term and for short-term PM_{10} concentrations. The long-term annual PM_{10} limit value is set at 40 µg.m^{-3}. The short-term limit value is that the daily average PM_{10} concentration should not exceed 50 µg.m^{-3} more than 35 days per year and is the limit value that is most often exceeded in Europe. It corresponds to the 90.4 percentile of daily PM_{10} concentrations in one year. The Air Quality Guideline recommended by the World Health Organization (WHO, 2005) for the PM_{10} annual average is 20 µg.m^{-3}.

This chapter presents the 2014 updates of these two PM_{10} health related indicators: annual average and the 90.4 percentile of the daily averages that is a more relevant indicator in the context of the AQ Directive (EU, 2008) than the formerly used 36th highest daily mean (Horálek et al., 2016b). The separate rural and urban background concentration maps are calculated on the 10x10 km resolution grid and the subsequent final combined concentration map are based on the 1x1 km gridded population density map. All maps here are presented in this 1x1 km grid resolution. The population exposure tables are calculated based on these maps in this resolution.

Annex 3 provides details on the regression and kriging parameters applied for deriving the maps of the two PM_{10} indicators, as well as the uncertainty analysis of the maps. Annex 4 discusses briefly the inter-annual changes observed in the concentration maps and the relevant population exposure.

2.1 PM_{10} annual average

2.1.1 Concentration map

Map 2.1 presents the final combined concentration map for the 2014 PM_{10} annual average as the result of interpolation and merging of the separate maps as described in Annex 1 (for a more detailed description see Horálek et al., 2007, and De Smet et al 2011). Red and purple areas indicate exceedances of the limit value (LV) of 40 µg.m^{-3}.

The most relevant linear regression submodel for the use of the PM_{10} mapping has been identified earlier in Horálek et al. (2008) and De Smet et al. (2009, 2010, 2011). Supplementary data used in the linear regression for rural areas consisted of EMEP model output, altitude, wind speed and surface solar radiation and for urban background areas it was EMEP model output only (Annex 3, Section A3.1). The linear regression and ordinary kriging on its residuals is applied on the logarithmically transformed data of both measurement and modelled PM_{10} values.

The final combined concentration map presented in Map 2.1 is presented on a 1x1 km grid resolution (Annex 1). Contrary to the past years, the final map is not aggregated any longer into the 10x10 km grid resolution. The reason is to prevent smoothing out of urbanised areas surrounded by the dominating pattern of extended rural areas. Next to this, the station points are not presented in the map, in order to better visualise the urban areas. However, concentration values from measurements at the station points used in the kriging interpolation methodology (Annex 3) is considered to provide relevant information. In Map A5.1 of Annex 5 these point values are presented on top of Map 2.1 and illustrate the smoothing effect the interpolation methodology can have on the gridded concentration fields.

Map 2.1 shows LV exceedances in southern Spain near Almeria, in urban areas of the Ostrava–Katowice region of southern Poland and north-eastern Czech Republic, and in some urban areas in Bulgaria, FYR of Macedonia and Serbia.

The uncertainty of the concentration map can be expressed in relative terms of the absolute Root Mean Square Error (RMSE) uncertainty related to the mean air pollution indicator value for all stations (see

Annex 1). This *relative mean uncertainty* (RRMSE) of the final combined map of PM_{10} annual average is 20.7 % for rural areas and 17.7 % for urban areas (Annex 3).

Map 2.1 Concentration map of PM_{10} annual average, 2014

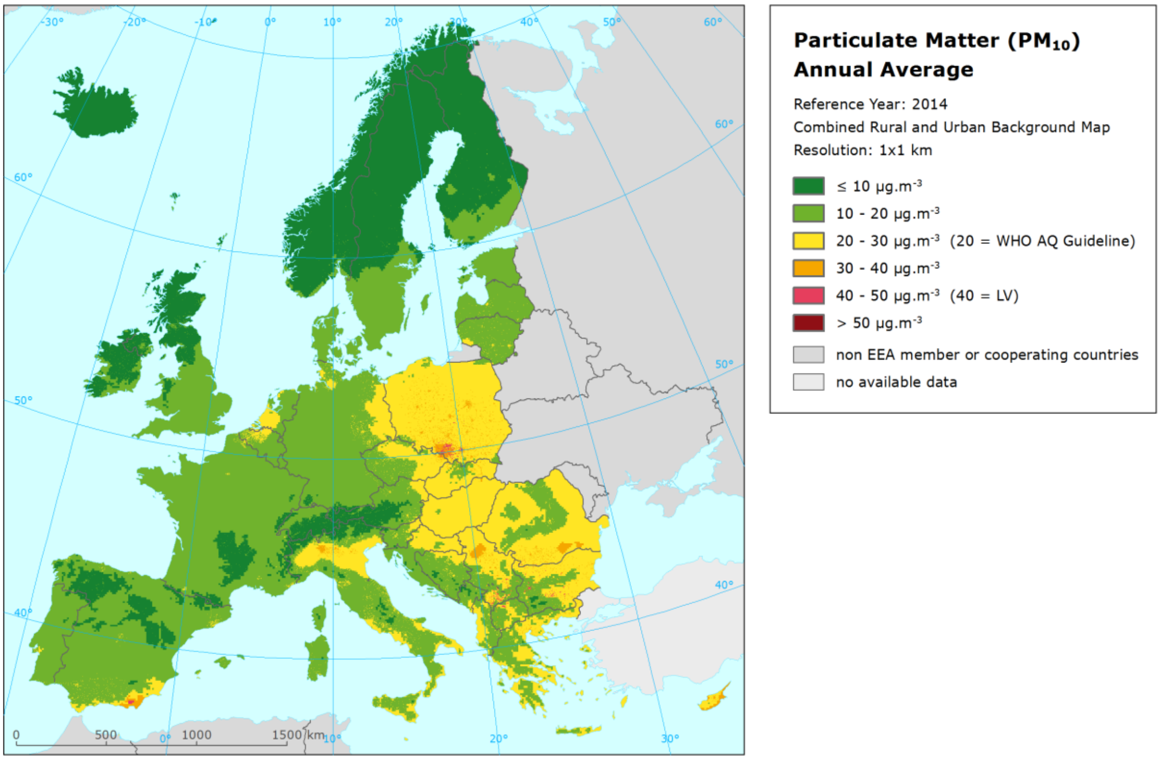

2.1.2 Population exposure

Table 2.1 gives the population frequency distribution for a limited number of exposure classes, as well as the population weighted concentration for individual countries and for Europe as a whole according to Equation A1.5.

About 44 % of the European population (and 43 % of the EU-28 population) has been exposed to annual average concentrations above the Air Quality Guideline of 20 µg.m^{-3} recommended by the World Health Organization (WHO, 2005). CSI004 (EEA, 2016c) estimates that about 50% of the population in urban agglomerations in the EU-28 was exposed in 2014 to levels above the WHO guideline. The latter estimate accounts for the urban population of the EU-28. It therefore represents areas where, in general, considerably higher PM_{10} concentrations occur. The estimates in Table 2.1 account for the total European and EU-28 population, *including* the population in rural areas, smaller cities and villages that are in general exposed to lower levels of PM_{10}.

The population exposure exceeding the EU limit value of 40 µg.m^{-3} is about 2 % for the population of the total of European area considered and the EU-28. In Bulgaria, FYR of Macedonia, Poland and Serbia more than 10 % of the population is exposed to concentrations above the LV. A limited fraction of the population (0.1 – 1.6%) is exposed to concentrations above the LV in the Czech Republic, Romania, and Spain. However, as the current mapping methodology tends to underestimate high values (see Annex 3, Section A3.1), the exceedance percentage will most likely be underestimated. Additional exceedances could be expected in countries like Cyprus, Greece, Romania and Slovakia, due to the estimated percentage of the population living in areas with the concentration levels above 30 µg.m^{-3} in these countries.

Table 2.1 Population exposure and population-weighted concentration, PM_{10} annual average, 2014

Country		Population	PM_{10} annual average, exposed population [%]						Population weighted conc.
			< LV				> LV		
		[inhbs . 1000]	< 10 $\mu g.m^{-3}$	10 - 20 $\mu g.m^{-3}$	20 - 30 $\mu g.m^{-3}$	30 - 40 $\mu g.m^{-3}$	40 - 45 $\mu g.m^{-3}$	> 45 $\mu g.m^{-3}$	[$\mu g.m^{-3}$]
Albania	AL	2 896	0.0	7.7	88.9	3.5			25.7
Andorra	AD	73	0.8	2.5	96.7				21.3
Austria	AT	8 507	4.2	58.8	37.0				17.8
Belgium	BE	11 204		42.2	57.8				20.2
Bosnia & Herzegovina	BA	3 831	0.1	24.9	75.0				22.1
Bulgaria	BG	7 246	0.0	3.1	16.2	40.0	40.7		36.2
Croatia	HR	4 247	0.0	25.6	74.4				21.7
Cyprus	CY	858		0.1	8.6	91.4			32.1
Czech Republic	CZ	10 512		9.6	78.8	10.3	1.3		25.5
Denmark	DK	5 627	0.1	95.8	4.1				18.5
Estonia	EE	1 316	0.1	99.9					14.8
Finland	FI	5 451	15.1	84.9					12.0
France (metropolitan)	FR	63 989	0.9	93.6	5.5	0.0			16.7
Germany	DE	80 767	0.1	80.9	19.0				18.7
Greece	GR	10 927		3.1	74.0	23.0			27.4
Hungary	HU	9 877		0.6	99.0	0.4			25.4
Iceland	IS	326	9.8	90.2					12.7
Ireland	IE	4 606	20.2	79.2	0.6				13.7
Italy	IT	60 783	0.3	15.0	75.3	9.4			24.0
Latvia	LV	2 001		35.3	64.7				20.3
Liechtenstein	LI	37	6.5	93.5					13.1
Lithuania	LT	2 943		24.7	75.3				21.7
Luxembourg	LU	550		100.0					17.4
Macedonia, FYROM of	MK	2 066		1.8	9.7	44.1	44.5		39.3
Malta	MT	425			100.0				28.9
Monaco	MC	38			100.0				22.3
Montenegro	ME	622	0.5	17.8	79.1	2.6			24.6
Netherlands	NL	16 829		40.9	59.1				20.2
Norway	NO	5 108	24.9	75.1	0.0				12.6
Poland	PL	38 018		0.4	42.2	45.1	12.3		31.5
Portugal (excl. Az., Mad.)	PT	9 922	0.3	91.3	8.4				16.9
Romania	RO	19 947		5.1	74.3	20.0	0.6		25.9
San Marino	SM	33		15.4	84.6				21.2
Serbia (incl. Kosovo*)	RS	7 147	0.0	3.5	33.9	46.4	16.2		32.1
Slovakia	SK	5 416		0.7	75.2	24.1			27.2
Slovenia	SI	2 061	0.1	36.7	63.2				20.3
Spain (excl. Canarias)	ES	44 397	0.7	58.6	39.4	1.3	0.1		19.7
Sweden	SE	9 645	7.7	92.3					13.8
Switzerland	CH	8 140	3.7	94.8	1.5				16.5
United Kingdom (& dep.)	UK	64 351	1.3	98.6	0.1				16.6
Total		**532 738**	**1.2**	**54.7**	**34.3**	**7.8**	**2.0**		**21.1**
			55.9				**2.0**		
EU-28		**502 424**	**1.0**	**55.5**	**34.6**	**7.3**	**1.6**		**20.9**
			56.5				**1.6**		

Kosovo*	KS	1 821	0.0	3.4	16.5	27.6	52.4		37.5
Serbia (excl. Kosovo*)	RS	7 147		3.5	38.1	51.0	7.4		30.8

*) under the UN Security Council Resolution 1244/99

Note 1: Turkey is not included in the calculation due to the lack of air quality data.
Note 2: The percentage value "0.0" indicates an exposed population exists, but it is small and estimated less than 0.05 %. Empty cells mean: no population in exposure.

The European-wide population-weighted concentration of the annual average for 2014 is estimated to be about 21 µg.m^{-3}, the same as for the EU28 only. This is the lowest level of the ten years period 2005 – 2014 (Table 6.1).

2.2 PM_{10} – 90.4 percentile of daily means

The AQ Directive (EU, 2008) describes the PM_{10} daily limit as "daily average 50 µg.m^{-3} not to be exceeded more than 35 times a calendar year". This requirement can be evaluated by the indicator 36th highest daily mean, which is in principle equivalent to the indicator 90.4 percentile of daily means. However, for measurement data these two indicators are equivalent only if no data is missing, which is in general not the case. As shown in de Leeuw (2012), the additional uncertainty related to the incomplete time series is substantially smaller when using percentile values instead of the x-th highest value. Furthermore, the AQ Directive requires the use of the 90.4 percentile when random measurements are used to assess the requirements of the PM_{10} daily limit value. Thus, from this report onward, the 90.4 percentile of daily means is and will be used as indicator, instead of the formerly used 36th highest daily mean.

2.2.1 Concentration map

Map 2.2 presents the final combined map, where red and purple marked areas indicate exceedances of the limit value (LV) of 50 µg.m^{-3} on more than 35 measurement days. The similar mapping procedure as in the case of the annual average is used. The mapping details and the uncertainty analysis are presented in Annex 3.

Large areas above the daily LV can be seen in northern Italy (i.e. the Po Valley), in southern Poland and north-eastern Czech Republic (i.e. Ostrava – Katowice region), in southern Romania and northern Serbia, and in the most of the urban areas in Poland, Bulgaria and Serbia. In general, the central and the eastern parts of Europe appear with higher concentrations than the western and the northern parts.

The *relative mean uncertainty* (relative RMSE) of the final combined map of the 90.4 percentile of PM_{10} daily means is 21.5 % for rural areas and 20.4 % for urban areas (Annex 3).

The final combined map *including* the measurement data at station points is presented in Map A5.2 of Annex 5.

Map 2.2 Concentration map of PM_{10} indicator 90.4 percentile of daily means, 2014

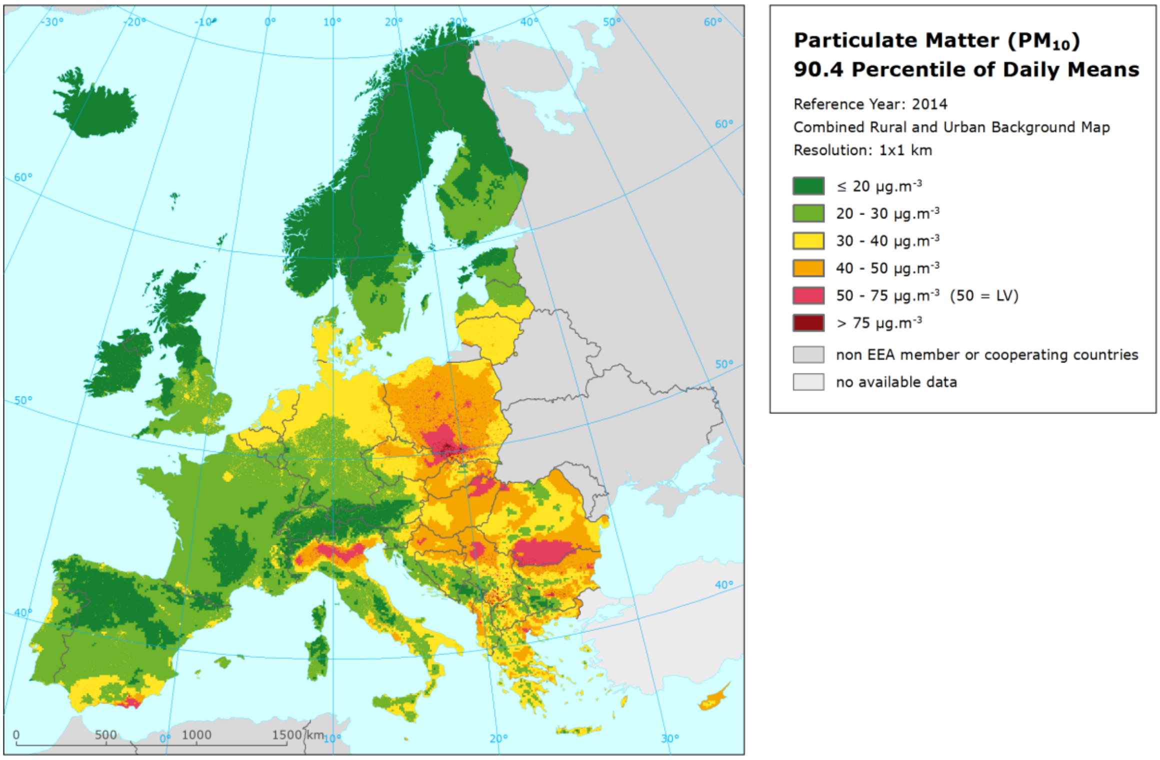

2.2.2 Population exposure

Table 2.2 gives the population frequency distribution for a limited number of exposure classes calculated at 1x1 km grid resolution, as well as the population-weighted concentration for individual countries and for Europe as a whole. Annex 4 shows details on the ten years evolution of population exposure.

It has been estimated that in 2014 about 13 % of the European population lived in areas where the 90.4 percentile of the PM_{10} daily means exceeded the EU limit value of 50 µg.m^{-3}. In Bulgaria, FYR of Macedonia, Montenegro, Poland and Serbia the population-weighted indicator concentration was above or around the LV and more than half of the population was exposed to concentrations exceeding the LV. In Albania, Czech Republic, Greece, Romania and Slovakia the portion of the population living in areas with concentrations above the LV was between 25 and 50 percent.

For the EU-28 around 12% lived in areas where the 90.4 percentile of the PM_{10} daily mean exceeded the EU limit value of 50 µg.m^{-3}. According to CSI004 (EEA, 2016c), in 2014 about 16 % of the urban population in the EU-28 was exposed to PM_{10} above this limit value. The difference between the two estimates is because the EEA accounts for the urban population of the larger agglomerations only, while Table 2.2 provides estimates also including inhabitants in rural areas, smaller cities and villages.

The European-wide population-weighted concentration of the 90.4 percentile of PM_{10} daily means is estimated for 2014 at about 37 µg.m^{-3}, the same as for the EU28 only.

Like in previous years, also in 2014 the most stringent EU PM_{10} indicator to determine population exposure exceedance in rural and urban background areas appears to be the daily limit value over the annual limit value.

Table 2.2 Population exposure and population-weighted concentrations, PM_{10} indicator 90.4 percentile of daily means, 2014

Country		Population	PM_{10}, 90.4 percentile of daily means, exposed population [%]						Pop. weighted conc.
			< LV				> LV		
		[inhbs . 1000]	< 20 $\mu g.m^{-3}$	20 - 30 $\mu g.m^{-3}$	30 - 40 $\mu g.m^{-3}$	40 - 50 $\mu g.m^{-3}$	50 - 75 $\mu g.m^{-3}$	> 75 $\mu g.m^{-3}$	[$\mu g.m^{-3}$]
Albania	AL	2 896	0.0	1.5	16.8	37.6	42.9	1.2	47.4
Andorra	AD	73	0.8	1.1	1.5	96.7			41.9
Austria	AT	8 507	5.7	30.5	60.0	3.7			32.4
Belgium	BE	11 204	0.0	5.7	94.3				35.0
Bosnia & Herzegovina	BA	3 831	0.1	5.6	18.1	52.2	24.0		44.2
Bulgaria	BG	7 246	0.1	1.2	3.7	10.2	40.1	44.7	68.4
Croatia	HR	4 247	0.0	5.2	29.1	62.3	3.4		42.1
Cyprus	CY	858		0.1	1.3	98.6			47.4
Czech Republic	CZ	10 512	0.0	1.6	13.2	59.9	23.8	1.4	47.3
Denmark	DK	5 627	0.3	10.1	89.6				32.6
Estonia	EE	1 316	8.5	66.8	24.6				26.4
Finland	FI	5 451	12.4	85.9	1.7				22.4
France (metropolitan)	FR	63 989	2.0	62.8	35.0	0.1	0.1		28.2
Germany	DE	80 767	0.3	23.6	67.2	8.9	0.0		33.0
Greece	GR	10 927	0.0	0.7	14.5	57.1	27.7	0.0	46.4
Hungary	HU	9 877		0.0	14.0	74.0	11.9		45.3
Iceland	IS	326	12.8	86.1	1.1				22.3
Ireland	IE	4 606	32.6	51.7	15.6	0.0			23.6
Italy	IT	60 783	0.5	5.9	40.6	31.6	21.4		42.1
Latvia	LV	2 001		11.4	80.1	8.6			36.1
Liechtenstein	LI	37	7.1	92.9					23.6
Lithuania	LT	2 943			63.5	36.5			38.8
Luxembourg	LU	550		24.2	75.8				29.6
Macedonia, FYROM of	MK	2 066	0.0	0.4	2.0	2.4	31.5	63.7	80.9
Malta	MT	425		0.6	2.5	97			42.4
Monaco	MC	38			100.0				34.8
Montenegro	ME	622	2.4	10.1	6.9	27.4	53.3		49.2
Netherlands	NL	16 829		0.2	99.8				34.5
Norway	NO	5 108	31.8	66.9	1.3				22.4
Poland	PL	38 018		0.0	5.6	28.2	52.6	13.7	58.0
Portugal (excl. Az., Mad.)	PT	9 922	1.3	39.1	59.6				29.9
Romania	RO	19 947		0.7	30.8	40.5	27.0	1.0	45.4
San Marino	SM	33		4.9	70.9	24			38.5
Serbia (incl. Kosovo*)	RS	7 147	0.0	1.3	6.0	15.9	54.5	22.3	63.3
Slovakia	SK	5 416		0.0	4.4	62.3	33.2	0.0	48.7
Slovenia	SI	2 061	0.1	9.9	50.5	39.4			37.3
Spain (excl. Canarias)	ES	44 397	1.7	31.5	57.8	7.9	1.0		32.0
Sweden	SE	9 645	9.7	78.7	11.6				24.3
Switzerland	CH	8 140	6.4	53.2	38.9	1.5			28.3
United Kingdom (& dep.)	UK	64 351	2.3	53.3	44.4	0.0			28.7
Total		**532 738**	**1.9**	**26.8**	**42.2**	**15.8**	**11.0**	**2.3**	**37.1**
			86.7				**13.3**		
EU-28		**502 424**	**1.6**	**26.9**	**43.9**	**15.8**	**10.1**	**1.8**	**36.6**
			88.1				**11.9**		

Kosovo*	KS	1 821	0.0	0.7	5.5	7.2	19.2	67.4	78.0
Serbia (excl. Kosovo*)	RS	7 147	0.0	1.5	6.1	18.0	63.1	11.3	59.7

*) under the UN Security Council Resolution 1244/99

Note 1: Turkey is not included in the calculation due to the lack of air quality data.
Note 2: The percentage value "0.0" indicates an exposed population exists, but it is small and estimated less than 0.05 %. Empty cells mean: no population in exposure.

3 $PM_{2.5}$

In the Ambient Air Quality Directive (EU, 2008), the target value for the annual average $PM_{2.5}$ concentrations was set at 25 µg.m^{-3}. This TV became a limit value (LV) for the year 2015. In the AQ directive there is also an indicative LV of 20 µg.m^{-3} defined as Stage 2 that should become potentially into force in 2020. The Air Quality Guideline recommended by the World Health Organization (WHO, 2005) for the $PM_{2.5}$ annual average is 10 µg.m^{-3}.

The current number of $PM_{2.5}$ measurement stations is yet limited and its spatial distribution is irregular over Europe. Deriving a reasonably reliable European wide spatially interpolated $PM_{2.5}$ annual average map on the basis of these $PM_{2.5}$ measurement data alone is not feasible. The resulting map would not be suitable for being used in population exposure assessments.

The mapping of the health-related indicator $PM_{2.5}$ annual average is, therefore, in this paper based on a mapping methodology developed in Denby et al. (2011a, 2011b). This methodology derives additional *pseudo* $PM_{2.5}$ annual mean concentrations from PM_{10} annual mean measurement concentrations. As such, it increases the number and spatial coverage of $PM_{2.5}$ 'data points' and these data is used to derive a European wide map of annual mean $PM_{2.5}$. Pseudo $PM_{2.5}$ stations data are estimated using PM_{10} measurement data, surface solar radiation, latitude and longitude. Separate urban and rural background concentration maps are calculated on a grid of 10x10 km resolution and the subsequent final combined concentration map is based on the 1x1 km gridded population density map. The final $PM_{2.5}$ map is presented in this 1x1 km grid resolution. The population exposure table is calculated based on this maps in this resolution.

Annex 3 provides details on the regression and kriging parameters applied for deriving the $PM_{2.5}$ annual average map, as well as the uncertainty analysis of the map. Annex 4 discusses briefly the inter-annual changes observed in the concentration maps and the relevant population exposure.

3.1 $PM_{2.5}$ – Annual mean

3.1.1 Concentration map

Map 3.1 presents the final combined map for the 2014 $PM_{2.5}$ annual average as result of the interpolation and merging of the separate rural and urban maps. The purple areas exceed the target value (TV) of 25 µg.m^{-3}. Red areas show exceedances of the indicative LV of 20 µg.m^{-3} defined as Stage 2.

Supplementary data in the regression used for rural areas consist of EMEP model output, altitude, wind speed, surface solar radiation and population density. The relevant supplementary data for estimating both the pseudo $PM_{2.5}$ station data and the linear regression sub-model with its residual kriging in the rural areas were identified earlier in Denby et al. (2011a, 2011b). Based on advice of Horálek et al. (2015), EMEP model output is used as supplementary data source for the urban areas. Prior to linear regression and kriging of its residuals, the $PM_{2.5}$ measurement and the modelled pseudo data is logarithmically transformed as that provides better results. After regression, these results are back-transformed.

According to Map 3.1, the areas with the highest $PM_{2.5}$ concentrations seem to be the Katowice (PL) – Ostrava (CZ) industrial region, together with the Po Valley in Northern Italy. Furthermore, the areas around the cities of Belgrade and Novi Sad in Serbia also show elevated $PM_{2.5}$ annual average concentrations. Like in the case of PM_{10}, the central and the eastern parts of Europe show higher concentrations than the western and the northern parts.

The *relative mean uncertainty* of the final combined map of $PM_{2.5}$ annual average is 22.4 % for rural areas and 16.4 % for urban areas and determined exclusively on the actual $PM_{2.5}$ measurement data points, i.e. not on the pseudo stations (Annex 3).

Map 3.1 Concentration map of $PM_{2.5}$ annual average, 2014

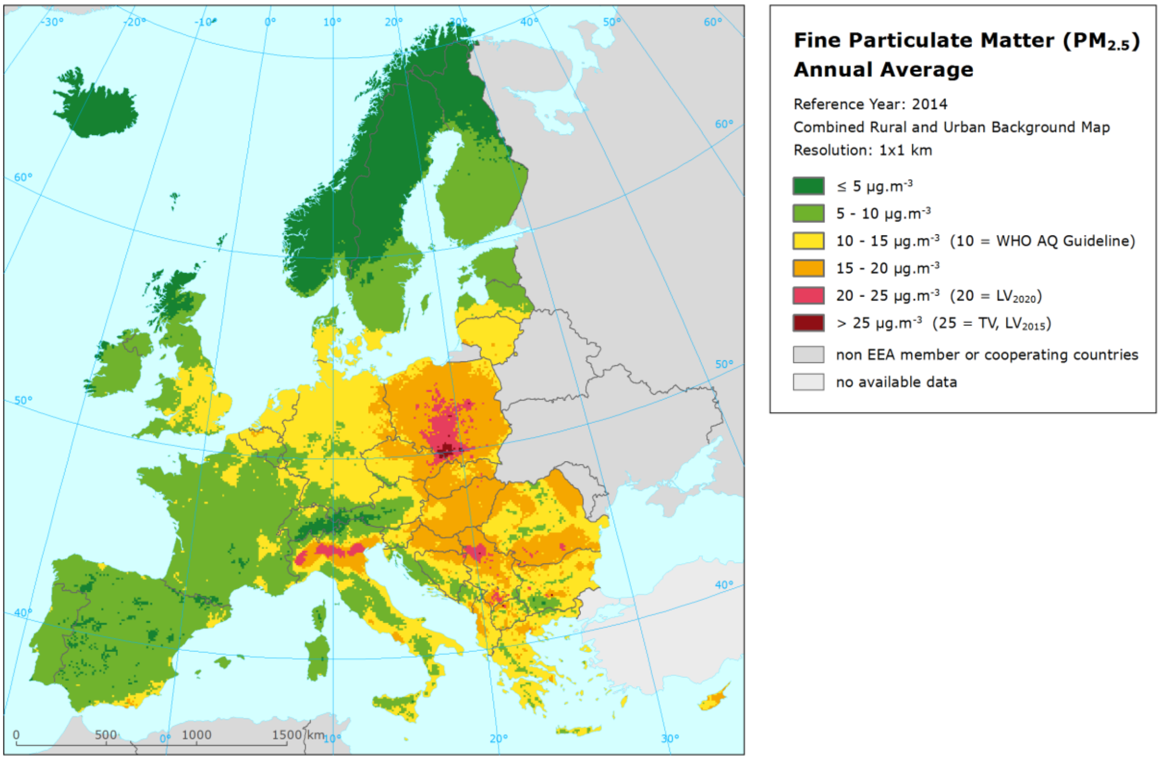

In order to provide more complete information of the air quality across Europe, the final combined map including the measurement data at station points is presented in Map A5.3 of Annex 5.

3.1.2 Population exposure

Table 3.1 gives the population frequency distribution for a limited number of exposure classes calculated on a grid of 1x1 km resolution, as well as the population-weighted concentration for individual countries and for Europe as a whole according to Equation A1.5 of Annex 1. Annex 4 shows details on the eight year evolution of population exposure.

In 2014, about 83 % of the European population has been exposed to $PM_{2.5}$ annual mean concentrations above the Air Quality Guideline of 10 μg.m^{-3} defined by the World Health Organization (WHO, 2005). The European wide and EU-28 population exposure exceeding the EU target value (TV) of 25 μg.m^{-3} is for both about 4 %. The indicative Stage 2 limit value LV_{2020} of 20 μg.m^{-3} is exceeded for about 11 – 12 %. In Bulgaria, Czech Republic, Greece, Italy, FYR of Macedonia, Poland, Romania, Serbia and Slovakia, 20 % or more of the population is exposed to concentrations above the LV_{2020}. As the current mapping methodology tends to underestimate high values (Annex 3), the exceedance percentages and/or the number of countries with population exposed to concentrations above both the TV and the LV_{2020} will most likely be higher.

Table 3.1 Population exposure and population-weighted concentration, $PM_{2.5}$ annual average 2014

Country		Population	$PM_{2.5}$ annual average, exposed population [%]						Population weighted conc.
			< LV_{2020}				> LV_{2020}		
			< TV					> TV	
			< 5	5 - 10	10 - 15	15 - 20	20 - 25	> 25	
		[inhbs . 1000]	$\mu g.m^{-3}$	$\mu g.m^{-3}$	$\mu g.m^{-3}$	$\mu g.m^{-3}$	$\mu g.m^{-3}$	$\mu g.m^{-3}$	[$\mu g.m^{-3}$]
Albania	AL	2 896		0.0	24.2	72.8	2.2	0.8	16.5
Andorra	AD	73	0.5	2.7	96.7				10.0
Austria	AT	8 507	0.4	13.0	54.0	32.5			12.9
Belgium	BE	11 204		2.7	67.2	30.0			13.7
Bosnia & Herzegovina	BA	3 831		1.7	47.9	47.4	3.0		15.3
Bulgaria	BG	7 246		0.9	8.4	12.0	33.4	45.2	24.0
Croatia	HR	4 247		4.8	31.8	63.1	0.3		15.6
Cyprus	CY	858			5.0	95.0			17.0
Czech Republic	CZ	10 512		0.2	9.5	69.3	13.8	7.2	18.7
Denmark	DK	5 627	0.4	4.2	95.4				11.6
Estonia	EE	1 316		94.9	5.1				8.7
Finland	FI	5 451	1.1	98.4	0.5				7.4
France (metropolitan)	FR	63 989	0.0	31.5	67.4	1.1			11.0
Germany	DE	80 767	0.0	2.3	85.5	12.3			13.4
Greece	GR	10 927		0.4	29.1	50.6	11.9	8.0	17.0
Hungary	HU	9 877			6.6	89.2	4.1		17.3
Iceland	IS	326	9.6	90.4					6.6
Ireland	IE	4 606	1.2	76.5	22.2				9.0
Italy	IT	60 783	0.0	3.7	44.5	32.2	19.5		15.8
Latvia	LV	2 001		10.6	38.2	51.2			14.1
Liechtenstein	LI	37	0.1	99.9					9.0
Lithuania	LT	2 943			28.5	71.5			15.5
Luxembourg	LU	550		8.7	91.3				11.9
Macedonia, FYROM of	MK	2 066		0.0	2.2	10.3	11.8	75.6	27.4
Malta	MT	425		0.4	99.6				12.0
Monaco	MC	38			100.0				12.9
Montenegro	ME	622		3.7	36.5	59.9			15.6
Netherlands	NL	16 829		0.0	98.7	1.3			13.8
Norway	NO	5 108	21.7	75.9	2.4				7.2
Poland	PL	38 018			1.9	29.6	35.3	33.3	22.9
Portugal (excl. Az., Mad.)	PT	9 922	0.1	90.5	9.4				8.7
Romania	RO	19 947		0.1	28.9	47.5	20.1	3.5	17.5
San Marino	SM	33			100.0				13.5
Serbia (incl. Kosovo*)	RS	7 147		0.1	3.1	30.5	41.9	24.4	22.4
Slovakia	SK	5 416			1.0	65.4	32.3	1.4	19.2
Slovenia	SI	2 061		1.1	37.8	61.1			15.1
Spain (excl. Canarias)	ES	44 397	0.1	43.6	55.1	1.2	0.0		10.7
Sweden	SE	9 645	4.0	82.0	13.9				7.6
Switzerland	CH	8 140	0.8	16.6	81.1	1.6			11.6
United Kingdom (& dep.)	UK	64 351	0.2	13.9	86.0				11.6
Total		**532 738**	**0.4**	**16.4**	**52.8**	**18.6**	**7.7**	**4.2**	**14.1**
			16.7		**71.4**		**11.9**		
EU-28		**502 424**	**0.1**	**16.3**	**54.2**	**18.3**	**7.3**	**3.7**	**14.0**
			16.4		**72.5**		**11.0**		

Kosovo*	KS	1 821		0.0	2.4	15.3	15.1	67.3	26.4
Serbia (excl. Kosovo*)	RS	7 147		0.1	3.3	34.2	48.4	13.9	21.4

*) under the UN Security Council Resolution 1244/99

Note 1: Turkey is not included in the calculation due to the lack of air quality data.

Note 2: The percentage value "0.0" indicates an exposed population exists, but it is small and estimated less than 0.05 %. Empty cells mean: no population in exposure.

According to EEA CSI004 (EEA, 2016c), about 8 % of the urban population in the EU-28 was exposed to $PM_{2.5}$ above the target value threshold in 2014. The difference with the estimated 4 % in Table 3.1 is because the EEA accounts for the urban population in the larger agglomerations only. Whereas, Table 3.1 provides estimates, including the population in rural areas, smaller cities and villages. When it comes to the WHO AQ guideline, the urban population exposed to concentrations above this value (10 $\mu g.m^{-3}$) in 2014 was estimated at 85 %, more in line with the total population estimation presented in Table 3.1.

The European-wide population-weighted concentration of the $PM_{2.5}$ annual average is estimated for 2014 at about 14 $\mu g.m^{-3}$ (the same as for the EU28 only). This is the lowest level of the limited series 2007 –2014 (with no 2009 data, see Table 6.2).

4 Ozone

For ozone, two health-related indicators (93.2 percentile of maximum daily 8-hour means, see below, and SOMO35) and two vegetation-related indicators (AOT40 for vegetation and AOT40 for forests) are considered. For the definition of SOMO35 and AOT40 indicators, see following sections and Annex 2.

The separate rural and urban background *health*-related indicator fields are calculated at a resolution of 10x10 km. Subsequently, the final health-related indicator maps are created by combining rural and urban areas based on the 1x1 km gridded population density map. We present these maps on this 1x1 km grid resolution. The population exposure tables are calculated based on these health-related indicator maps.

The *vegetation*-related indicator maps are calculated from observations at rural background stations and are representative for rural areas only (assuming urban areas do not cover vegetation). The maps have a resolution of 2x2 km. This resolution serves the needs of the EEA Core Set Indicator 005 (EEA, 2016d) on ecosystem exposure to ozone.

Annex 3 provides details on the regression and kriging parameters applied for deriving the maps of the ozone indicators, as well as the uncertainty analysis of the maps. Annex 4 discusses briefly the inter-annual changes observed in the concentration maps and the relevant population and vegetation exposure.

4.1 Ozone – 93.2 percentile of maximum daily 8-hour means

The AQ Directive (EU, 2008) describes the ozone daily target value as "a maximum daily 8-hour mean of 120 μg.m^{-3} not to be exceeded on more than 25 times a calendar year, averaged over three years". On an annual basis, it can be evaluated by the indicator 26th maximum daily 8-hour mean, which is in principle equivalent to the indicator 93.2 percentile of maximum daily 8-hour means. However, for measurement data these two indicators are equivalent only if no data is missing, which is in general not the case. As shown in de Leeuw (2012), the additional uncertainty related to the incomplete time series is substantially smaller when using percentile values instead of the x-th highest value. Thus, from this report onward, the 93.2 percentile of maximum daily 8-hour means is and will be used as indicator, instead of the formerly used 26th maximum daily 8-hour mean.

4.1.1 Concentration map

Map 4.1 presents the final combined map for 93.2 percentile of the maximum daily 8-hour means as a result of combining the separate rural and urban interpolated maps following the procedures as described in Annex 1 (for a more detailed description, see Horálek et al., 2007, 2010). The supplementary data used are EMEP model output, altitude and surface solar radiation for rural areas and EMEP model output, wind speed and surface solar radiation for urban areas (Annex 3).

In the final combined map the red and purple areas show values above 120 μg.m^{-3} on more than 25 days in 2014. Note that in the AQ Directive (EU, 2008) the target value is actually defined as 120 μg.m^{-3} not to be exceeded on more than 25 days per calendar year *averaged over three years*. Here only 2014 data are presented, and no three-year average is calculated.

In the map most of the areas with values above 120 μg.m^{-3} on more than 25 days in 2014 are in the Alpine region, northern and southern Italy, southern France, central and south-western Spain, Greece and Cyprus. In general, the southern parts of Europe show higher ozone concentrations than the northern parts, which is caused mainly by higher solar radiation and temperature in these areas. Higher levels of ozone do also occur more frequently in mountainous areas than in lowlands. The relative mean uncertainty of the 2014 map of the 93.2 percentile of daily 8-h ozone maximums is about 7 % for both rural and urban areas (Annex 3).

In order to provide more complete information of the air quality across Europe, the final combined map including the measurement data at station points is presented in Map A5.4 of Annex 5.

Map 4.1 Concentration map of ozone indicator 93.2 percentile of maximum daily 8-hour means, 2014

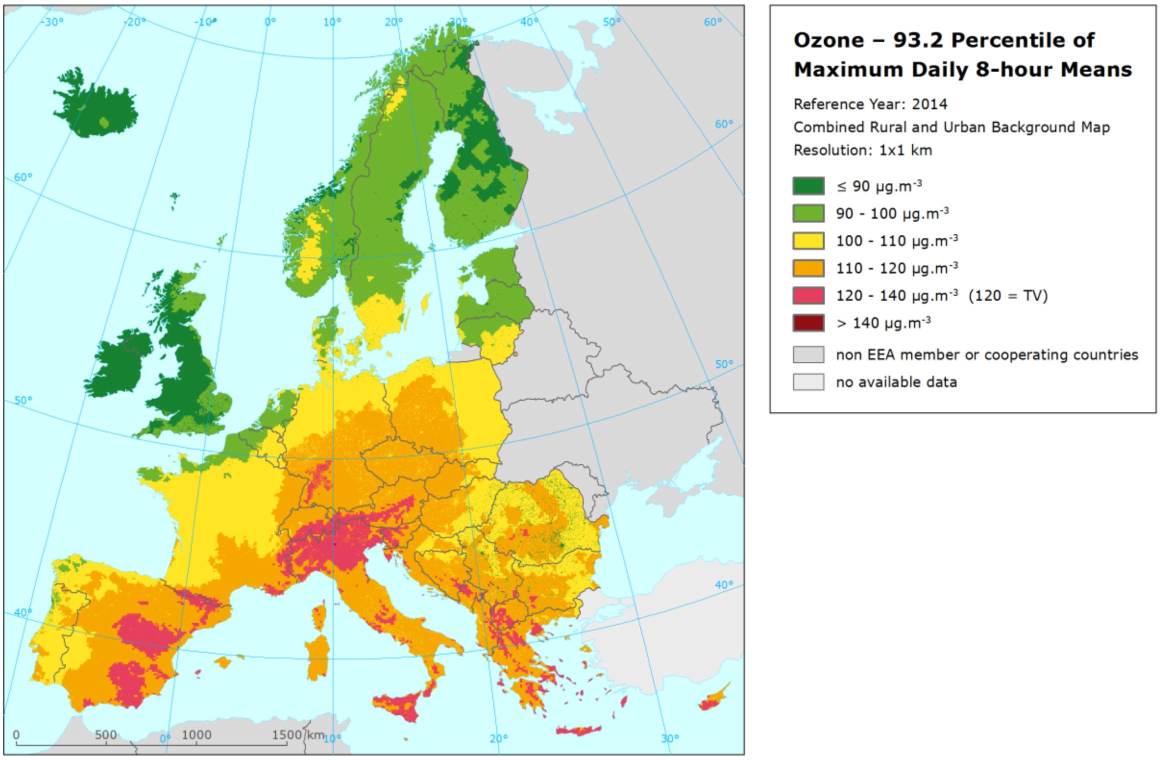

4.1.2 Population exposure

Table 4.1 gives, for 93.2 percentile of maximum daily 8-hour running means, the population frequency distribution for a limited number of exposure classes, as well as the population-weighted concentration for individual countries and for Europe as a whole. Annex 4 presents the ten year evolution of population exposure.

It has been estimated that in 2014 some 6 % of the European population lived in areas where the ozone concentration exceeded the health related target value threshold (TV of 120 μg.m^{-3}). This is the lowest value of the ten years period 2005 – 2014 (Table 6.3). According to CSI004 (EEA, 2016c), about 8 % of the urban population in the EU-28 was exposed to ozone above the target value threshold in 2014.

In Italy, Spain and Slovenia more than 5 % of the population was exposed to concentrations exceeding the TV threshold. As the current mapping methodology tends to underestimate high values due to interpolation smoothing (Annex 3), the exceedance percentage is most likely somewhat underestimated; additional exceedances might be expected in countries like Austria, Croatia, Greece and Switzerland. The reason is that in these countries the estimated percentage population exposed to the concentrations above 110 μg.m^{-3} is high (more than 50 %).

Table 4.1 Population exposure and population-weighted concentrations, ozone indicator 93.2 percentile of maximum daily 8-hour means, 2014

Country		Population [inhbs . 1000]	Ozone, 93.2nd percentile of max. daily 8-h means, exposed population: < TV: < 90 μg.m-3	< TV: 90 - 100 μg.m-3	< TV: 100 - 110 μg.m-3	< TV: 110 - 120 μg.m-3	> TV: 120 - 140 μg.m-3	> TV: > 140 μg.m-3	Population-weighted conc. [μg.m-3]
Albania	AL	2 896			76.8	22.3	0.8		107.4
Andorra	AD	73				97.7	2.3		117.4
Austria	AT	8 507			28.0	70.1	1.9		112.0
Belgium	BE	11 204	0.1	66.3	33.6				99.0
Bosnia & Herzegovina	BA	3 831		4.0	78.5	17.4	0.1		105.6
Bulgaria	BG	7 246	20.4	62.8	11.6	5.1	0.0		94.6
Croatia	HR	4 247		1.0	43.6	53.5	1.9		109.5
Cyprus	CY	858		21.7	61.4	13.1	3.8		104.6
Czech Republic	CZ	10 512			60.5	39.5			109.6
Denmark	DK	5 627	0.8	86.7	12.6	0.0			96.6
Estonia	EE	1 316	2.7	97.1	0.2				92.8
Finland	FI	5 451	62.8	37.2	0.0				89.1
France (metropolitan)	FR	63 989		18.3	60.1	21.4	0.3		105.6
Germany	DE	80 767		2.6	62.0	35.1	0.3		107.9
Greece	GR	10 927		5.7	33.1	57.6	3.6		112.2
Hungary	HU	9 877	4.7	18.2	69.4	7.7			103.2
Iceland	IS	326	100						69.0
Ireland	IE	4 606	100						58.1
Italy	IT	60 783		0.1	21.0	43.6	35.2	0.0	116.2
Latvia	LV	2 001	39.6	59.8	0.6				91.8
Liechtenstein	LI	37				100			113.4
Lithuania	LT	2 943	0.2	85.3	14.5				96.5
Luxembourg	LU	550			97.4	2.6			105.5
Macedonia, FYROM of	MK	2 066		20.5	74.0	5.0	0.4		102.0
Malta	MT	425				97.3	2.7		115.8
Monaco	MC	38				100			116.3
Montenegro	ME	622		9.5	67.2	21.6	1.7		105.6
Netherlands	NL	16 829		84.3	15.7				97.5
Norway	NO	5 108	70.2	29.6	0.2				88.7
Poland	PL	38 018		4.6	71.8	23.6			107.2
Portugal (excl. Az., Mad.)	PT	9 922	6.1	32.8	56.4	4.6			101.0
Romania	RO	19 947	75.4	9.0	12.0	3.5	0.0		83.3
San Marino	SM	33				99.3	0.7		118.4
Serbia (incl. Kosovo*)	RS	7 147	32.0	44.2	14.0	9.8	0.1		95.6
Slovakia	SK	5 416		0.6	36.9	62.5			110.2
Slovenia	SI	2 061			10.5	81.5	7.9		115.0
Spain (excl. Canarias)	ES	44 397	0.2	4.9	23.8	55.2	15.8		112.2
Sweden	SE	9 645	8.0	82.8	9.2	0.0			95.4
Switzerland	CH	8 140			11.2	85.9	2.9		113.8
United Kingdom (& dep.)	UK	64 351	95.9	4.1	0.1	0.0			84.1
Total		**532 738**	**17.9**	**15.0**	**35.7**	**25.8**	**5.6**	**0.0**	**102.9**
			32.9		**61.5**		**5.6**		
EU-28		**502 424**	**17.7**	**14.8**	**36.1**	**25.6**	**5.9**	**0.0**	**103.0**
			32.5		**61.7**		**5.9**		

Kosovo*	KS	1 821		56.2	28.5	15.1	0.2		101.8
Serbia (excl. Kosovo*)	RS	7 147	39.8	41.2	10.5	8.4	0.0		94.1

*) under the UN Security Council Resolution 1244/99

Note 1: Turkey is not included in the calculation due to the lack of air quality data.
Note 2: The percentage value "0.0" indicates an exposed population exists, but it is small and estimated less than 0.05 %. Empty cells mean: no population in exposure.

The overall European and EU-28 population-weighted ozone concentrations in terms of the 93.2 percentile of maximum daily 8-hour means were estimated for 2014 as being 103 $\mu g.m^{-3}$, which is the lowest value during the period 2005 – 2014.

4.2 Ozone – SOMO35

SOMO35 is the annually accumulated ozone daily 8-hourly maximum concentration in excess of 35 ppb (i.e. 70 $\mu g.m^{-3}$). It is not subject to any of the EU air quality directives and there are no limit or target values defined. Comparison of the 93.2 percentile of maximum daily 8-hour means versus the SOMO35 for all background stations shows there is no simple relation between the two indicators, however it seems that the target value of the 93.2 percentile of maximum daily 8-hour means (being 120 $\mu g.m^{-3}$) is related approximately with SOMO35 in the range 6 000 – 8 000 $\mu g.m^{-3}.d$. This comparison motivates a somewhat arbitrarily chosen threshold of 6 000 $\mu g.m^{-3}.d$, in order to facilitate the discussion of the observed distributions of SOMO35 levels in their spatial and temporal context. This threshold is used in this and previous papers (Horálek et al. 2016b and the references cited therein) in the population exposure.

4.2.1 Concentration map

Map 4.2 presents the final combined map for SOMO35 as result of combining the separate rural and urban interpolated maps following the similar procedure as for 93.2 percentile of the maximum daily 8-hour means. The mapping details and the uncertainty analysis are presented in Annex 3. In the final combined map the red and purple areas show values above 8 000 $\mu g.m^{-3}.d$, while the orange areas show values above 6 000 $\mu g.m^{-3}.d$.

Like in the case of the 93.2 percentile of the maximum daily 8-hour means, the southern parts of Europe show higher ozone SOMO35 concentrations than the northern parts. Higher levels of ozone do also occur more frequently in mountainous areas than in lowlands. The relative mean uncertainty of the 2014 map of the SOMO35 is about 29 % for both rural and urban areas (Annex 3).

In order to provide more complete information of the air quality across Europe, the final combined map including the measurement data station points is presented in Map A5.5 of Annex 5.

Map 4.2 Concentration map of ozone indicator SOMO35, 2014

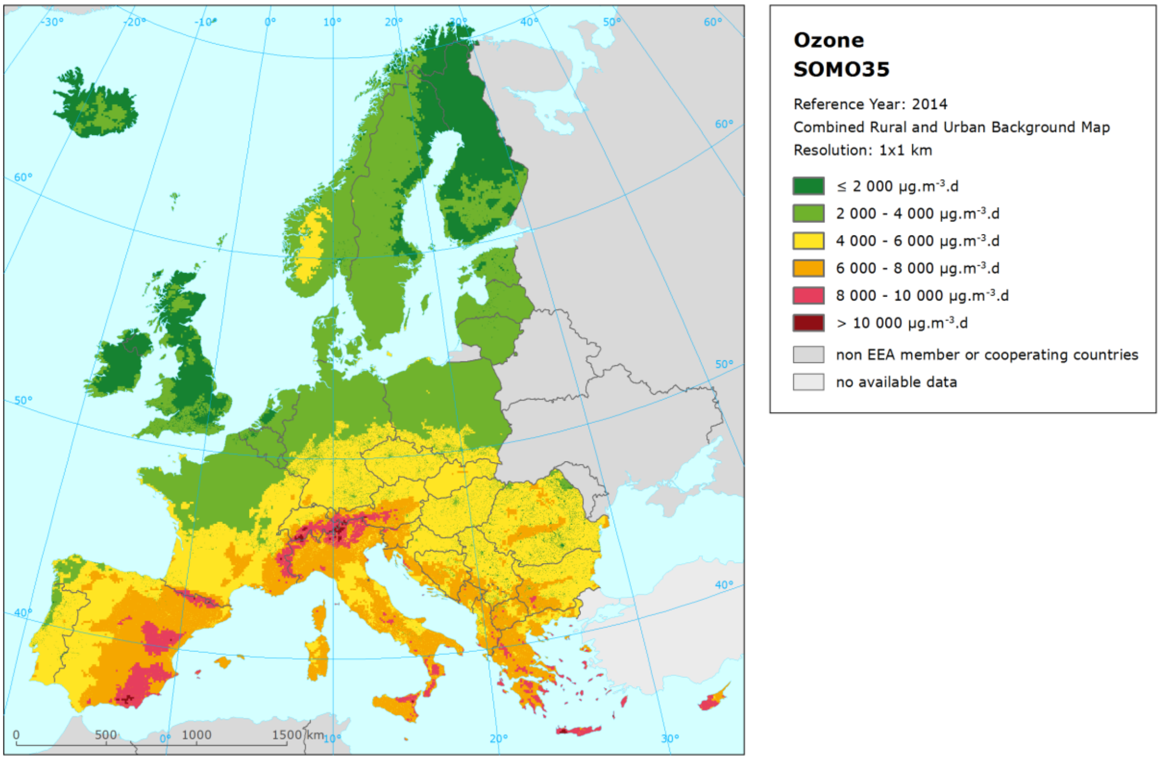

4.2.2 Population exposure

Table 4.2 gives for SOMO35 the population frequency distribution for a limited number of exposure classes, as well as the population-weighted concentration for individual countries and for Europe as a whole. Annex 4 shows details on the ten-year evolution of population exposure.

It has been estimated that in 2014 about 9 % of the European population lived in areas with SOMO35 values above 6 000 µg.m^{-3}.d. (For the motivation of this indicative threshold, see above.) This is the lowest value of the ten years period 2005 – 2014 (Table 6.3).

In 2014, the northern and north-western European countries do not have people exposed to SOMO35 concentrations above 6 000 µg.m^{-3}.d, and almost no people above 4 000 µg.m^{-3}.d. Most of the countries in southern and south-eastern Europe show exposures above or well above 6 000 µg.m^{-3}.d, specifically Malta, Greece, Spain, Italy, Slovenia and Cyprus. This can also be seen in Map 4.2.

In 2014, the total European and the EU-28 population-weighted ozone concentrations, in terms of SOMO35, were estimated to be 3 500 µg.m^{-3}.d, which is the lowest of the ten years period 2005 – 2014 (Table 6.3).

Table 4.2 Population exposure and population-weighted concentrations, ozone indicator SOMO35, 2014

Country		Population [inhbs.1000]	Ozone, SOMO35, exposed population [%] < 2000 µg.m^{-3}.d	2000 - 4000 µg.m^{-3}.d	4000 - 6000 µg.m^{-3}.d	6000 - 8000 µg.m^{-3}.d	8000 - 10000 µg.m^{-3}.d	> 10000 µg.m^{-3}.d	Population-weighted conc. [µg.m^{-3}.d]
Albania	AL	2 896		43.8	45.2	10.9	0.1		4 376
Andorra	AD	73				98.2	1.8		6 692
Austria	AT	8 507		29.2	63.2	7.0	0.6	0.0	4 423
Belgium	BE	11 204	12.0	88.0					2 297
Bosnia & Herzegovina	BA	3 831		65.7	30.5	3.8			3 852
Bulgaria	BG	7 246	32.1	53.9	12.1	2.0	0.0		2 519
Croatia	HR	4 247		36.0	55.9	8.1	0.0		4 503
Cyprus	CY	858			81.1	12.7	6.2		5 426
Czech Republic	CZ	10 512		73.7	26.3	0.0			3 822
Denmark	DK	5 627	1.2	98.5	0.4				2 611
Estonia	EE	1 316	44.3	55.7					1 991
Finland	FI	5 451	89.8	10.2					1 615
France (metropolitan)	FR	63 989	0.6	65.4	27.2	6.8	0.1		3 786
Germany	DE	80 767		82.7	17.2	0.1	0.0		3 287
Greece	GR	10 927	0.3	13.3	33.6	49.8	2.9	0.0	5 926
Hungary	HU	9 877	0.2	79.0	20.8	0.0			3 620
Iceland	IS	326	99.9	0.1					218
Ireland	IE	4 606	92.1	7.9					868
Italy	IT	60 783		2.0	67.8	29.6	0.6	0.0	5 569
Latvia	LV	2 001	23.0	77.0					2 213
Liechtenstein	LI	37			98.2	1.8			4 360
Lithuania	LT	2 943	6.7	93.3					2 457
Luxembourg	LU	550		100.0					2 872
Macedonia, FYROM of	MK	2 066		92.6	5.2	2.2	0.0		3 215
Malta	MT	425				97.6	2.4		6 946
Monaco	MC	38				100			7 112
Montenegro	ME	622		70.6	16.1	13.3	0.0		4 012
Netherlands	NL	16 829	26.9	73.1					2 244
Norway	NO	5 108	50.1	49.5	0.4				2 113
Poland	PL	38 018		93.3	6.7	0.0			3 425
Portugal (excl. Az., Mad.)	PT	9 922	2.9	57.9	39.0	0.1			3 519
Romania	RO	19 947	70.3	16.9	12.5	0.3			1 842
San Marino	SM	33			84.6	15.4			5 949
Serbia (incl. Kosovo*)	RS	7 147	25.5	56.9	16.2	1.3			2 762
Slovakia	SK	5 416		16.0	83.9	0.0			4 344
Slovenia	SI	2 061		10.0	69.5	20.4	0.1		5 086
Spain (excl. Canarias)	ES	44 397	0.2	15.5	43.1	40.4	0.8	0.0	5 436
Sweden	SE	9 645	18.0	82.0	0.0				2 318
Switzerland	CH	8 140		16.1	80.1	3.0	0.7	0.0	4 417
United Kingdom (& dep.)	UK	64 351	91.4	8.4	0.2				1 337
Total		**532 738**	**18.5**	**46.9**	**25.2**	**9.1**	**0.2**	**0.0**	**3 500**
			90.6			**9.4**			
EU-28		**502 424**	**18.7**	**46.9**	**24.7**	**9.5**	**0.2**	**0.0**	**3 506**
			90.3			**9.7**			

Kosovo*	KS	1 821	2.4	75.2	20.2	2.2			3 149
Serbia (excl. Kosovo*)	RS	7 147	31.2	52.5	15.2	1.1			2 668

*) under the UN Security Council Resolution 1244/99

Note 1: Turkey is not included in the calculation due to the lack of air quality data.
Note 2: The percentage value "0.0" indicates an exposed population exists, but is small and estimated less than 0.05 %. Empty cells mean no population in exposure.

4.3 Ozone – AOT40 vegetation and AOT40 forests

In the Ambient Air Quality Directive (EU, 2008) a target value (TV) and a long-term objective (LTO) for the *vegetation protection* from high ozone concentrations accumulated during the growing season have been defined. TV and LTO are specified using "accumulated ozone exposure over a threshold of 40 parts per billion" (AOT40). This is calculated as a sum of the difference between hourly concentrations greater than 80 $\mu g.m^{-3}$ (i.e. 40 parts per billion) and 80 $\mu g.m^{-3}$, using only observations between 08:00 and 20:00 Central European Time (CET) each day, calculated over three months from 1 May to 31 July. The TV is 18 000 $\mu g.m^{-3}.h$ (averaged over five years) and the LTO is 6 000 $\mu g.m^{-3}.h$.

Note that the term *vegetation* as used in the Air Quality Directive (EU, 2008) is not further defined. Nevertheless, the target value used in the directive is the same as the critical load used in the Mapping Manual (UNECE, 2004) for "agricultural crops", so we have interpreted the term *vegetation* in the AQ directive as primarily agricultural crops. Therefore, the exposure of *agricultural crops* has been evaluated here based on the AOT40 for vegetation as defined in the AQ directive and the agricultural areas, defined as the CORINE Land Cover level-1 class *2 Agricultural areas* (encompassing the level-2 classes *2.1 Arable land, 2.2 Permanent crops, 2.3 Pastures* and *2.4 Heterogeneous agricultural areas)*, see Section 4.3.2. Note that in addition to these agricultural areas there are several other CLC classes that could be considered "vegetation", namely level-2 classes *1.4 Artificial, non-agricultural vegetated areas* (encompassing the level-3 classes *1.4.1 Green urban areas* and *1.4.2 Sport and leisure facilities*), *2.3 Forests* (see below) and *2.4 Scrub and/or herbaceous vegetation associations*.

Next to the AOT40 for vegetation protection, the AQ Directive (EU, 2008) defines also the AOT40 for *forest protection*, which is calculated similarly as the AOT40 for vegetation, but is summed over six months from 1 April to 31 September. For AOT40 for forests there is no TV defined. However, there is a critical level (CL) established by UNECE (UNECE, 2004). This CL is set at 10 000 $\mu g.m^{-3}.h$.

For the exposure of forests evaluation, the CORINE Land Cover level-2 class *3.1 Forests* has been used.

The ecosystem based accumulative ozone indicators described in this section are specifically prepared for calculation of EEA Core Set Indicator 005 (EEA, 2016d). For the estimation of the vegetation and forested area exposure to accumulated ozone, the maps in this section are created on a grid of 2x2 km resolution. The exposure frequency distribution outcomes are based on the overlay with the 100x100 m grid resolution of the CLC2006 land cover classes.

4.3.1 Concentration maps

The interpolated map of AOT40 for vegetation and of AOT40 for forests are created for rural areas only, as urban areas are considered not to represent agricultural or forested areas. These maps are therefore applicable to rural areas only, and as such they are based on AOT40 data derived from rural background station observations only. These AOT40 monitoring data are combined in the mapping with the supplementary data sources EMEP model output, altitude and surface solar radiation. These supplementary data sources are the same as those selected at the human health related ozone indicators.

Map 4.3 presents the final map of AOT40 for *vegetation* in 2014. Note that in Directive 2008/50/EC the target value is actually defined as 18 000 $\mu g.m^{-3}.h$ *averaged over five years*. Here only 2014 data are presented, and no five-year average is calculated.

The areas in the map with concentrations above the target value (TV) threshold of 18 000 $\mu g.m^{-3}.h$ are marked in red and dark red. The areas below the long term objective (LTO) are marked in green. The high AOT40 levels for vegetation do occur specifically in the southern, south-western and south-eastern regions of Europe. The relative mean uncertainty of the 2014 map of the AOT40 for vegetation is about 31 % (Annex 3).

Map 4.3 Concentration map of ozone indicator AOT40 for vegetation, rural map, 2014

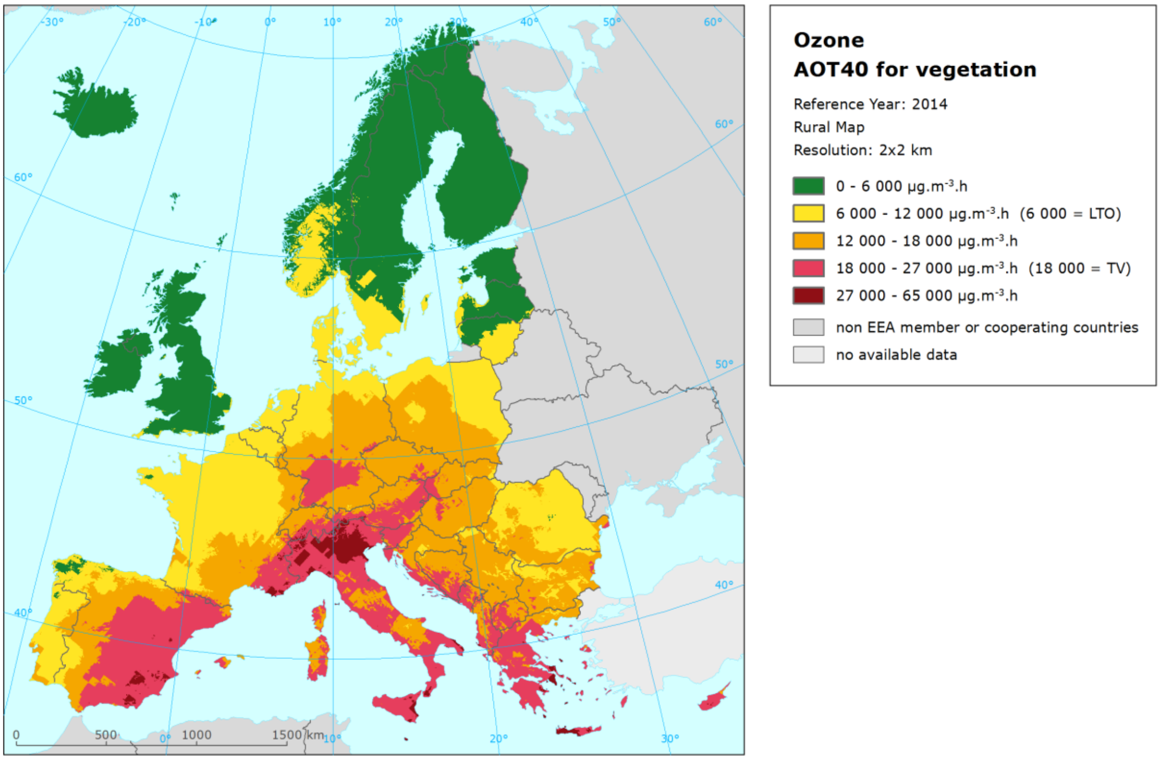

Map 4.4 Concentration map of ozone indicator AOT40 for forests, rural map, 2014

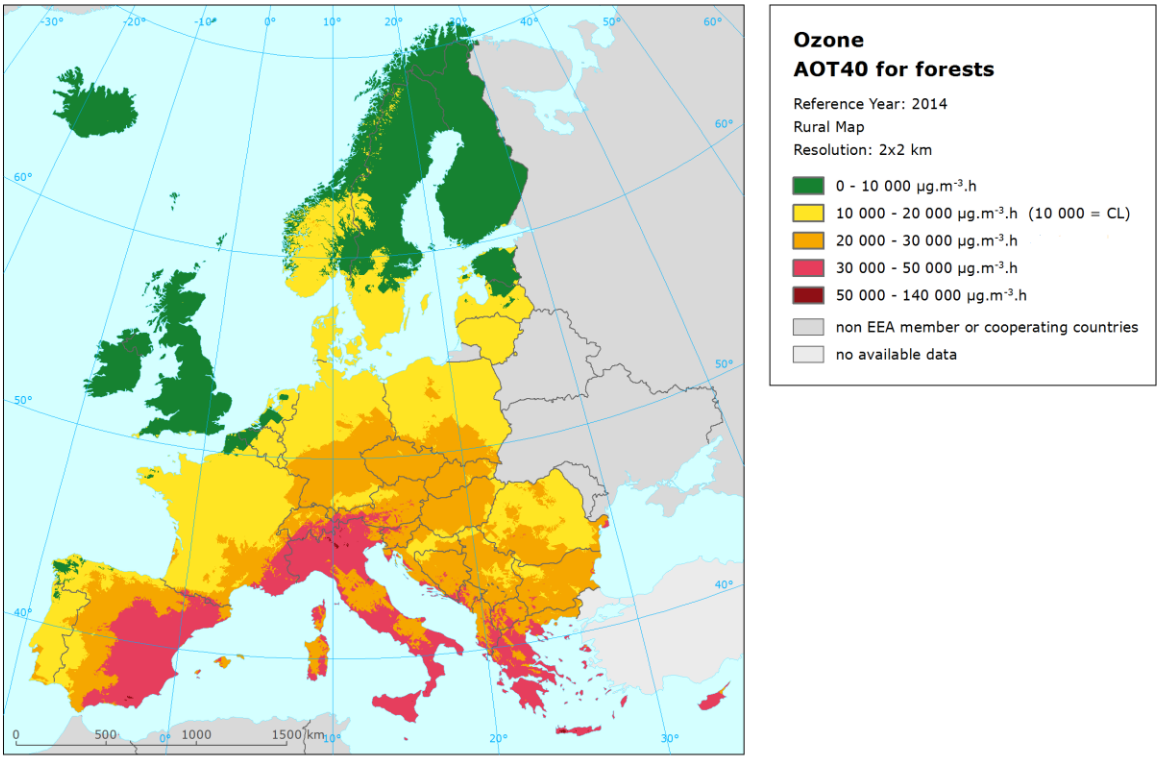

Map 4.4 presents the final map of AOT40 for *forests* in 2014. The areas in the map with concentrations above the critical level (CL) defined by UNECE (2004) are marked in yellow, orange, red and dark red. One can see large European forested areas exceeding this level.

Like at the AOT40 for vegetation indicator, the high levels of the AOT40 for forests are found in the same south-western, southern and south-eastern European regions. The relative mean uncertainty of the 2014 map of the AOT40 for forests is about 34 % (Annex 3).

In order to provide more complete information of the air quality across Europe, the AOT40 maps including the data at rural background measurement station points are presented in Maps A5.6 and A5.7 of Annex 5.

4.3.2 Vegetation exposure

Agricultural crops

The rural map with ozone indicator AOT40 for vegetation has been combined with the land cover CLC2006 map. Following a similar procedure as described in Horálek et al. (2007), the exposure of agricultural areas (as defined above) has been calculated at the country-level.

Table 4.3 gives the absolute and relative agricultural area for each country and for four European regions where the ozone target value (TV) threshold and long-term objective (LTO) for protection of vegetation as defined in the AQ Directive (EU, 2008) are exceeded. The frequency distribution of the agricultural area over the exposure classes per country is presented as well.

The table indicates the country grouping with corresponding colours of the region; *Northern Europe*: Denmark, Estonia, Finland, Latvia, Lithuania, Norway, and Sweden. *North-western Europe*: Belgium, France north of 45 degrees latitude, Ireland, Iceland, Luxembourg, the Netherlands, and United Kingdom. *Central and Eastern Europe*: Austria, Bulgaria, Czech Republic, Germany, Hungary, Liechtenstein, Poland, Slovakia, Switzerland, and Romania. *Southern Europe*: Albania, Bosnia-Herzegovina, Croatia, Cyprus, France south of 45 degrees latitude, Greece, Italy, F.Y.R. of Macedonia, Malta, Monaco, Montenegro, Portugal, San Marino, Serbia (including Kosovo under the UN Security Council Resolution 1244/99), Slovenia, and Spain.

Table 4.3 illustrates that in 2014, some 18 % of all European agricultural land was exposed to ozone exceeding the target value (TV) threshold of 18 000 $\mu g.m^{-3}.h$. This is the lowest percentage of the ten year period 2005 – 2014, see Table 6.4.

Considering the long-term objective (LTO) of 6 000 $\mu g.m^{-3}.h$ the area in excess is about 86 %, which is more than in 2013 and similar to 2010 – 2012 according to Table 6.4. Iceland and Ireland were the only countries with ozone levels not being in excess of the LTO. In half of the southern European countries, more than half of their agricultural area experienced exposures above the less stringent TV threshold in 2014.

Forests

The rural map with ozone indicator AOT40 for forests was combined with the land cover CLC2006 map. Following a similar procedure as described in Horálek et al. (2007), the exposure of forest areas (as defined above) has been calculated for each country, for the same four European regions as for crops and for Europe as a whole.

Table 4.3 Agricultural area exposure and exceedance, ozone indicator AOT40 for vegetation, 2014

Country	Agricultural Area, 2014					Percentage of agricultural area, 2014 [%]				
	Total area	> LTO (6 000 μg.m^{-3}.h)		> TV (18 000 μg.m^{-3}.h)		< 6 000	6 000 - 12 000	12 000 - 18 000	18 000 - 27 000	> 27 000
	[km^2]	[km^2]	[%]	[km^2]	[%]	μg.m^{-3}.h	μg.m^{-3}.h	μg.m^{-3}.h	μg.m^{-3}.h	μg.m^{-3}.h
Albania	7877	7877	100	3875	49.2			50.8	49.1	0.1
Austria	27222	27222	100	10576	38.9		0.1	61.1	38.8	0.0
Belgium	17597	17597	100				92.7	7.3		
Bosnia-Herzegovina	18840	18840	100	3089	16.4		1.0	82.6	16.4	
Bulgaria	57402	57402	100	455	0.8		38.7	60.5	0.8	
Croatia	22502	22502	100	4002	17.8		4.9	77.3	17.6	0.2
Cyprus	4290	4290	100	4003	93.3			6.7	92.7	0.6
Czech Republic	45117	45117	100	2876	6.4			93.6	6.4	
Denmark (no Faroes)	32042	32042	100				99.9	0.1		
Estonia	14644	371	2.5			97.5	2.5			
Finland	29023	3	0.0			100.0	0.0			
France (metropolitan)	327710	326977	99.8	8937	2.7	0.2	76.1	20.9	2.6	0.2
Germany	212177	212177	100	28364	13.4		36.9	49.7	13.4	
Greece (CLC2000)	51575	51575	100	39691	77.0		1.6	21.5	71.8	5.2
Hungary	62219	62219	100	3041	4.9		5.8	89.3	4.9	
Iceland	2378					100				
Ireland	46141					100				
Italy	156491	156491	100	122411	78.2		0.2	21.6	63.7	14.5
Latvia	28253	3572	12.6			87.4	12.6			
Liechtenstein	41	41	100					100.0		
Lithuania	39815	22423	56.3			43.7	56.3			
Luxembourg	1389	1389	100					100.0		
Macedonia, FYR of	9316	9316	100	2990	32.1			67.9	32.1	
Malta	124	124	100	124	100					100
Monaco	0									
Montenegro	2297	2297	100	1149	50.0			50.0	50.0	
Netherlands	24238	24238	100				100.0			
Norway	15673	2489	15.9			84.1	15.9			
Poland	195798	195798	100				50.8	49.2		
Portugal (excl. Az., Mad.)	41909	41528	99.1			0.9	81.9	17.2		
Romania	135293	135080	100	22	0.0	0.2	75.9	24.0	0.0	
San Marino	42	42	100	42	100				100.0	
Serbia (incl. Kosovo*)	48639	48639	100	80	0.2		15.1	84.7	0.2	
Slovakia	23660	23660	100	3960	16.7		6.4	76.8	16.7	
Slovenia	7104	7104	100	4047	57.0			43.0	57.0	
Spain (excl. Canarias)	251578	247023	98.2	138262	55.0	1.8	12.1	31.1	54.2	0.7
Sweden	38647	14303	37.0			63.0	37.0			
Switzerland	11806	11806	100	1471	12.5		0.0	87.5	12.3	0.2
United Kingdom(& Man)	138874	5019	3.6			96.4	3.6			
Total	**2149741**	**1838591**	**85.5**	**383466**	**17.8**	**14.5**	**35.0**	**32.7**	**16.5**	**1.3**
EU-28	**2032485**	**1737192**	**85.5**	**370769**	**18.2**	**14.5**	**36.5**	**30.7**	**16.9**	**1.4**
France over 45N	259931	259197	99.7	409	0.2	0.3	87.4	12.2	0.2	
France below 45N	67779	67779	100	8528	12.6	89.0	11.0			
Kosovo*	4438	4438	100	14	0.3			99.7	0.3	
Serbia (excl. Kosovo*)	44201	44201	100	66	0.1		16.6	83.2	0.1	
Northern	198097	75203	38.0			62.0	37.9	0.0		
North-western	490547	307439	62.7	409	0.1	37.3	55.6	7.0	0.1	
Central & Eastern	770734	770521	100	50764	6.6	0.0	39.9	53.5	6.6	0.0
Southern	690363	685428	99.3	332292	48.1	0.7	14.0	37.1	44.1	4.1

*) under the UN Security Council Resolution 1244/99

Note 1: Countries not included due to the lack of land cover data: Andorra, Turkey.
Note 2: The percentage value "0.0" indicates an exposed agricultural area exists, but is small and estimated less than 0.05 %. Empty cells mean: no agricultural area in exposure.

Table 4.4 Forested area exposure and exceedance, ozone indicator AOT40 for forests, 2014

Country	Forested area, 2014					Percentage of forested area, 2014 [%]				
	Total area	> CL (10 000 µg.m^{-3}.h)		> RV (20 000 µg.m^{-3}.h)		< 10 000	10 000 - 20 000	20 000 - 30 000	30 000 - 50 000	> 50 000
	[km^2]	[km^2]	[%]	[km^2]	[%]	mg.m^{-3}.h	mg.m^{-3}.h	mg.m^{-3}.h	mg.m^{-3}.h	mg.m^{-3}.h
Albania	7589	7589	100	7589	100			56.2	43.8	
Austria	37223	37223	100	35311	94.9		5.1	83.6	11.3	
Belgium	6092	5907	97.0			3.0	97.0			
Bosnia-Herzegovina	22806	22806	100	21209	93.0		7.0	90.1	2.9	
Bulgaria	34635	34635	100	33154	95.7		4.3	94.5	1.2	
Croatia	20094	20094	100	15018	74.7		25.3	62.7	12.0	
Cyprus	1535	1535	100	1535	100			1.7	98.3	
Czech Republic	26092	26092	100	26053	99.8		0.2	99.8		
Denmark (no Faroes)	3731	3731	100	8	0.2		99.8	0.2		
Estonia	20559	3657	17.8			82.2	17.8			
Finland	194003	458	0.2			99.8	0.2			
France (metropolitan)	141881	141107	99.5	51954	36.6	0.5	62.8	26.5	10.1	
Germany	104143	104143	100	57398	55.1		44.9	55.1	0.1	
Greece (CLC2000)	23562	23562	100	23533	99.9		0.1	27.6	72.0	0.3
Hungary	17520	17520	100	16010	91.4		8.6	91.4		
Iceland	318					100.0				
Ireland	2835					100.0				
Italy	78246	78246	100	78246	100			26.8	72.5	0.7
Latvia	26158	21468	82.1			17.9	82.1			
Liechtenstein	85	85	100	83	97.6		2.4	97.6		
Lithuania	18728	18728	100				100.0			
Luxembourg	931	931	100				100.0			
Macedonia, FYR of	8232	8232	100	8232	100			62.1	37.9	
Malta	2	2	100	2	100				100.0	
Monaco	0.44	0.44	100	0.44	100				100.0	
Montenegro	5736	5736	100	5736	100			74.8	25.2	
Netherlands	3100	2487	80.2			19.8	80.2			
Norway	103846	41180	39.7	0	0.0	60.3	39.7	0.0		
Poland	93919	93919	100	24042	25.6		74.4	25.6		
Portugal (excl. Az., Mad.)	20132	19802	98.4	2179	10.8	1.6	87.5	10.8		
Romania	69989	69989	100	31064	44.4		55.6	44.3	0.1	
San Marino	6	6	100	6	100				100.0	
Serbia (incl. Kosovo)	26875	26875	100	24260	90.3		9.7	89.8	0.4	
Slovakia	19683	19683	100	18922	96.1		3.9	96.1		
Slovenia	11471	11471	100	11471	100.0		0.0	82.3	17.7	
Spain (excl. Canarias)	90274	87449	96.9	68243	75.6	3.1	21.3	31.7	43.7	0.2
Sweden	243521	66526	27.3			72.7	27.3			
Switzerland	12530	12530	100	11701	93		6.6	68.0	25.3	0.0
United Kingd. (& Man)	20056	55	0.3			89.0	11.0			
Total	**1518137**	**1035457**	**68.2**	**572956**	**37.7**	**31.8**	**30.5**	**27.8**	**9.9**	**0.0**
EU-28	**1330081**	**910420**	**68.4**	**494141**	**37.2**	**31.6**	**31.3**	**26.7**	**10.4**	**0.1**
France over 45N	88005	87231	99.1	16683	19.0	0.9	80.2	18.0	1.0	
France below 45N	53876	53876	100	35271	65.5	89.0	11.0			
Kosovo*	4292	4292	100	4283	100		0.2	97.0	2.7	
Serbia (excl.Kosovo)*	22583	22583	100	19977	88.5		11.5	88.5		
Northern	610546	155748	25.5	8	0.0	74.5	25.5	0.0		
North-western	121336	96609	79.6	16683	13.7	20.4	65.9	13.1	0.7	
Central & Eastern	415821	415821	100	253736	61.0		39.0	59.1	1.9	0.0
Southern	370434	367280	99.1	302529	81.7	0.9	17.5	43.3	38.1	0.2

*) under the UN Security Council Resolution 1244/99

Note 1: Countries not included due to the lack of land cover data: Andorra, Turkey.
Note 2: The percentage value "0.0" indicates an exposed forested area exists, but is small and estimated less than 0.05 %. Empty cells mean: no forested area in exposure.

Table 4.4 gives the absolute and relative forest area where the Critical Level (CL) as defined in UNECE (2004) and the value 20 000 µg.m^{-3}.h (which is equal to the earlier used Reporting Value, RV, as was defined in the repealed ozone directive 2002/3/EC) are exceeded.

Next to the forest area in exceedance, Table 4.4 presents the frequency distribution of the forest area over the exposure classes.

The Critical Level was exceeded in 2014 at about 68 % of all European forested area which is within the range of exceedances between 62 – 69 % as observed for the years 2009 – 2012 (Table 6.4). As in previous years, most countries continue to have in 2014 considerable forest areas in excess to the CL, with specifically almost all forest area in central, eastern and southern European countries.

In this context, it should be mentioned that the AOT40 indicator probably is not the best proxy for the vegetation damage. E.g., it does not take into account that the Mediterranean vegetation closes its stomata in the warmest and driest season protecting itself from the exposure to ozone. A flux approach – as done e.g. in the EMEP model – taking into account the reduced deposition when stomata are closed would be better. However, there is still a damage to Mediterranean forests – e.g. the Aleppo pine in the southern France seems to be quite sensitive to ozone exposure and suffering damage, UNECE (2016).

5 NO_2 and NO_x

Annual average maps for NO_2 (related to protection of health) and for NO_x (related to protection of vegetation) have been produced and are presented in the regular mapping report for the first time.

The methodology for creating the concentration maps follows the same principle as for the rest of pollutants: a linear regression model on the basis of European wide station measurement data, followed by kriging of the residuals produced from that regression model (residual kriging).

The maps on NO_2 are created for the rural and urban background areas separately on a grid at 10x10 km resolution. Subsequently, these rural and urban background maps are merged into one combined air quality indicator map using a population density grid at 1x1 km resolution. We present this final combined map in this 1x1 km grid resolution. It should be noted that this map refers to background areas only, as hotspot and traffic locations are not taken into consideration. The exposure table for NO_2 has been calculated and is presented in this report for the first time.

The map of the vegetation-related indicator NO_x annual average is created on a grid at 2x2 km resolution, based on rural background measurements only, as vegetation is considered not to be extensively present at urban and suburban areas. Hence, this map is applicable to rural areas only. The resolution is chosen equally to the one of the vegetation indicator for ozone.

Annex 3 provides details on the regression and kriging parameters applied for deriving the maps, as well as the uncertainty analysis of the maps.

5.1 NO_2 – Annual mean

5.1.1 Concentration map

The Ambient Air Quality Directive (EU, 2008) sets the Limit Value (LV) for the NO_2 annual average at the level of 40 $\mu g.m^{-3}$. This is the same concentration level as recommended by the World Health Organization for the NO_2 annual average as the Air Quality Guideline (WHO, 2005).

Map 5.1 presents the final combined concentration 1x1 km gridded map for the 2014 NO_2 annual average as the result of interpolation and merging of the separate maps as described in Annex 1.

Supplementary data used in the linear regression are in principle the same as in Horálek et al. (2014): for rural areas they consist of EMEP model output, altitude and wind speed; for urban background areas the EMEP model output and wind speed are supplemented with population density (Annex 3).

The most of the European area shows NO_2 levels below 20 $\mu g.m^{-3}$, with most of the rural areas below 10 $\mu g.m^{-3}$. Some areas above 20 $\mu g.m^{-3}$ can be found in the Po valley, the Benelux, the German Ruhr region and in central and southern England. According to the measurements from monitoring stations, the Limit Value (LV) of 40 $\mu g.m^{-3}$ is exceeded specifically in several large agglomerations all over Europe. However, it should be noted that the interpolated map refers to the rural and urban *background* situations only, while the exceedances of the NO_2 limit values occur mostly at local *hotspots* such as densely urbanised and industrialised areas, and dense traffic locations.

The relative mean uncertainty of the NO_2 annual average map is 44 % for rural and 26 % for urban areas (Annex 3).

In order to provide more complete information of the air quality across Europe, the final combined map including the measurement data at station points is presented in Map A5.8 of Annex 5.

Map 5.1 Concentration map of NO_2 annual average, 2014

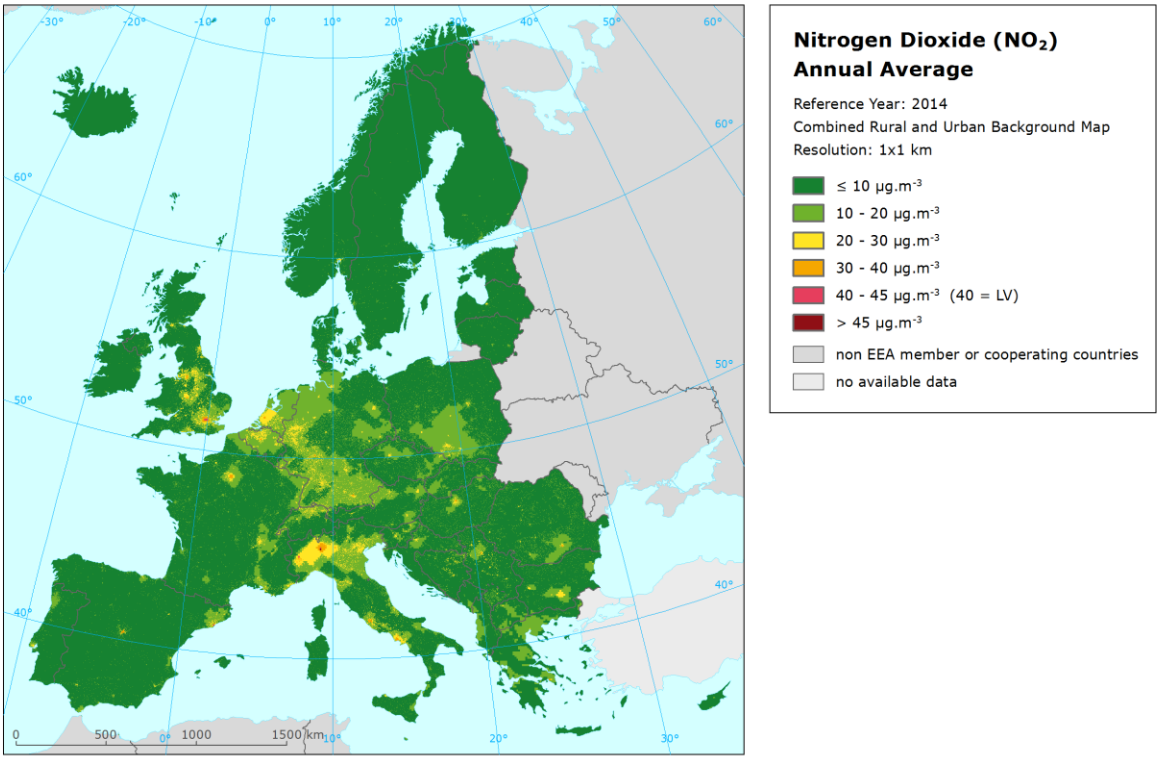

5.1.2 Population exposure

Table 5.1 gives the population frequency distribution for a limited number of exposure classes calculated on a grid of 1x1 km resolution, as well as the population-weighted concentration for individual countries and for Europe as a whole according to Equation A1.5 of Annex 1.

The human exposure to NO_2 has been calculated and is presented in this report for the first time. It should be mentioned that – as for other pollutants – the population exposure refer to the rural and urban *background* areas only. However, the high concentration levels of NO_2 do occur mostly on a local scale at, so called, *hotspots* and traffic locations, which are not resolved by this type of exposure estimate.

It has been estimated that in 2014 about 1 % of the European population and also the EU-28 population lived in areas with NO_2 annual average concentrations above the EU limit value of 40 µg.m^{-3}. CSI004 (EEA, 2016c) estimates that about 7 % of the population in urban agglomerations in the EU-28 was exposed in 2014 to levels above the EU limit value. The difference with the estimated 1 % in Table 5.1 is mainly because the EEA accounts for the urban population in the agglomerations only (where, as pointed out above, hotspots are most frequent). Whereas, Table 5.1 provides estimates, including the population in rural areas, smaller cities and villages.

The European-wide population-weighted concentration of the NO_2 annual average for 2014 is estimated to be about 19 µg.m^{-3}, the same as for the EU28 only.

As is stated above, the presented population exposure refer to people living in the rural and urban background areas only, assuming the most of the population live just in these background areas. However, in order to improve the assessment of the population exposed to excessive levels of NO_2, the mapping methodology should be in future improved by accounting for the NO_2 hotspots. It concerns local air pollution caused by intensive human activities and specifically traffic. Such improvement effort is currently executed by the ETC/ACM in parallel to this report. It focusses on mapping and exposure assessment for local traffic conditions in addition to the background concentrations.

Table 5.1 Population exposure and population-weighted concentration, NO_2 annual average, 2014

Country		Population [inhbs . 1000]	NO_2 annual average, exposed population [%]						Population weighted conc. [μg.m^{-3}]
			< LV				> LV		
			< 10 μg.m^{-3}	10 - 20 μg.m^{-3}	20 - 30 μg.m^{-3}	30 - 40 μg.m^{-3}	40 - 45 μg.m^{-3}	> 45 μg.m^{-3}	
Albania	AL	2 896	11.2	88.8					14.2
Andorra	AD	73	1.8	98.2					15.4
Austria	AT	8 507	11.7	46.2	42.1				18.1
Belgium	BE	11 204	1.3	38.5	52.0	8.3			21.3
Bosnia & Herzegovina	BA	3 831	18.3	41.3	40.4				17.0
Bulgaria	BG	7 246	9.5	64.9	25.6				16.4
Croatia	HR	4 247	16.1	61.2	22.7				16.4
Cyprus	CY	858	65.9	34.1					9.2
Czech Republic	CZ	10 512	9.5	77.1	13.4				16.9
Denmark	DK	5 627	25.7	74.3					11.9
Estonia	EE	1 316	31.0	69.0					10.2
Finland	FI	5 451	56.7	43.3					9.0
France (metropolitan)	FR	63 989	19.4	53.2	19.3	8.1			17.2
Germany	DE	80 767	3.1	42.1	53.2	1.6			20.1
Greece	GR	10 927	26.5	50.1	10.7	12.6			15.0
Hungary	HU	9 877	7.2	69.9	15.9	7.0			17.3
Iceland	IS	326	13.2	86.2	0.7				13.7
Ireland	IE	4 606	58.1	41.9					8.6
Italy	IT	60 783	5.1	35.4	42.9	13.0	1.9	1.7	22.7
Latvia	LV	2 001	28.2	53.3	18.6				12.5
Liechtenstein	LI	37	3.9	11.9	84.3				19.3
Lithuania	LT	2 943	30.4	69.6					11.4
Luxembourg	LU	550	3.0	33.0	64.0				19.5
Macedonia, FYROM of	MK	2 066	2.3	83.6	14.1				17.0
Malta	MT	425	3.2	96.8					12.8
Monaco	MC	38			100				21.3
Montenegro	ME	622	16.9	83.1					15.8
Netherlands	NL	16 829	0.2	36.7	60.1	3.1			21.6
Norway	NO	5 108	31.7	46.4	21.9				13.7
Poland	PL	38 018	16.5	66.6	16.9				15.2
Portugal (excl. Az., Mad.)	PT	9 922	29.3	57.6	13.1				12.8
Romania	RO	19 947	13.7	68.6	11.8	5.9			16.7
San Marino	SM	33	4.0	96.0					16.5
Serbia (incl. Kosovo*)	RS	7 147	10.6	41.9	40.7	6.9			19.8
Slovakia	SK	5 416	7.8	92.2					15.2
Slovenia	SI	2 061	15.9	50.6	33.5				16.4
Spain (excl. Canarias)	ES	44 397	8.5	59.1	21.1	8.2	3.1		18.9
Sweden	SE	9 645	31.9	68.1					10.8
Switzerland	CH	8 140	4.8	35.9	59.3				20.2
United Kingdom (& dep.)	UK	64 351	5.7	25.9	55.0	10.1	3.2		23.0
Total		**532 738**	**11.7**	**49.0**	**32.8**	**5.6**	**0.9**	**0.2**	**18.6**
			98.9				**1.1**		
EU-28		**502 424**	**11.5**	**49.0**	**32.6**	**5.8**	**0.9**	**0.2**	**18.7**
			98.9				**1.1**		
Kosovo*	KS	1 821	10.1	83.3	6.6				16.5
Serbia (excl. Kosovo*)	RS	7 147	10.7	31.8	49.0	8.5			20.6

*) under the UN Security Council Resolution 1244/99

Note 1: Turkey is not included in the calculation due to the lack of air quality data.
Note 2: Empty cells mean: no population in exposure.

5.2 NO_x – Annual mean

5.2.1 Concentration map

The AQ Directive (EU, 2008) sets a Critical Level (CL) for the protection of vegetation for the NO_x annual mean at 30 µg.m^{-3}. According to this directive, the sampling points targeted at the protection of vegetation and natural ecosystems shall be in general sited more than 20 km away from agglomerations or more than 5 km away from other built-up areas. Thus, the observations at rural background stations only are used for the NO_x mapping and the resulting map is representative for rural areas only.

The number of NO_x measurement stations is limited and some countries (e.g. Belgium, France) did not report NO_x measurement data for 2014. The mapping of the NO_x annual average is therefore performed on the basis of an approach presented in Horálek et al. (2007). This approach derives additional *pseudo* NO_x annual mean concentrations from NO_2 annual mean measurement concentrations and increases as such the number and spatial coverage of NO_x 'data points', and applies these data to the NO_x mapping. Section A1.1 of Annex 1 provides some details

Map 5.2 presents the concentration map of NO_x annual average. It concerns rural areas only, representing an indicator for vegetation exposure to NO_x. The supplementary data used are the same as in Horálek et al. (2014), i.e. EMEP model, altitude and wind speed.

Map 5.2 Concentration map of NO_x annual average, rural map, 2014

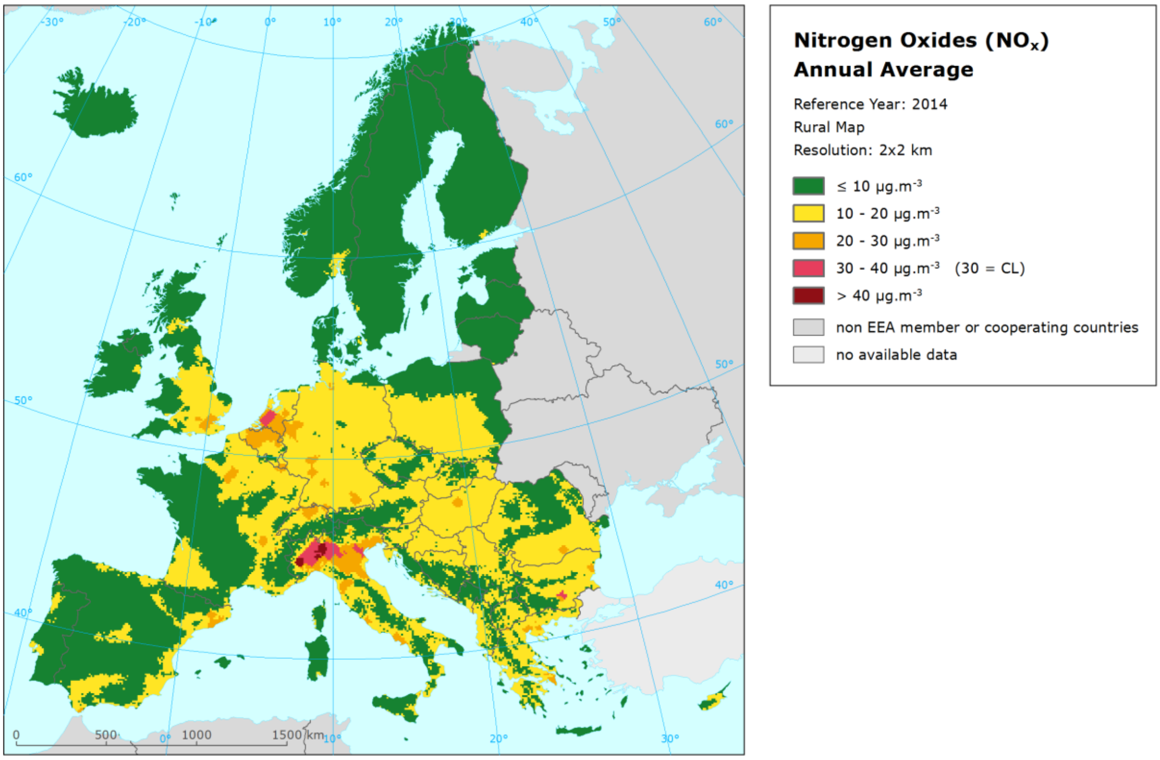

Most of the European area shows NO_x levels below 20 µg.m^{-3}. However, at the Po valley, the western part of the Netherlands and around Haskovo in Bulgaria elevated NO_x concentrations above the Critical Level (CL) are observed. Furthermore, around many larger European cities, typically often being the national capital, concentrations just below the CL are observed. These concentrations are expected to be the result of large emissions from transport in and around the cities, as well as energy production and industrial facilities taking place at these areas. However, this is relevant only if there is vegetation around those larger cities.

The NO_x annual average rural map has a relative mean uncertainty of 47 %.

The NO_x annual average rural map including the data measured at rural background stations is presented in Map A5.9 of Annex 5. The map illustrates the lack of the NO_x rural stations in the Balkan area.

Vegetation exposure is not calculated for NO_x, as the critical level (CL) applies actually to vegetation only, which is by nature mostly allocated in rural areas where there is little CL exceedance observed. Therefore, the vegetation exposure exceedance would occur in limited vegetation areas only and, as such, is considered not to provide relevant information from the European scale perspective. Furthermore, contrary to vegetation exposure to high ozone concentrations in Europe that leads to considerable damage, vegetation exposure to NO_x pollution is of minor importance in terms of actual impacts. On the other hand, NO_x concentrations lead to NO_x deposition, which have acidifying and eutrophying effects on vegetation and is still very important in Europe. However, these effects on vegetation cannot be easily expressed by an exposure table.

Concerning the potential NO_x vegetation and natural ecosystems exposure estimate there is an additional dilemma: which receptor types should be selected to estimate the exposure and critical level exceedance of vegetation and natural ecosystems? An option would be the use of CLC classes (e.g. like in Horálek et al., 2008), nevertheless this classification is too general. Other option would be the NATURA2000 database. However, that source contains a wide series of receptor types, species and classes. It would need serious additional resources to conclude on the most relevant set of receptors from the NATURA 2000 geographical database. Besides, the yet large uncertainty of the NO_x concentration map in general, and the lack of NO_x stations in the Balkan region do not allow for good quality exposure exceedance estimates at national scale. As a compromise we could derive some exposure numbers for Europe as a whole only like in Horálek et al. (2014), but, as already pointed out, there is still a need to define which representative receptors should be used for exposure estimates of vegetation and natural ecosystems.

6 Exposure trend estimates

6.1 Mapping and exposure results

This paper has presented the interpolated maps for 2014 on the PM_{10}, $PM_{2.5}$, ozone and NO_2 *human health* related air pollution indicators. It has showed the maps of annual average and the 90.4 percentile of PM_{10} daily mean(s), annual average for $PM_{2.5}$, the 93.2 percentile of maximum daily 8-hour value(s) and the SOMO35 for ozone, together with the frequency distribution of the estimated population exposures and exceedances. Next to this, the map of the human health indicator annual average for NO_2 has been presented. However, in this report no exposure estimates are made for this indicator.

Furthermore, interpolated maps on ozone and NO_x *vegetation* related air pollution indicators have been produced. These have been the maps of ozone indicators AOT40 for vegetation and AOT40 for forests, including their frequency distribution of estimated land area exposures and exceedances. In addition, the map of the annual average for NO_x has been produced, but without exposure estimates.

A mapping approach similar to previous years (De Smet et al. 2011 and references cited therein, Denby et al. 2011b) based primarily on observational data was used. With the interpolated air pollution maps and exposure estimates for the year 2014, a ten-year overview on comparable exposure estimates was obtained. In this chapter we provide such ten-year overviews of exposure estimates for each of the indicators of PM_{10}, $PM_{2.5}$ and ozone. The trend analysis is provided in Annex 4.

Maps for the nitrogen related indicators were not produced on a multi-annual basis and therefore no time series are given in this chapter.

For the human health indicators, we express the exposure estimates on the one hand as the population-weighted concentration and on the other hand as the percentage of population exposed to concentrations above the limit/target values. For the vegetation related indicators, the exposure estimates are expressed as the agricultural or forest areas exposed to concentrations above defined thresholds.

It should be noted that the percentage of population exposed is less robust indicator compared to a population weighted concentration, as a small concentration increase (or decrease) can lead into a major increase (or decrease) of the population exposed. Thus, the trend analysis is done for the population weighted concentrations only.

When thinking about a trend, we should take into account (i) the meteorologically induced variations, (ii) the uncertainties involved in the interpolation (Annex 3), and (iii) the station densities and their spatial distributions over the European regions. Next to this, we should be aware that different trends in various parts of Europe may take place. However, bearing in mind these limitations we provide here and in Annex 4 for the first time a trend analysis for the period 2005 – 2014 on the population-weighted concentrations for individual countries and for Europe as a whole.

6.1.1 Human health PM_{10} indicators

Table 6.1 summarises over the ten year period 2005 – 2014 for both *human health PM_{10} indicators* the average concentration to which the European population is exposed to, expressed as the population-weighted concentration and the percentage of population exposed to PM_{10} concentrations above the limit values (LV).

In 2014 the population exposed to *annual mean* concentrations of PM_{10} above the limit value of 40 $\mu g.m^{-3}$ is at least 2.0 % of the total population, which is somewhat less than in 2013 and the smallest percentage in the time series. Furthermore, it is estimated that European inhabitants living in background (neither hot-spot nor industrial) areas –regardless if these areas are urban or rural – are exposed on average to an annual mean PM_{10} concentration of 21 µg.m^{-3}.

Table 6.1 Population-weighted concentration and percentage of the European population exposed to concentrations above the PM_{10} limit values (LV) for the protection of health for 2005 to 2014

PM_{10}			2005	2006	2007	2008	2009	2010	2011	2012	2013	2014
Annual average												
Population-weighted concentratio	[µg.m^{-3}]		28.0	28.5	26.2	24.8	24.6	24.3	22.1	22.7	22.2	21.1
Population exposed > LV (40 µg.m	[%]		13.3	10.3	6.8	5.8	6.0	5.2	2.5	3.4	2.6	2.0
36th highest daily mean / 90.4 percentile of daily means												
Population-weighted concentratio	[µg.m^{-3}]	36th highest d. m.	46.8	47.8	44.1	41.3	41.2	41.9	39.0	39.7	38.6	
Population-weighted concentratio	[µg.m^{-3}]	90.4 perc. of d. m.								40.6	39.4	37.1
Population exposed > LV (50 µg.m	[%]	36th highest d. m.	34.3	35.7	26.2	19.4	16.5	20.6	15.8	16.5	16.4	
Population exposed > LV (50 µg.m	[%]	90.4 perc. of d. m.								17.7	17.3	13.3

In comparison with the previous nine years, the number of people living in areas with concentrations above the LV is the lowest in 2014. The overall picture of the population-weighted concentration of the European totals (i.e. totals of 40 European countries considered) demonstrates a downward trend of -0.8 for the years 2005 – 2014 (Annex 4). This trend is statistically significant and expresses a mean decrease of 0.8 µg.m^{-3} per year.

In 2014 at least some 13 % of the European population lived in areas where the PM_{10} daily limit value (calculated using the *90.4 percentile*) was exceeded, being less than in previous years. The overall European population-weighted concentration of the 90.4 percentile of the PM_{10} daily means (formerly the 36th highest daily mean) for the background areas is estimated to be at least 37 µg.m^{-3} in 2014, which is the lowest in the ten years considered. The population-weighted concentration of the European totals (i.e. totals of 40 European countries considered) in Annex 4 demonstrate a downward trend of -1.0 for the years 2005 – 2014, which is statistically significant and expresses a mean decrease of 1.0 µg.m^{-3} per year.

For years 2012 and 2013 both the 36th highest value and the 90.4 percentile of daily mean(s) have been calculated. Their results demonstrate an underestimation of almost 1 µg.m^{-3} at the 36th highest daily mean. One may conclude that this underestimation has its cause in the fact that when calculating the 36th highest daily mean value there is no correction for the missing values in incomplete time series. Whereas the 90.4 percentile of daily mean(s) adjusts for such missing data.

Bearing in mind the above mentioned underestimation of the 36th highest daily mean, it should be emphasized that the population-weighted concentration in 2014 is the lowest of the ten years period 2005 – 2014, even if the 90.4 percentile of the PM_{10} daily means has been used in the 2014 calculation.

6.1.2 Human health $PM_{2.5}$ indicator

Table 6.2 summarises for *human health $PM_{2.5}$ indicator* (annual average) the population-weighted concentration and the percentage of European population exposed to $PM_{2.5}$ concentrations above the EU target value (TV) for the years 2007 to 2014 (without 2009, for which neither a map nor a population exposure was prepared).

Table 6.2 Population-weighted concentration and percentage of the European population exposed to concentrations above the $PM_{2.5}$ target value (TV) for the protection of health for 2007 to 2014

$PM_{2.5}$		2007	2008	2009	2010	2011	2012	2013	2014
Annual average									
Population-weighted concentration	[µg.m^{-3}]	16.3	16.3	not mapped	16.8	15.9	15.6	15.3	14.1
Population exposed > TV (25 µg.m^{-3})	[%]	7.8	7.6		8.3	6.2	9.0	5.8	4.2

The percentage of population exposed in 2014 to annual mean concentrations of $PM_{2.5}$ above the target value (TV) of 25 µg.m^{-3} is about 4 %, which is the lowest in the limited time series. Furthermore, it is estimated that European inhabitants living in background (neither hot-spot, nor industrial) areas – regardless if these areas are urban or rural – are exposed on average to an annual mean $PM_{2.5}$ concentration of about 14 µg.m^{-3}, again the lowest in the time series.

Annex 4 provides the trend analysis of the population-weighted concentrations across the period 2007 – 2014 for individual countries and for Europe as a whole. At European scale a slightly downward trend can be observed, estimated to be -0.3, which means a decrease in the population-weighted concentration of 0.3 µg.m^{-3} per year.

This means that over the years both the population-weighted concentration and the percentage of people living above the TV seem to decrease slightly.

6.1.3 Human health ozone indicators

Table 6.3 summarises for both *human health ozone indicators* the exposure levels of the European inhabitants in terms of population-weighted concentrations. Furthermore, it presents the percentage of European population exposed to concentrations above the target value (TV) threshold and above a level of 6 000 µg.m^{-3}.d for the SOMO35 for the years 2005 to 2014.

Table 6.3 Population-weighted concentration and percentage of the European population exposed to concentrations above the target value (TV) threshold for the protection of health and a SOMO35 threshold of 6 000 µg.m^{-3}.d for 2005 to 2014

Ozone		2005	2006	2007	2008	2009	2010	2011	2012	2013	2014
26th highest daily max. 8-h mean / 93.2 percentile of daily max. 8-h means											
Popul.-weighted concentr. [µg.m^{-3}]	26th highest d. max8h	112.1	118.2	110.7	109.8	108.1	106.8	108.9	107.9	108.3	
Popul.-weighted concentr. [µg.m^{-3}]	93.2 perc. of d. max8h								108.5	108.9	102.9
Popul. exposed > TV (120 µg.m^{-3}) [%]	26th highest d. max8h	31.6	51.4	27.1	15.0	16.0	16.3	16.5	20.7	15.0	
Popul. exposed > TV (120 µg.m^{-3}) [%]	93.2 perc. of d. max8h								21.9	15.9	5.6
SOMO35											
Popul.-weighted concentration	[µg.m^{-3}.d]	4706	5167	4411	4275	4275	3917	4414	4279	4088	3500
Popul. exposed > 6000 µg.m^{-3}.d	[%]	27.0	29.5	28.1	19.6	24.6	16.6	23.6	24.5	18.8	9.4

The table presents the results obtained with the 1x1 km merging resolution as tested on the 2006 data in Horálek et al (2010), then recomputed for 2005 and 2007, and finally implemented fully on the 2008 data and onwards.

Using the *93.2 percentile of ozone maximum daily 8-hour means* it is estimated that almost 6 % of the population lived in 2014 in areas where concentrations were above the ozone target value (TV) threshold of 120 µg.m^{-3}, which is considerably lower than in the previous nine years. The overall European population-weighted ozone concentration in terms of the 93.2 percentile maximum daily 8-

hour means in the background areas is estimated at about 103 µg.m^{-3}, which is the lowest value of the whole ten years period (please be aware that for 2005–2011 the 26th highest value of the maximum daily eight-hour mean was considered instead).

For 2012 and 2013 both the 26th highest value and the 93.2nd percentile of maximum daily 8-hour mean(s) have been calculated. It demonstrates an underestimation of about 0.6 µg.m^{-3} at the 26th maximum daily 8-hour mean, which is caused by the fact that when calculating this indicator there is no correction for the missing values in the incomplete measurement time series.

Examining the time series 2005 – 2014, it can be concluded that 2006 is an exceptional year with elevated ozone concentrations, leading to increased exposure levels compared to the other nine years. In 2006, a relative long warm summer period induced long lasting elevated ozone concentration levels all over Europe. Additionally, the population exposed to ozone levels above the target value threshold in the period 2008 – 2014 is lower than in the preceding period of 2005 – 2007.

Annex 4 presents some details on the trend analysis of the population-weighted concentrations across the period 2005 – 2014 for individual countries and for Europe as a whole. The population-weighted concentration of the European totals (i.e. totals of 40 European countries considered) demonstrates a downward trend of -1.0 that is statistically significant and expresses a mean decrease of about 1 µg.m^{-3} per year.

A similar tendency is observed for the *SOMO35*: In 2006 – 2007 almost one-third of the population lived in areas where a level of 6 000 µg.m^{-3}.d[1] was exceeded, with the highest level in 2006. In the period of 2008 – 2013 it fluctuates from about 19 % to 25 % of the population, while in 2014 it is about 9 % of the population. The population-weighted SOMO35 concentrations show a quite similar kind of pattern over time. Trend analysis in Annex 4 on the population-weighted concentration of the European totals shows a slightly downward trend of about -134, for the period 2005 – 2014, which is statistically significant and expresses a mean decrease of about 134 µg.m^{-3}·d per year.

6.1.4 Vegetation and forest ozone indicators

Exposure indicators describing the *agricultural and forest areas exposed to accumulated ozone* concentrations above defined thresholds are summarised in Table 6.4. Those thresholds are the target value (TV) threshold of 18 000 µg.m^{-3}.h and the long-term objective (LTO) of 6 000 µg.m^{-3}.h for the AOT40 for vegetation, and the former Reporting Value (RV) of 20 000 µg.m^{-3}.h and the Critical Level (CL) of 10 000 µg.m^{-3}.h for the AOT40 for forests.

[1] Note that the 6 000 µg.m^{-3}.d does not represent a health-related legally binding 'threshold'. In this and previous papers it concerns a somewhat arbitrarily chosen threshold to facilitate the discussion of the observed distributions of SOMO35 levels in their spatial and temporal context. For motivation of this choice, see Section 4.2.

Table 6.4 Percentages of the European agricultural and forest area exposed to ozone concentrations above the target value (TV) threshold and the long-term objective (LTO) for AOT40 for vegetation, and above Critical Level (CL) and Reporting Value (RV) for AOT40 for forests for 2005 to 2014

Ozone		2005	2006	2007	2008	2009	2010	2011	2012	2013	2014
AOT40 for vegetation											
Agricultural area % > TV (18 000 µg.m^{-3}.	[%]	48.5	69.1	35.7	37.8	26.0	21.3	19.2	30.0	22.1	17.8
Agricultural area % > LTO (6 000 µg.m^{-3}.l	[%]	88.8	97.6	77.5	95.5	81.0	85.4	87.9	86.4	81.0	85.5
AOT40 for forests											
Forest area exposed > RV (20 000 µg.m^{-3}.	[%]	59.1	69.4	48.4	50.2	49.2	49.3	53.0	47.2	44.1	37.7
Forest area exposed > CL (10 000 µg.m^{-3}.	[%]	76.4	99.8	62.1	79.6	67.4	63.4	68.6	65.0	67.2	68.2

In 2014, some 18 % of all agricultural land (*crops*) was exposed to accumulated ozone concentrations (AOT40 for vegetation) exceeding the target value (TV) threshold, which is the lowest percentage of the whole ten years period. Almost 86 % of all agricultural land (crops) was exposed to levels in excess of the long-term objective (LTO), which is within the range of 81 – 89 % as observed at most of the years.

For the ozone indicator AOT40 for *forests* the level of 20 000 µg.m^{-3}.h (earlier used Reporting Value, RV) was exceeded in about 38 % of the European forest area in 2014, which is the lowest of the whole time series and clearly below the percentages of the years 2005 – 2013. The forest area exceeding the Critical Level (CL) was in 2014 about 68 %, which is within the range of exceedances between 62 – 69 % as observed for the years 2007 and 2009 – 2012 and well below the exceedances of 2005 and 2008 (with 76 – 80 %) and 2006 where all forest areas were exposed to concentrations exceeding the CL.

The temporal pattern of the AOT40 for forests exceedances shows some similarity with those of the AOT40 for vegetation, despite their different definitions and receptors. Their annual variability is, however, heavily dependent on meteorological variability.

References

Cressie N (1993). Statistics for spatial data. Wiley series, New York.

Danielson JJ, Gesch DB (2011). Global multi-resolution terrain elevation data 2010 (GMTED2010): U.S. Geological Survey Open-File Report 2011–1073. https://lta.cr.usgs.gov/GMTED2010

De Leeuw F (2012). AirBase: a valuable tool in air quality assessments at a European and local level. ETC/ACM Technical Paper 2012/4.
http://acm.eionet.europa.eu/reports/ETCACM_TP_2012_4_AirBase_AQassessment

Denby B, Schaap M, Segers A, Builtjes P, Horálek J (2008). Comparison of two data assimilation methods for assessing PM_{10} exceedances on the European scale. Atmospheric Environment 42, 7122–7134.

Denby B, Gola G, De Leeuw F, De Smet P, Horálek J (2011a). Calculation of pseudo $PM_{2.5}$ annual mean concentrations in Europe based on annual mean PM10 concentrations and other supplementary data. ETC/ACC Technical Paper 2010/9.
http://acm.eionet.europa.eu/reports/ETCACC_TP_2010_9_pseudo_PM2.5_stations

Denby B, Horálek J, de Smet P, de Leeuw F (2011b). Mapping annual mean $PM_{2.5}$ concentrations in Europe: application of pseudo $PM_{2.5}$ station data. ETC/ACM Technical Paper 2011/5.
http://acm.eionet.europa.eu/reports/ETCACM_TP_2011_5_spatialPM2.5mapping

De Smet P, Horálek J, Coňková M, Kurfürst P, de Leeuw F, Denby B (2009). European air quality maps of ozone and PM_{10} for 2006 and their uncertainty analysis. ETC/ACC Technical Paper 2008/8.
http://acm.eionet.europa.eu/reports/ETCACC_TP_2008_8_spatAQmaps_2006

De Smet P, Horálek J, Coňková M, Kurfürst P, de Leeuw F, Denby B (2010). European air quality maps of ozone and PM_{10} for 2007 and their uncertainty analysis. ETC/ACC Technical Paper 2009/9.
http://acm.eionet.europa.eu/reports/ETCACC_TP_2009_9_spatAQmaps_2007

De Smet P, Horálek J, Coňková M, Kurfürst P, de Leeuw F, Denby B (2011). European air quality maps of ozone and PM_{10} for 2008 and their uncertainty analysis. ETC/ACC Technical Paper 2010/10.
http://acm.eionet.europa.eu/reports/ETCACC_TP_2010_10_spatAQmaps_2008

EC (2008). Directive 2008/50/EC of the European Parliament and of the Council of 21 May 2008 on ambient air quality and cleaner air for Europe. OJ L 152, 11.06.2008, 1-44.
http://eur-lex.europa.eu/LexUriServ/LexUriServ.do?uri=OJ:L:2008:152:0001:0044:EN:PDF

ECMWF: Meteorological Archival and Retrieval System (MARS). http://www.ecmwf.int/

EEA (2008). ORNL Landscan 2008 Global Population Data conversion into EEA ETRS89-LAEA5210 1km grid (eea_r_3035_1_km_landscan-eurmed_2008, by Hermann Peifer of EEA).

EEA (2011). Guide for EEA map layout. EEA operational guidelines. August 2011, version 4.
http://www.eionet.europa.eu/gis/docs/GISguide_v4_EEA_Layout_for_map_production.pdf

EEA (2013a). Corine land cover 2000 (CLC2000) raster data. 100x100m gridded version 17 (12/2013). http://www.eea.europa.eu/data-and-maps/data/corine-land-cover-2000-raster-3

EEA (2013b). Corine land cover 2006 (CLC2006) raster data. 100x100m gridded version 17 (12/2013) http://www.eea.europa.eu/data-and-maps/data/corine-land-cover-2006-raster-3

EEA (2016a). Air Quality e-Reporting. Air quality database. http://www.eea.europa.eu/data-and-maps/data/aqereporting-1

EEA (2016b). Air quality in Europe – 2016 Report. EEA Report 28/2016. http://www.eea.europa.eu/publications/air-quality-in-europe-2016

EEA (2016c). Exceedance of air quality limit values in urban areas. CSI004 indicator assessment. http://www.eea.europa.eu/data-and-maps/indicators/exceedance-of-air-quality-limit-3/assessment-2

EEA (2016d). Exposure of ecosystems to acidification, eutrophication and ozone. http://www.eea.europa.eu/data-and-maps/indicators/exposure-of-ecosystems-to-acidification-3/assessment-2

Eurostat (2014). GEOSTAT 2011 grid dataset. Population distribution dataset. http://ec.europa.eu/eurostat/web/gisco/geodata/reference-data/population-distribution-demography

Eurostat (2016). Total population for European states for 2014. http://epp.eurostat.ec.europa.eu/tgm/table.do?tab=table&language=en&pcode=tps00001&tableSelection=1&footnotes=yes&labeling=labels&plugin=1

EMEP (2016). Transboundary particular matter, photo-oxidants, acidifying and eutrophying components. EMEP Report 1/2016. http://emep.int/publ/reports/2016/EMEP_Status_Report_1_2016.pdf

Gilbert, RO (1987). Statistical Methods for Environmental Pollution Monitoring. Van Nostrand Reinhold, New York.

Guerreiro C, Horálek J, de Leeuw F, Couvidat F (2015). Mapping ambient concentrations of benzo(a)pyrene in Europe. ETC/ACM Technical paper 2014/6. http://acm.eionet.europa.eu/reports/ETCACM_TP_2014_6_BaP_HIA

Horálek J, Kurfürst P, Denby B, de Smet P, de Leeuw F, Brabec M, Fiala J (2005). Interpolation and assimilation methods for European scale air quality assessment and mapping. Part II: Development and testing new methodologies. ETC/ACC Technical paper 2005/8. http://acm.eionet.europa.eu/docs/ETCACC_TechnPaper_2005_8_SpatAQ_Part_II.pdf

Horálek J, Denby B, de Smet P, de Leeuw F, Kurfürst P, Swart R, van Noije T (2007). Spatial mapping of air quality for European scale assessment. ETC/ACC Technical paper 2006/6. http://acm.eionet.europa.eu/reports/ETCACC_TechnPaper_2006_6_Spat_AQ

Horálek J, de Smet P, de Leeuw F, Denby B, Kurfürst P, Swart R (2008). European air quality maps for 2005 including uncertainty analysis. ETC/ACC Technical paper 2007/7. http://acm.eionet.europa.eu/reports/ETCACC_TP_2007_7_spatAQmaps_ann_interpol

Horálek J, de Smet P, de Leeuw F, Coňková M, Denby B, Kurfürst P (2010). Methodological improvements on interpolating European air quality maps. ETC/ACC Technical Paper 2009/16. http://acm.eionet.europa.eu/reports/ETCACC_TP_2009_16_Improv_SpatAQmapping

Horálek J, Kurfürst P, de Smet P (2014). Additional 2011 European air quality maps. ETC/ACM Technical Paper 2014/5. http://acm.eionet.europa.eu/reports/ETCACM_TP_2014_5_add_2011_aqmaps

Horálek J, de Smet P, Kurfürst P, de Leeuw F, Benešová N (2015). European air quality maps of PM and ozone for 2012 and their uncertainty. ETC/ACM Technical Paper 2014/4. http://acm.eionet.europa.eu/reports/ETCACM_TP_2014_4_spatAQmaps_2012

Horálek J, Benešová N, de Smet P (2016a). Application of FAIRMODE Delta tool to evaluate interpolated European air quality maps for 2012. ETC/ACM Technical Paper 2015/2. http://acm.eionet.europa.eu/reports/ETCACM_TP_2015_2_Delta_Evaluation_AQMaps2012

Horálek J, de Smet P, Kurfürst P, de Leeuw F, Benešová N (2016b). European air quality maps of PM and ozone for 2013 and their uncertainty. ETC/ACM Technical Paper 2015/5. http://acm.eionet.europa.eu/reports/ETCACM_TP_2015_5_spatAQmaps_2013

Horálek J, Guerreiro C., de Leeuw, de Smet (2017). Potential improvements on benzo(a)pyrene (BaP) mapping. ETC/ACM Technical Paper 2016/3. http://acm.eionet.europa.eu/reports/ETCACM_TP_2016_3_BaP_improved_mapping

IPCC (2010). Guidance note for lead authors of the IPCC Fifth Assessment Report on consistent treatment of uncertainties. Jasper Ridge, USA. http://www.ipcc.ch/pdf/supporting-material/uncertainty-guidance-note.pdf

JRC (2009). Population density disaggregated with Corine land cover 2000. 100x100 m grid resolution, EEA version popu01clcv5.tif of 24 Sep 2009. http://www.eea.europa.eu/data-and-maps/data/population-density-disaggregated-with-corine-land-cover-2000-2

Mareckova K, Pinterits M, Wankmüller R, Tista M (2016). Inventory Review 2016. Review of emission data reported under the LRTAP Convention and NEC Directive. Stage 1 and 2 review & Status of gridded and LPS data. EEA/CEIP Technical Report 1/2016. http://www.ceip.at/review_proces_intro/review_reports

NILU (2016). EBAS, database of atmospheric chemical composition and physical properties (NILU, Norway). http://ebas.nilu.no/

NMI (2016). EMEP/MSC-W modelled air concentrations and depositions. Yearly, monthly, daily and hourly gridded data. http://thredds.met.no/thredds/catalog/data/EMEP/2016_Reporting/catalog.html

ORNL (2008). ORNL LandScan high resolution global population data set. http://www.ornl.gov/sci/landscan/landscan_documentation.shtml

Simpson D, Benedictow A, Berge H, Bergström R, Emberson LD, Fagerli H, Hayman GD, Gauss M, Jonson JE, Jenkin ME, Nyíri A, Richter C, Semeena VS, Tsyro S, Tuovinen J-P, Valdebenito A, Wind P (2012). The EMEP MSC-W chemical transport model – technical description. Atmospheric Chemistry and Physics, 12, 7825–7865, doi:10.5194/acp-12-7825-2012. http://www.atmos-chem-phys.net/12/7825/2012/acp-12-7825-2012.html

UNECE (2004). Manual on methodologies and criteria for modelling and mapping critical loads and levels and air pollution effects, risks and trends. UNECE Convention on Long-range Transboundary Air Pollution. http://www.icpmapping.org/Mapping_Manual

UNECE (2016). Forest condition in Europe. 2016 report of ICP Forests. UNECE Convention on Long-range Transboundary Air Pollution. http://www.wsl.ch/info/mitarbeitende/schaub/ICPF_TR_2016.pdf

UN (2015). World Population Prospects, the 2015 Revision. United Nations. Department of Economic and Social Affairs, Population Division. http://esa.un.org/unpd/wpp/Download/Standard/Population/

WHO (2005). WHO Air quality guidelines for particulate matters, ozone, nitrogen dioxide and sulphur dioxide. Global update 2005. http://www.who.int/phe/health_topics/outdoorair/outdoorair_aqg/en/index.html

Annex 1 Methodology

A1.1 Mapping method

Previous technical papers prepared by Horálek et al. (2005, 2007, 2008, 2010, 2014), De Smet et al. (2011), Denby et al. (2011a, 2011b) discuss methodological developments and details on spatial interpolations and their uncertainties. No changes took place in the mapping methodology of PM_{10} and ozone indicators compared to the five preceding reports (Horálek et al., 2016b and references cited therein), $PM_{2.5}$ mapping methodology paper (Denby et al., 2011b), and paper describing the NO_2 and NO_x maps (Horálek et al., 2014). This annex summarizes the currently applied method for these indicators. The mapping method has been evaluated with the FAIRMODE Delta tool in Horálek et al. (2016a). The method can be described as a regression – interpolation – merging mapping.

Pseudo $PM_{2.5}$ and NO_x station data estimation

To supplement $PM_{2.5}$ measurement data, in the mapping procedure we also use data from so-called *pseudo $PM_{2.5}$ stations*. These data are the estimates of $PM_{2.5}$ concentrations at the locations of PM_{10} stations with no $PM_{2.5}$ measurement. These estimates are based on PM_{10} measurement data and different supplementary data, using linear regression:

$$\hat{Z}_{PM2.5}(s) = c + b.Z_{PM10}(s) + a_1.X_1(s) + \ldots + a_n.X_n(s) \qquad \text{(A1.1)}$$

where $\hat{Z}_{PM2.5}(\mathrm{s})$ is the estimated value of $PM_{2.5}$ at the station *s*,
$Z_{PM10}(\mathrm{s})$ is the measurement value of PM_{10} at the station *s*,
$X_1(s), \ldots, X_n(s)$ are the values of other supplementary variables at the station *s*,
$c, b, a_1, \ldots, a_n$ are the parameters of the linear regression model calculated based on the data at the points of measuring stations with both $PM_{2.5}$ and PM_{10} measurements,
n is the number of other supplementary variables used in the linear regression model (apart from PM_{10}).

When applying this estimation method, all background stations (either classified as rural, urban or suburban) are handled together. For details, see Denby et al. (2011b).

To supplement NO_x measurement data, we estimate NO_x values at the locations of NO_2 stations with no NO_x data. The estimates are calculated similarly as in Horálek et al. (2007), using quadratic regression:

$$\hat{Z}_{NOx}(s) = a.Z_{NO2}(s)^2 + b.Z_{NO2}(s) + c \qquad \text{(A1.2)}$$

where $\hat{Z}_{NOx}(\mathrm{s})$ is the estimated value of NO_x at the station *s*,
$Z_{NO2}(\mathrm{s})$ is the measurement value of NO_2 at the station *s*,
a, b, c are the parameters of the quadratic regression calculated based on the data at the points of measuring stations with both NO_x and NO_2 measurements.

Interpolation

The mapping method used is a linear regression model followed by kriging of the residuals produced from that model (residual kriging). Interpolation is therefore carried out according to the relation:

$$\hat{Z}(s_0) = c + a_1.X_1(s_0) + a_2.X_2(s_0) + \ldots + a_n.X_n(s_0) + \eta(s_0) \qquad \text{(A1.3)}$$

where $\hat{Z}(\mathrm{s}_0)$ is the estimated value of the air pollution indicator at the point s_o,
$X_1(s_0), X_2(s_0), \ldots, X_n(s_0)$ are the *n* number of individual supplementary variables at the point s_o

$c, a_1, a_2, ..., a_n$ are the $n+1$ parameters of the linear regression model calculated based on the data at the points of measurement,

$\eta(s_0)$ is the spatial interpolation of the residuals of the linear regression model at the point s_o calculated based on the residuals at the points of measurement.

For different pollutants and area types (rural, urban) different supplementary data are used, depending on their improvement to the fit of the regression. Ordinary kriging is used to interpolate the residuals:

$$\hat{R}(s_0) = \sum_{i=1}^{N} \lambda_i R(s_i), \ \sum_{i=1}^{N} \lambda_i = 1, \qquad \text{(A1.4)}$$

where $R(s_i)$ are the residuals in the points of the measuring stations s_i,

$\lambda_1, ..., \lambda_N$ are the weights estimated based on variogram,

N is the number of the stations used in the interpolation.

The variogram (as a measure of a spatial correlation) is estimated using a spherical function (with parameters *nugget, sill, range*). For details, see Horálek et al. (2007), Section 2.3.5 and Cressie (1993).

For $PM_{2.5}$ and NO_x, both measurement data and the estimated data from the pseudo stations are used.

For the PM_{10} and $PM_{2.5}$ indicators we apply, prior to linear regression and interpolation, a logarithmic transformation to measurement and EMEP model concentrations. In the case of $PM_{2.5}$ rural map creation, population density is also log-transformed. After interpolation, we apply a back-transformation. For details, see De Smet et al. (2011) and Denby et al. (2008). In the case of urban background $PM_{2.5}$ map, we do not use any supplementary data – we apply just lognormal kriging.

For the vegetation related indicators (AOT40 for vegetation and forests and NO_x) we only construct rural maps based on rural background stations, based on the assumption that no vegetation is located in urban areas. For the health related indicators, we construct the rural and urban background maps separately and then we merge them.

Merging of rural and urban background maps

Health related indicator maps are constructed (using linear regression with kriging of its residuals) for the rural and urban background areas separately on a grid at 10x10 km resolution. The rural map is based on rural background stations and the urban background map on urban and suburban background stations. (Throughout the paper, both urban and suburban background stations are handled together.) Subsequent to this, the rural and urban background maps are merged into one combined air quality indicator map using a European-wide population density grid at 1x1 km resolution. For the 1x1 km grid cells with a population density less than a defined value of α_1, we select the rural map value and for grid cells with a population density greater than a defined value α_2, we select the urban background map value. For areas with population density within the interval (α_1, α_2) a weighting function of α_1 and α_2 is applied (for details and the setting of the parameters α_1 and α_2, see Horálek et al., 2005, 2007, 2010). This applies to the grid cells where the estimated rural value is lower (PM_{10} and $PM_{2.5}$) or higher (ozone), than the estimated urban background map value. In the exceptional cases when this criterion does not hold, we apply a joint urban/rural map (created using all background stations regardless their type), as far as its value lies in between the rural and urban background map value. For details, see De Smet et al. (2011).

Summarising, the separate rural, urban and joint urban/rural maps are constructed at a resolution of 10x10 km; their merging however takes place on the basis of the 1x1 km resolution population density grid, resulting in a final combined pollutant indicator map on this 1x1 km resolution grid. This map is used both for the population exposure estimates and for presentational purposes. We refer to the applied chain of optimised combinations of spatial resolutions, the process of *interpolation -> merging -> exposure estimate*, as the '10-1-1' (in km).

In all calculations and map presentations the EEA standard projection ETRS89-LAEA5210 (also known as ETRS89 / LAEA Europe, see www.epsg-registry.org) is used. The interpolation and mapping domain consists of the areas of all EEA member and cooperating countries, as far as they fall into the EEA map extent *Map_1c* (EEA, 2011). The mapping area covers the whole Europe apart from Belarus, Moldova, Ukraine and the European parts of Russia and Kazakhstan.

For further details and discussion on subjects briefly addressed in this section, refer to De Smet et al. (2011), Chapter 2.

A1.2 Calculation of population and vegetation exposure

Population and vegetation exposure estimates are based on the interpolated concentration maps, population density data and land cover data.

Population exposure

Population exposure for individual countries and for Europe as a whole is calculated from the air quality maps and population density data, both at 1x1 km resolution. For each concentration class, the total population per country as well as the European-wide total is determined. In addition, we express per-country and European-wide exposure as the population-weighted concentration, i.e. the average concentration weighted according to the population in a grid cell:

$$\hat{c} = \frac{\sum_{i=1}^{N} c_i p_i}{\sum_{i=1}^{N} p_i} \qquad \text{(A1.5)}$$

where $\hat{c}$ is the population-weighted average concentration in the country or in the whole Europe,
p_i is the population in the i^{th} grid cell,
c_i is the concentration in the i^{th} grid cell,
N is the number of grid cells in the country or in Europe as a whole.

Estimation of trends

For detecting and estimating the trends in time series of annual values of population exposure, the nonparametric Mann-Kendall's test for testing the presence of the monotonic increasing or decreasing trend is used. Next to that, the nonparametric Sen's method for estimating the slope of a linear trend is executed. For details, see Gilbert (1987). The significance of the Mann-Kendal test is shown by the usual way, i.e. + for 0.1, * for 0.05, ** for 0.01, and *** for 0.001.

Vegetation exposure

Vegetation exposure for individual countries and for Europe as a whole is calculated based on the air quality maps and land cover data, both in 2x2 km grid resolution. For each concentration class, the total vegetation area per country as well as European-wide is determined.

A1.3 Methods for uncertainty analysis

The uncertainty estimation of the European map is based on cross-validation. The cross-validation method computes the quality of the spatial interpolation for each measurement point from all available information except from the point in question, i.e. it withholds one data point and then makes a prediction at the spatial location of that point. This procedure is repeated for all measurement points in the available set. The predicted and measurement values at these points are plotted in the form of a scatter plot. With help of statistical indicators the quality of the predictions is demonstrated objectively. The advantage of the nature of this cross-validation technique is that it enables evaluation of the quality of the predicted values at locations without measurements, as long as they are within the area covered by the measurements.

In addition, we make a simple comparison between the point measurements and interpolated values of the 10x10 km grid for the separate rural and urban maps and the 1x1 km grid for the final combined maps, for the health-related indicators, resp. the 2x2 km grid in the case of AOT40 and NO_x. Note that the grid cell value is the averaged result of the interpolation in this grid cell area. The interpolated value within a grid cell will only approximate the predicted value(s) at the station(s) lying within that cell.

Another method to estimate uncertainties is based on geostatistical theory: together with the prediction, the prediction standard error is computed at all the grid cells, which represents in fact the interpolation uncertainty map (see Cressie, 1993 for a detailed discussion). Based on the concentration and the uncertainty map, the exceedance probability map is created.

Cross-validation

The results of cross-validation are described by the statistical indicators and scatter plots. The main indicator used is root mean squared error (RMSE) and additional is bias (mean prediction error, MPE):

$$RMSE = \sqrt{\frac{1}{N}\sum_{i=1}^{N}(\hat{Z}(s_i) - Z(s_i))^2} \quad \text{(A1.6)}$$

$$bias(MPE) = \frac{1}{N}\sum_{i=1}^{N}(\hat{Z}(s_i) - Z(s_i)) \quad \text{(A1.7)}$$

where $Z(s_i)$ is the air quality indicator value derived from the measured concentration at the i^{th} point, $i = 1, ..., N$,

$\hat{Z}(s_i)$ is the air quality estimated indicator value at the i^{th} point using other information, without the indicator value derived from the measured concentration at the i^{th} point,

N is the number of the measuring points.

Next to the RMSE expressed in the absolute units, one could express this uncertainty in relative terms by relating the RMSE to the mean of the air pollution indicator value for all stations:

$$RRMSE = \frac{RMSE}{\bar{Z}}.100 \quad \text{(A1.8)}$$

where $RRMSE$ is the relative RMSE, expressed in percent,

$\bar{Z}$ is the arithmetic average of the indicator values $Z(s_1), ..., Z(s_N)$, as derived from measurement concentrations at the station points $i = 1, ... , N$.

Other indicators are R^2 and the regression equation parameters *slope* and *intercept*, following from the scatter plot between the predicted (using cross-validation) and the observed concentrations

RMSE should be as small as possible, bias (MPE) should be as close to zero as possible, R^2 should be as close to *1* as possible, slope *a* should be as close to *1* as possible, and intercept *c* should be as close to zero as possible (in the regression equation $y = a.x + c$).

In the cross-validation of $PM_{2.5}$ and NO_x, only stations with $PM_{2.5}$ resp. NO_x measurement data are used (not the pseudo $PM_{2.5}$ resp. NO_x stations).

Comparison of the point measurement and interpolated grid values

The comparison of point measurement and predicted grid values is described by the linear regression equation and its parameters and statistical values. The comparison is executed separately for rural and urban background maps and for the final combined map. In the case of $PM_{2.5}$ and NO_x, only the stations with actual $PM_{2.5}$ resp. NO_x measurement data are used (not the pseudo $PM_{2.5}$ resp. NO_x stations).

The point observation – point cross-validation prediction analysis (Annex 3) describes interpolation performance at point locations when there is no observation (as it follows the leave-one-out approach). In this case, the smoothing effect of the interpolation is most prevalent.

The point observation – grid prediction approach indicates performance of the value for the 10x10 km (resp. 2x2 km or 1x1 km) grid cell with respect to the observations that are located within that cell. As such, some variability is due to smoothing but it also includes smoothing due to spatial averaging into the 10x10 km (2x2 km) grid cells. As such, the point-grid validation approach tells us how well our interpolated and aggregated grid values approximate the measurements at the actual station (point) locations. Whereas the point-point approach tells us how well our interpolated values estimate the indicator at a point where there is no actual measurement at that location, under the constrained that the point lies within the area covered by measurements.

Exceedance probability mapping

The maps with the probability of exceedance (PoE) of a specific threshold value (e.g. limit or target value) are constructed using the concentration and uncertainty maps:

$$PoE(x) = 1 - \Phi\left(\frac{LV - C_c(x)}{\sigma_c(x)}\right) \qquad \text{(A1.9)}$$

where $PoE(x)$ is the probability of limit/target value (*LV/TV*) exceedance in the grid cell *x*,
$\Phi(\,)$ is the cumulative distribution function of the normal distribution,
LV is the limit or target value of the relevant indicator,
$C_c(x)$ is the interpolated concentration in the grid cell *x*,
$\sigma_c(x)$ is the standard error of the estimation in the grid cell *x*.

The standard error of the probability map of the combined (rural and urban background) map is calculated from the standard errors of the separate rural and urban background maps; see Horálek et al. (2008), Section 2.3 and De Smet et al. (2011), Chapter 2. The maps with the probability of threshold value exceedance (PoE) are constructed in 1 x 1 km grid resolution.

In the probability of exceedance maps in this paper, the areas with 33–50 % and 50–66 % probability of LV exceedance are marked in yellow and orange respectively. The yellow colour indicates the areas with the estimated concentrations below limit value, but for which there exists a *modest* probability of exceeding the limit. The orange coloured areas have estimated concentrations above the limit value, but with a *moderate* chance of non-exceedance caused by its accompanying uncertainty. On the contrary, the areas with 66–90 % and 90–100 % are marked with red colour in two shades, indicating large or high probability of LV exceedance. Similarly, the areas with 0–10 % and 10–33 % are marked with green in two shades, indicating little or low probability of LV exceedance. Table A1.1 summarises the classes and terminology for probability (i.e. likelihood) that are distinguished in this paper.

Table A1.1 Probability mapping classes and terminology use in this paper

Map class colour	Percentage probability of threshold exceedance	Degree of probability (or likelihood) of exceedance	Likelihood of exceedance	
Green	0 – 10	Little	Very unlikely	More unlikely than likely
Light green	10 – 33	Low	Unlikely	
Yellow	33 – 50	Modest	About as likely as not	
Orange	50 – 66	Moderate		More likely than not
Light red	66 – 90	Large	Likely	
Dar red	90 – 100	High	Very likely	

The probability classes are used based on the classification used in IPCC (2010). Its basic likelihood scale of “very likely”, “likely”, “about as likely as not”, “unlikely” and “very unlikely” is combined with an additional option of “more likely than not”.

Annex 2 Input data

The types of input data in this paper are not different from that of Horálek et al. (2016b). The air quality and meteorological data has been updated. No further changes in selecting and processing of the input data have been implemented. For readability of this paper, we reproduce here the list of the input data. The key data is the air quality measurements at the monitoring stations extracted from Air Quality e-Reporting database, including geographical coordinates (*latitude*, *longitude*). The supplementary data cover the whole mapping domain and are converted into the EEA reference projection ETRS89-LAEA5210 on a 10 x 10 km grid resolution. The data for the AOT40 maps, however, were converted – like in the previous reports (Horálek et al., 2016b and references cited therein) – into a 2 x 2 km resolution to allow accurate land cover exposure estimates to be prepared for use in Core Set Indicator 005 of the EEA.

A2.1 Air quality monitoring data

Air quality station monitoring data for the relevant year are extracted from the official EEA Air Quality e-Reporting database, made public on 26 April 2016, EEA (2016a). This data set is supplemented with several EMEP rural background stations from the database EBAS (NILU, 2016) not reported to the Air Quality e-Reporting database. (Specifically, 16 additional rural background stations for PM_{10}, 14 for $PM_{2.5}$, 11 for NO_2 and 3 for NO_x from the EBAS database are added.) Only data from stations classified as *background* (for the three types of area, *rural*, *suburban* and *urban*) are used. *Industrial* and *traffic* station types are not considered; they represent local scale concentration levels not applicable at the mapping resolution employed. The following pollutants and aggregations are considered:

PM_{10} – annual average [$\mu g.m^{-3}$], year 2014
– 90.4 percentile of the daily average values [$\mu g.m^{-3}$], year 2014

$PM_{2.5}$ – annual average [$\mu g.m^{-3}$], year 2014

Ozone – 93.2 percentile of the maximum daily 8-hour average values [$\mu g.m^{-3}$], year 2014
– SOMO35 [$\mu g.m^{-3}.day$], year 2014
– AOT40 for vegetation [$\mu g.m^{-3}.hour$], year 2014
– AOT40 for forests [$\mu g.m^{-3}.hour$], year 2014

NO_2 – annual average [$\mu g.m^{-3}$], year 2014

NO_x – annual average [$\mu g.m^{-3}$], year 2014

NO – annual average [$\mu g.m^{-3}$], year 2014 (for the purposes of NO_x mapping only)

The exact values of percentiles are actually 90.41 in the case of PM_{10} daily means and 93.15 in the case of ozone maximum daily 8-hour means.

For a considerable number of stations NO_x is measured, but it is not reported as such but separately as NO and NO_2. For these stations reporting NO and NO_2 separately, the NO_x concentrations were derived according to the equation

$$NO_x = NO_2 + \frac{46}{30} \cdot NO \qquad \text{(A2.1)}$$

where all components are expressed in $\mu g.m^{-3}$, with a molecular mass for NO of 30 and for NO_2 of 46 $g.mol^{-1}$.

SOMO35 is the annual sum of the differences between maximum daily 8-hour concentrations above 70 $\mu g.m^{-3}$ (i.e. 35 ppb) and 70 $\mu g.m^{-3}$. AOT40 is the sum of the differences between hourly concentrations greater than 80 $\mu g.m^{-3}$ (i.e. 40 ppb) and 80 $\mu g.m^{-3}$, using only observations between 08:00 and 20:00 CET, calculated over the three months from May to July for AOT40 for vegetation and over the six months from April to September for AOT40 for forests.

Only the stations with annual data coverage of at least 75 percent are used. In the case of SOMO35 and AOT40 indicators, a correction for the missing data is applied according to the equation

$$I_{corr} = I \cdot \frac{N_{\max}}{N} \qquad \text{(A2.2)}$$

where I_{corr} is the corrected indicator (SOMO35, AOT40 for vegetation or AOT40 for forests),
I is the value of the given indicator without any correction,
N is the number of the available daily resp. hourly data in a year for the given station,
N_{max} is the maximum possible number of the days or hours applicable for the given indicator.

For the xth highest values (i.e. for the PM_{10} indicator 36th highest daily mean and for the ozone indicator 26th highest maximum daily 8-hour running mean) used in the previous reports (Horálek et al., 2016b and references cited therein), no correction for missing data was applied. The most straightforward way to solve the missing data issue in these cases is to use the percentiles instead of the xth highest values. Thus, from this report onward, the percentiles (i.e. 90.4 percentile of PM_{10} daily means and 93.2 percentile of ozone maximum daily 8-hour means) are and will be used.

For the indicators relevant to human health (i.e. for all PM_{10} and $PM_{2.5}$ indicators, ozone indicators 93.2nd percentile of maximum daily 8-hour means and SOMO35, and NO_2 annual average), data from *rural*, *urban* and *suburban background* stations are considered. (Throughout the paper, the urban and suburban stations are handled together.) For the indicators relevant to vegetation damage (i.e. for both ozone AOT40 parameters and NO_x annual average), only *rural background* stations are considered. In case of existing data (with sufficient annual time coverage) from two or more different measurement devices in the same station location, the average of these data is used.

We excluded the stations from French overseas areas (departments), Svalbard, Azores, Madeira and Canary Islands. These areas outside the EEA map extent *Map_1c* (EEA, 2011) were excluded from the interpolation and mapping domain.

Table A2.1 shows the number of the measurement stations selected for the individual pollutants and their respective indicators. Compared to 2013, the number of rural background stations selected for 2014 increased by approximately 11 % for PM_{10} stations, by about 18 % for $PM_{2.5}$ stations and by approximately 1 – 4 % for ozone. The number of the urban/suburban background stations increased by approximately 7 % for PM_{10}, by approximately 11 % for $PM_{2.5}$, and by about 4 – 6 % for ozone.

Table A2.1 Number of stations selected for each pollutant indicator and area type

Area type	PM_{10}		$PM_{2.5}$	ozone				NO_2	NO_x
	Ann. avg.	90.4 perc. of d. means	Annual average	93.2 perc. of max. d. 8h	SOMO35	AOT40 for crops	AOT40 for forests	Ann. avg.	Ann. avg.
Rural	346	346	173	505	505	501	501	410	322
Urban /Suburban	1074	1072	506	1021	1021			1126	

For the $PM_{2.5}$ mapping, 185 additional rural background and 634 additional urban/suburban background PM_{10} stations (at locations without $PM_{2.5}$ measurement) were also used for the purpose of calculating the pseudo $PM_{2.5}$ station data.

In the case of NO_x, for 295 stations NO_x data is reported, while for 17 stations NO_x values are calculated from reported NO_2 and NO data using Eq. A2.1. Next to this, for the NO_x mapping 90 additional rural background NO_2 stations (at locations without NO_x measurement) were also used for the purpose of calculating the pseudo NO_x station data.

Due to the lack of reporting stations in Turkey, no proper interpolation results could be presented for this country for any of the indicators. Therefore, we excluded Turkey from the production process of the maps and exposure tables of this paper.

A2.2 EMEP MSC-W model output

The chemical dispersion model used in this paper is the EMEP MSC-W (formerly called Unified EMEP) model (version rv4.9), which is an Eulerian model. Simpson et al. (2012) and https://wiki.met.no/emep/page1/emepmscw_opensource (web site of Norwegian Meteorological Institute) describe the model in more detail. Emissions for the relevant year 2014 (Mareckova et al., 2016) are used and the model is driven by ECMWF meteorology for the relevant year 2014. EMEP (2016) provides details on the EMEP modelling for 2014. The resolution of the model is circa 50x50 km. Information from this model was converted to 10x10 km grid resolution (for health related indicators), resp. into the 2x2 km grid resolution (for vegetation related indicators) for the interpolation process.

We downloaded the EMEP data from NMI (2016) in the form of annual means for NO_x, daily means for PM_{10} and $PM_{2.5}$ and NO_2, and hourly means for ozone. We aggregated these primary data to the same set of parameters as we have for the air quality observations:

PM_{10} – annual average [µg.m^{-3}], year 2014 (aggregated from daily means)
– 90.4 percentile of the daily average value [µg.m^{-3}], year 2014 (aggregated from daily means)

$PM_{2.5}$ – annual average [µg.m^{-3}], year 2014 (aggregated from daily means)

Ozone – 93.2 percentile of the highest maximum daily 8-hour average value [µg.m^{-3}], year 2014 (aggregated from hourly means)
– SOMO35 [µg.m^{-3}.day], year 2014 (aggregated from hourly means)
– AOT40 for vegetation [µg.m^{-3}.hour], year 2014 (aggregated from hourly means)
– AOT40 for forests [µg.m^{-3}.hour], year 2014 (aggregated from hourly means)

NO_2 – annual average [µg.m^3], year 2014 (aggregated from daily means)

NO_x – annual average [µg.m^3], year 2014

Due to the complete temporal data coverage available at the modelled data, the PM_{10} indicator 90.4 percentile of daily means is identical with the 36th highest daily mean and the ozone indicator 93.2 percentile of maximum daily 8-hour means is identical with the 26th highest maximum daily 8-hour mean.

In the original format of the model results, a point represents the centre of a grid cell (in 50x50 km resolution). The data are imported into *ArcGIS* as a point shapefile and converted into ETRS89-LAEA5210 projection, subsequently converted into a 100x100 m resolution raster grid and spatially aggregated into the reference EEA 10x10 km grid (for health related indicators), resp. into the 2x2 km grid (for vegetation related indicators).

A2.3 Other supplementary data

Altitude

We use the altitude data field (in meters) of *Global Multi-resolution Terrain Elevation Data 2010 (GMTED2010)*, with an original grid resolution of 15x15 arcseconds (some 463x463 m at 60N). Source: U.S. Geological Survey Earth Resources Observation and Science, see Danielson et al. (2011). We converted the field into the ETRS 1989 LAEA projection. (The resolution after projection was in 449.2x449.2 m). In the following step, we resampled the raster dataset to 100x100 m resolution and shifted it to the extent of EEA reference grid. As a final step, the dataset was spatially aggregated into 2x2 km and 10x10 km resolutions.

Meteorological parameters

Actual meteorological surface layer parameters were extracted from the *Meteorological Archival and Retrieval System (MARS)* of the *ECMWF (European Centre for Medium-range Weather Forecasts)*. Currently we use the following ECMWF variables (details specified in Horálek et al. 2007, Section 4.5) on a 0.25x0.25 degrees (about 28x28 km at 60N) resolution as supplementary data in the regressions:

Wind speed	– annual average [$m.s^{-1}$], year 2014 (aggregated from 6-hour means)
Surface solar radiation	– annual average of daily sum [$MWs.m^{-2}$], year 2014 (aggregated from daily sums)

The 6-hour mean wind speed used in the aggregation is derived from the 10 meter height wind speed in U (*10U*) and V (*10V*) directions (where U and V are perpendicular vectors in horizontal directions) with magnitude $\sqrt{(10U)^2 + (10V)^2}$.

The data are imported into *ArcGIS* as a point shapefile. Each point represents the centre of a grid cell. The shapefile is converted into ETRS89-LAEA5210 projection, converted into a 100x100 m resolution raster grid and spatially aggregated into the reference EEA 10x10 km grid, resp. into the 2x2 km grid.

Population density and population totals

Population density (in $inhbs.km^{-2}$, census 2011) is based on *Geostat 2011* grid dataset, Eurostat (2014). The dataset is in 1x1 km resolution, in the EEA reference grid.

For regions not included in the Geostat 2011, alternative sources were used. Primarily, *JRC (Joint Research Centre)* population data in resolution 100x100 m were used (JRC, 2009). The JRC 100x100 m population density data is spatially aggregated into the reference 1x1 km EEA grid. For regions that are neither included in the Geostat 2011 nor in the JRC database, we used population density data from *ORNL LandScan Global Population Dataset* (ORNL, 2008). This dataset is in 30x30 arcsec resolution; its values are based on the annual mid-year national population estimates for 2008 from the Geographic Studies Branch, US Bureau of Census, http://www.census.gov. The ORNL data is re-projected and converted from its original WGS1984 30x30 arcsecs grids into EEA's reference projection ETRS89-LAEA5210 at 1x1 km resolution by EEA (eea_r_3035_1_m_landscan-eurmed_2008, EEA, 2008).

The areas lacking Geostat 2011 data, and supplemented with JRC or ORNL data were: Gibraltar (JRC); Faroe Islands, British crown dependencies (Jersey, Guernsey and Man) and northern Cyprus (ORNL). As such, the Geostat 2011 1x1 km data and these supplements cover the entire mapping area.

To verify the consistency of merging Geostat 2011 with JRC and ORNL data, we compared the Geostat 2011 data and the JRC supplemented with ORNL data on the basis of the national population totals of the individual countries (see Horálek et al., 2015 for details). Additionally, we verified the national population totals for the Geostat 2011 gridded data with the Eurostat national population data for 2014 (Eurostat, 2016). Figure A2.1 presents both comparisons. From these verifications, one can conclude a high correlation of the national population totals of each data source. Slight underestimation of the supplemented JRC and ORNL data in comparison with the Geostat 2011 data can be seen, which is caused by the fact that the Geostat 2011 data is more up-to-date than both the JRC and the ORNL data source. Geostat 2011 and Eurostat 2014 data correlate even better and leads to a similar conclusion. Based on this, we used in the further calculations on national population totals the actual Eurostat data for 2014 (Eurostat, 2016), as described further.

Population density data can be used to classify the spatial distribution of each type of area (rural, urban or mixed population density) in Europe. We use this information to select and weight the air quality values, grid cell by grid cell and merge them into a final combined map (Annex 1). Furthermore, we use it to estimate population health exposure and exceedance numbers per country and for Europe as a whole, including involved uncertainties. These activities take place on the 1x1 km resolution grid in accordance with the recommendations of Horálek et al. (2010). The supplemented Geostat data (as described above) are used in all the calculations.

Figure A2.1 Correlation of national population totals for Geostat 2011 with JRC supplemented with ORNL, and with Eurostat 2014

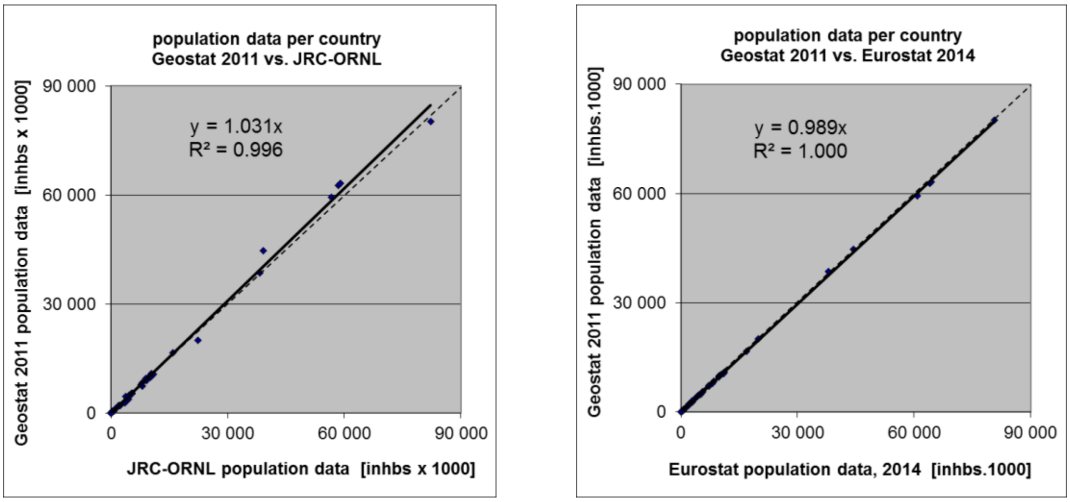

National population totals presented in the exposure tables of this paper are based on Eurostat national population data for 2014 (Eurostat, 2016). For France, Portugal and Spain, the population totals of areas outside the mapping area (i.e. Azores, Canarias, Madeira, French oversea departments) are subtracted. For Andorra and Monaco, which do not have 2014 data in the Eurostat database, the population total is based on UN population data (UN, 2015) for 2014.

Land cover

CORINE Land Cover 2006 – grid 100 x 100 m, Version 17 (12/2013) is used (CLC2006 – 100m, g100_06.zip; EEA, 2013b). The countries missing in this database are Andorra and Greece. Greece is missing in the CLC2006 but present in the CLC2000 version that we used in previous mapping years. Therefore, we inserted for Greece the CLC2000 data (grid 100 x 100 m, Version 17, 12/2013 EEA, 2013a). Due to the lack of land cover data for Andorra, we excluded this country from the process of exposure estimates related to the vegetation based AOT40 ozone indicators.

Annex 3 Technical details and mapping uncertainties

This annex contains technical details on the linear regression models and the residual kriging, including the performance. Furthermore, uncertainty estimates for the maps of the indicators are given.

A3.1 PM_{10}

Technical details on the interpolation model and uncertainty estimates for the maps of both PM_{10} indicators annual average and 90.4 percentile of daily means – i.e. for Maps 2.1 and 2.2 – are presented in this section.

Technical details on the interpolation model

Table A3.1 presents the estimated parameters of the linear regression models (c, a_1, a_2, …) and of the residual kriging (nugget, sill, range) and includes the statistical indicators of both the regression and the kriging, for both PM_{10} indicators. The linear regression and ordinary kriging on its residuals is applied on the logarithmically transformed data of both measurement and modelled PM_{10} values. In Table A3.1 the standard error and variogram parameters (nugget, sill and range) refer to these transformed data, whereas RMSE and bias refer to the interpolation after a back-transformation.

For the 90.4 percentile of daily means, surface solar radiation was found to be statistically non-significant and thus it was not used in 2014 mapping.

The adjusted R^2 and standard error are indicators for the fit of the regression relationship, where the adjusted R^2 should be as close to 1 as possible and the standard error should be as small as possible. The adjusted R^2 was 0.51 for the annual average (resp. 0.47 for the P90.4) for the rural areas and 0.15 for the annual average (resp. 0.11 for the P90.4) for urban areas.

RMSE (the smaller the better) and bias (the closer to zero the better), highlighted by orange, are the cross-validation indicators, showing the quality of the resulting map. The bias indicates to what extent the estimation on average is under- or overestimated. Further in this section, more detailed uncertainty analysis is presented. Annex 4 presents the comparison with results of the years 2005 – 2013.

Table A3.1 Parameters and statistics of linear regression model and ordinary kriging of PM_{10} indicators annual average and 90.4 percentile of daily means for 2014 in rural and urban areas for the final combined map

		Annual average		90.4 percentile of daily means	
		Rural areas	Urban areas	Rural areas	Urban areas
Linear regresion model (LRM, Eq. A1.3)	c (constant)	1.67	2.03	2.38	2.32
	a1 (log. EMEP model)	0.531	0.43	0.465	0.43
	a2 (altitude GTOPO)	-0.00047		-0.00050	
	a3 (wind speed)	-0.072		-0.079	
	a4 (s. solar radiation)	0.019		*non signif.*	
	Adjusted R^2	**0.51**	**0.15**	**0.47**	**0.11**
	Standard Error [μg.m^{-3}]	**0.28**	**0.30**	**0.28**	**0.34**
Ordinary kriging (OK) of LRM residuals	nugget	0.044	0.016	0.027	0.016
	sill	0.073	0.078	0.069	0.085
	range [km]	800	870	510	630
LRM + OK of its residuals	**RMSE [μg.m^{-3}]**	**3.5**	**4.2**	**6.5**	**8.6**
	Relative RMSE [%]	**20.7**	**17.7**	**21.5**	**20.4**
	Bias (MPE) [μg.m^{-3}]	**0.1**	**0.0**	**0.2**	**-0.1**

Uncertainty estimated by cross-validation

Using RMSE as the most common indicator, the *absolute mean uncertainty* of the final combined map at areas 'in between' the station measurements can be expressed in µg.m^{-3}. Table A3.1 shows that the absolute mean uncertainty of the final combined map of PM_{10} annual average resp. 90.4 percentile of daily means expressed by RMSE is 3.5 µg.m^{-3} resp. is 6.5 µg.m^{-3} for the rural areas and 4.2 µg.m^{-3} resp. 8.6 µg.m^{-3} for the urban areas. Alternatively, one can express this uncertainty in relative terms by relating the absolute RMSE uncertainty to the mean air pollution indicator value for all stations. This *relative mean uncertainty* (Relative RMSE) of the final combined map of PM_{10} annual average resp. 90.4 percentile of daily means is 20.7 % resp. 21.5 % for rural areas and 17.7 % resp. 20.4 % for urban areas. These relative uncertainty values fulfil the data quality objectives for models as set in Annex I of the air quality Directive 2008/50/EC (EU, 2008). See Annex 4 (and specifically Table A4.1) for a further discussion on uncertainties over the previous nine modelling years.

Figure A3.1 shows the cross-validation scatter plots, obtained according to Annex 1, for both rural and urban areas, for both PM_{10} indicators. The R^2 indicates that the variability is attributable to the interpolation for about 68 % at the rural areas and for about 76 % at the urban areas.

Figure A3.1 Correlation between cross-validated predicted (y-axis) and measurement values for PM_{10} indicators annual average (top) and 90.4 percentile of daily means (bottom) for 2014 for rural (left) and urban (right) areas

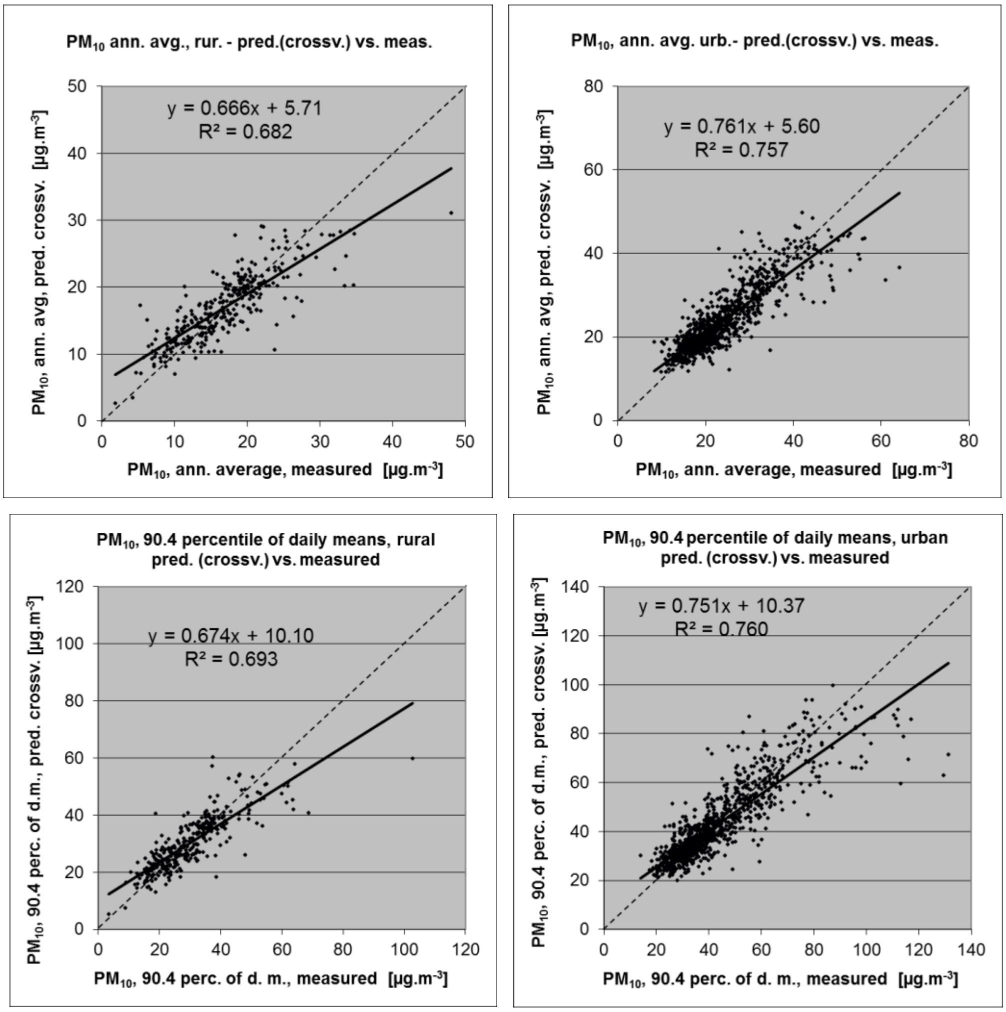

The scatter plots indicate that the interpolation methods tend to underestimate the high concentrations and overestimate the low concentrations. For example, in urban areas for annual average an observed value of 55 µg.m^{-3} is estimated in the interpolations to be about 47 µg.m^{-3}, about 14 % lower. This underestimation at high values is common to all spatial interpolation methods. It can be reduced by either using a higher number of stations with an improved spatial distribution, or by introducing an improved regression by using other supplementary data.

Comparison of point measurement values with the predicted grid value

In addition to the above point observation – point prediction cross-validation discussed in the previous subsection, a simple comparison has been made between the point observation values and interpolated prediction values spatially averaged at grid cells. This *point-grid* comparison indicates to what extent the predicted value of a grid cell represents the corresponding measurement values at stations located in that cell. The comparison has been made primarily for the separate rural and urban background map at 10x10 km resolution. (One can directly relate this comparison result to the cross-validation results of Figure A3.1). Next to this, the comparison has been done also for the final combined maps at 1x1 km resolution. Figure A3.2 shows the scatterplots for these comparisons, for PM_{10} annual average only as an illustration.

Figure A3.2 Correlation between predicted grid values from rural 10x10 km (upper left), urban 10x10 km (bottom left) and final combined 1x1 km (upper and bottom right) map (y-axis) versus measurements from rural (top), resp. urban/suburban (bottom) background stations (x-axis) for PM_{10} annual average 2014

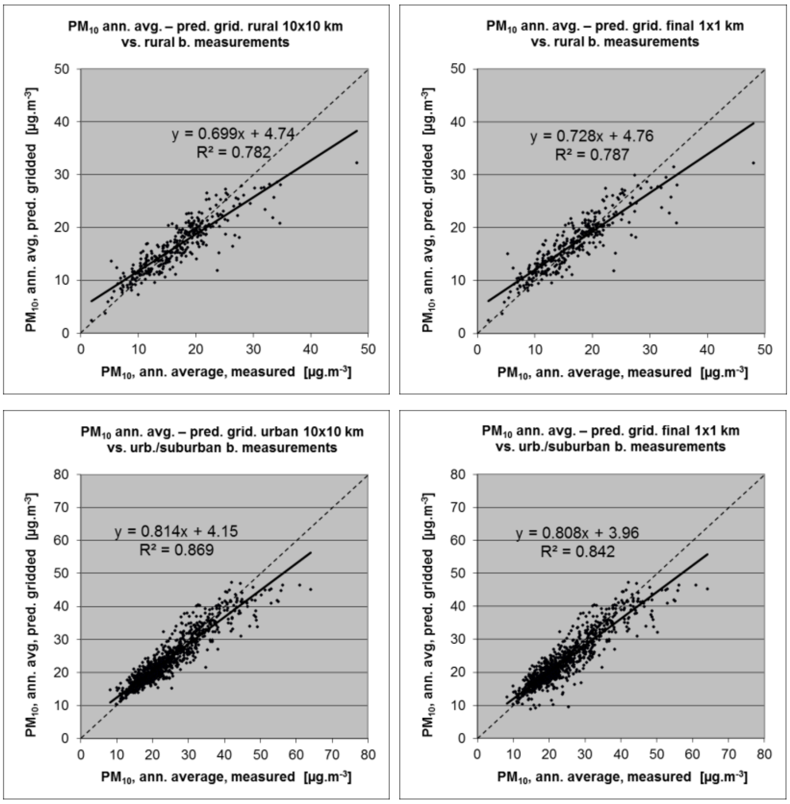

The results of the point observation – point prediction cross-validation of Figure A3.1 and those of the point-grid validation for separate rural and separate urban background maps, and for the final combined maps at both resolutions are summarised in Table A3.2 for both PM_{10} indicators.

By comparing the scatterplots and the statistical indicators for the separate rural and separate urban background map with the final combined maps in both resolutions, one can evaluate the level of representation of the rural resp. urban background areas in the final combined maps. Both the rural and the urban air quality is fairly well represented in the 1x1 km final combined map. This would not be the case in the urban areas for the aggregated final combined 10x10 km map (Horálek et al., 2016b). Therefore, we present the final combined maps just in the 1x1 km resolution, see Maps 2.1 and 2.2, contrary to the last years' reports (e.g. Horálek et. al, 2016b).

Table A3.2 Statistical indicators from the scatter plots for the predicted point values based on cross-validation and the predicted grid values from separate (rural resp. urban) 10x10 km and final combined 1x1 km map versus the measurement point values for rural (left) and urban (right) background stations for PM_{10} indicators annual average (top) and 90.4 percentile of daily means (bottom) for 2014

PM_{10}	rural backgr. stations				urban/suburban backgr. stations			
	RMSE	bias	R^2	lin. r. equation	RMSE	bias	R^2	lin r. equation
Annual average								
cross-valid. prediction, separate (r or ub) map	3.5	0.1	0.682	y = 0.666x + 5.71	4.2	0.0	0.757	y = 0.761x + 5.60
grid prediction, 10x10 km separate (r or ub) map	2.9	-0.3	0.782	y = 0.699x + 4.74	3.1	-0.2	0.869	y = 0.814x + 4.15
grid prediction, 1x1 km final combined map	2.9	0.2	0.787	y = 0.728x + 4.76	3.4	-0.6	0.842	y = 0.808x + 3.96
90.4 percentile of daily means								
cross-valid. prediction, separate (r or ub) map	6.5	0.2	0.693	y = 0.674x + 10.1	8.6	-0.1	0.760	y = 0.751x + 10.4
grid prediction, 10x10 km separate (r or ub) map	4.6	-0.4	0.860	y = 0.753x + 7.11	6.1	-0.5	0.887	y = 0.817x + 7.20
grid prediction, 1x1 km final combined map	4.6	0.3	0.855	y = 0.768x + 7.33	6.6	-1.0	0.867	y = 0.810x + 7.01

The Table A3.2 shows a better relation (i.e. lower RMSE, higher R^2, smaller intercept and slope closer to 1) between station measurements and the interpolated values of the corresponding grid cells at both rural and urban background map areas than it does at the point cross-validation predictions. That is because the simple comparison between point measurements and the gridded interpolated values shows the uncertainty at the actual station locations (points), while the point cross-validation prediction simulates the behaviour of the interpolation at point positions assuming no actual measurement would exist at that point. The uncertainty at measurement locations is caused partly by the smoothing effect of the interpolation and partly by the spatial averaging of the values in the 10x10 km grid cells. The level of the smoothing effect leading to underestimation at areas with high values is there smaller than in situations where no measurement is represented in such areas. For example, in urban areas the predicted interpolation gridded value in the separate urban background map will be about 49 $\mu g.m^{-3}$ at the corresponding station point with the measurement value of 55 $\mu g.m^{-3}$. This means an underestimation of about 11 %. It is less than the prediction underestimation of 14 % at the same point location, when leaving out this one actual measurement point and the interpolation is done without this station (see the previous subsection).

Probability of Limit Value exceedance

We constructed the map of probability of limit value exceedance. For this purpose, we used the final combined concentration map in the 1x1 km grid resolution. Based on this map, we derived, with support of the 1x1 km uncertainty map (Annex 1) and the limit value (40 $\mu g.m^{-3}$), the probability of exceedance (PoE) map at that same resolution. It is important to emphasize that the exceedance of the spatial average of a 10x10 km grid cell (as presented in the previous reports, e.g. Horálek et al., 2016b) would show low probability even though some smaller (e.g. urban) areas inside such a grid cell would show high probability of exceedance (becoming visible in case one would present the map on a higher grid cell resolution).

It is needed to keep in mind that the interpolated maps refer to the rural or urban/suburban *background* situations only, i.e. it cannot be excluded that exceedances of limit values may occur at *hotspot* and traffic locations throughout Europe, which are not resolved by this type of map.

The map shows areas with a probability of limit value exceedance (PoE) above 66 % marked in red (large or high PoE) and areas below 33 % in green (low or little PoE). Red in two shades indicate areas for which exceedance is *likely* or *very likely* (above 90 %) to occur due to either high concentrations close to or already above the LV accompanied with such uncertainty that exceedance is very likely, or areas with lower concentrations accompanied with high uncertainty levels so that excess is very likely. Vice versa, in the green areas of two shades (below 33 %) it is *unlikely* to exceed the LV because we have predicted concentrations and accompanying uncertainties at levels that do not sum above the LV. The areas with 33–50 % and 50–66 % probability of LV exceedance are marked in yellow and orange respectively. Table A4.5 summarises the classes and terminology for probability (i.e. likelihood) that are used in this paper.

Maps A3.1 and A3.2 present the probability of the LV exceedance for PM_{10} indicators annual average and 90.4 percentile of daily means. In case of the annual average (Map A3.1), only limited areas do show increased probability of LV exceedance, namely the surrounding of Almeria in southern Spain, urban areas in the Ostrava–Katowice region of southern Poland and north-eastern Czech Republic, and some urban areas in Bulgaria and FYR of Macedonia.

Map A3.1 Map with the probability of the limit value exceedance, PM_{10} annual average, 2014

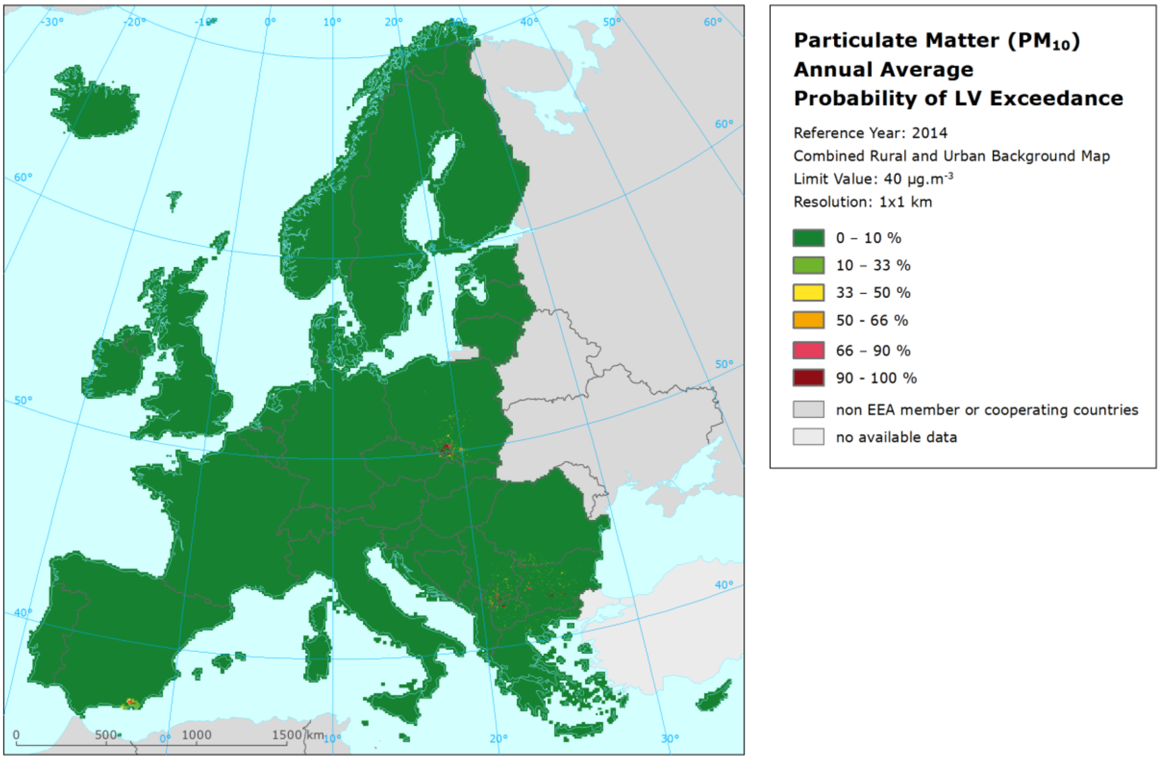

Note: Interpolation uncertainty is considered only, no other sources of uncertainty.

In case of the 90.4 percentile of daily means (Map A3.2), one can see larger areas with high levels of PoE, namely in southern Poland and north-eastern Czech Republic (with industrial Ostrava–Katowice region), the Po Valley in northern Italy, northern Serbia, southern Romania, and also the region around Almería in southern Spain. Next to this, urban areas of the most of the Poland, Serbia, Bulgaria and FYR of Macedonia show high levels of PoE.

Map A3.1 Map with the probability of the limit value exceedance, PM_{10} indicator 90.4 percentile of daily means, 2014

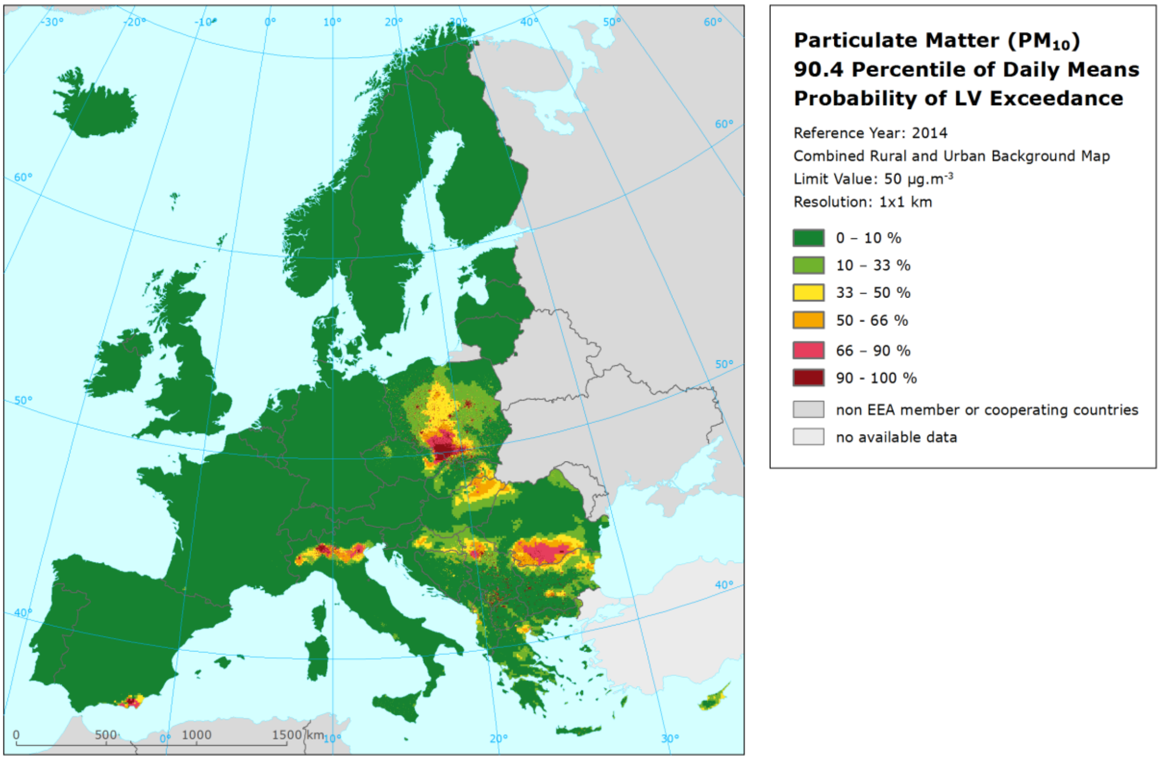

Note: Interpolation uncertainty is considered only, no other sources of uncertainty.

A3.2 $PM_{2.5}$

Technical details and uncertainty estimates for the map of $PM_{2.5}$ annual average – i.e. for Map 3.1 – are presented in this section.

Technical details on the interpolation model

Table A3.3 presents the regression coefficients determined for pseudo $PM_{2.5}$ stations data estimation, based on the stations with both $PM_{2.5}$ and PM_{10} measurements (see Section 2.1.1). The number of such type of stations is 546.

Table A3.3 Parameters and statistics of linear regression model for generation of pseudo $PM_{2.5}$ data, regardless of rural or urban/suburban area, for $PM_{2.5}$ annual average 2014

		Both rural and urban areas
Linear regresion model (LRM, Eq. A1.1)	c (constant)	21.8
	b (PM_{10} measurement data)	0.702
	a1 (surface solar radiation)	-1.092
	a2 (population density)	*non signif.*
	a3 (latitude)	-0.226
	a4 (longitude)	0.053
	Adjusted R^2	**0.90**
	Standard Error [$\mu g.m^{-3}$]	**2.0**

The same supplementary data as in Denby (2011b) are used. However, the inclusion of the population density in the regression model was found not be significant (like in 2010 – 2013), thus it will not be further used.

Table A3.4 presents the estimated parameters of the linear regression models (c, a_1, a_2,...) and of the residual kriging (*nugget, sill, range*) and includes the statistical indicators of both the regression and the kriging. Like in the case of PM_{10}, the linear regression is applied on the logarithmically transformed data of both measurement and modelled $PM_{2.5}$ values. Thus, the standard error and variogram parameters refer to these transformed data, whereas RMSE and bias refer to the interpolation after the back-transformation.

Surface solar radiation was not (in contrast to 2007 – 2008 and like in 2010 – 2013) found to be statistically significant and thus not used in 2014 mapping. Its further use is to be considered.

Table A3.4 Parameters and statistics of linear regression model and ordinary kriging of $PM_{2.5}$ annual average 2014 in rural and urban areas for final combined map

		Annual average	
		Rural areas	**Urban areas**
Linear regression model (LRM, Eq. A1.3)	c (constant)	1.16	1.45
	a1 (log. EMEP model)	0.604	0.56
	a2 (altitude GTOPO)	-0.00025	
	a3 (wind speed)	-0.051	
	a4 (s. solar radiation)	*non signif.*	
	a5 (log. population)	0.018	
	Adjusted R^2	**0.55**	**0.29**
	Standard Error [µg.m^{-3}]	**0.29**	**0.32**
Ordinary kriging (OK) of LRM residuals	nugget	0.035	0.016
	sill	0.083	0.080
	range [km]	680	830
LRM + OK of its residuals	**RMSE [µg.m^{-3}]**	**2.5**	**2.6**
	Relative RMSE [%]	**22.4**	**16.4**
	Bias (MPE) [µg.m^{-3}]	**0.0**	**0.1**

The adjusted R^2 and standard error are indicators for the quality of the fit of the regression relation, where the adjusted R^2 should at the best be as close to 1 as possible and the standard error should be as small as possible. The adjusted R^2 is 0.55 for the rural areas and 0.29 for urban areas.

RMSE and bias – highlighted in orange – are the cross-validation indicators, showing the quality of the resulting map; the bias indicates to what extent the estimation on average is under- or overestimated. Only stations with $PM_{2.5}$ measurement data are used for calculating RMSE and bias (i.e. non-pseudo $PM_{2.5}$ stations are used).

Uncertainty estimated by cross-validation

Table A3.4 shows that the absolute mean uncertainty of the final combined map of $PM_{2.5}$ annual average expressed as RMSE is 2.5 µg.m^{-3} for the rural areas and 2.6 µg.m^{-3} for the urban areas. On the other hand, the *relative mean uncertainty* (Relative RMSE) of the final combined map of $PM_{2.5}$ annual average is 22.4 % for rural areas and 16.4 % for urban areas. These relative uncertainty values fulfil the data quality objectives for models as set in Annex I of the air quality Directive 2008/50/EC (EU, 2008). Annex 4 (and specifically Table A4.5) summarises both the absolute and relative uncertainties of different years.

Figure A3.3 shows the cross-validation scatter plots, obtained according to Section A1.3, for both the rural and urban areas. The R^2 indicates that about 78 % of the variability is attributable to the interpolation for the rural areas and 81 % for the urban areas.

Figure A3.3 Correlation between cross-validated predicted and measurement values for $PM_{2.5}$ annual average 2014 for rural (left) and urban (right) areas

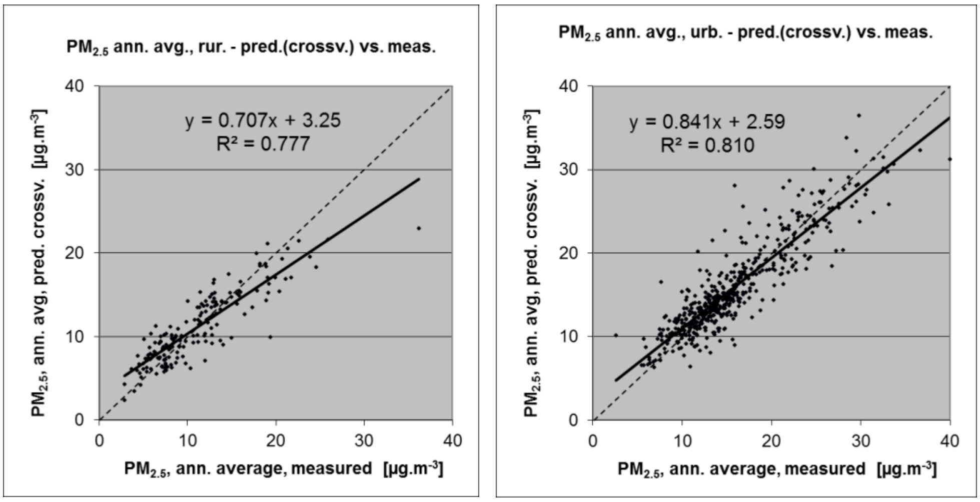

The scatter plots indicate that in areas with high concentrations the interpolation methods tend to underestimate the levels. For example, in rural areas an observed value of 25 $\mu g.m^{-3}$ is estimated in the interpolations to be about 21 $\mu g.m^{-3}$, about 16 % lower. This underestimation at high values is an inherent feature of all spatial interpolations. It can be reduced by either using a higher number of the stations at improved spatial distribution, or introducing a closer regression by using other supplementary data.

Comparison of point measurement values with the predicted grid value

Next to the cross-validation comparison, a simple comparison has been made between the point observation values and interpolated prediction values spatially averaged in grid cells. This point-grid comparison indicates to what extent the predicted value of a grid cell represents the corresponding measurement values at stations located in that cell. The comparison has been made primarily for the separate rural and urban map at 10x10 km resolution. Next to this, the comparison has been done also for the final combined maps at 1x1 km resolution. Figure A3.4 shows the scatterplots for these comparisons.

The results of the point observation – point prediction cross-validation of Figure A3.3 and those of the point-grid validation of Figure A3.4 for separate rural and separate urban background maps, and for the final combined maps at both resolutions are summarised in Table A3.5.

By comparing the scatterplots and the statistical indicators for the separate rural and separate urban background map with the final combined maps, one can evaluate the level of representation of the rural resp. urban background areas in the final combined maps. Similar results as for PM_{10} can be observed: Both the rural and urban air quality is fairly well represented in the 1x1 km final combined map.

Figure A3.4 Correlation between predicted grid values from rural 10x10 km (upper left), urban 10x10 km (bottom left) and final combined 1x1 km (both right) map (y-axis) versus measurements from rural (top), resp. urban/suburban (bottom) background stations (x-axis) for $PM_{2.5}$ annual average 2014

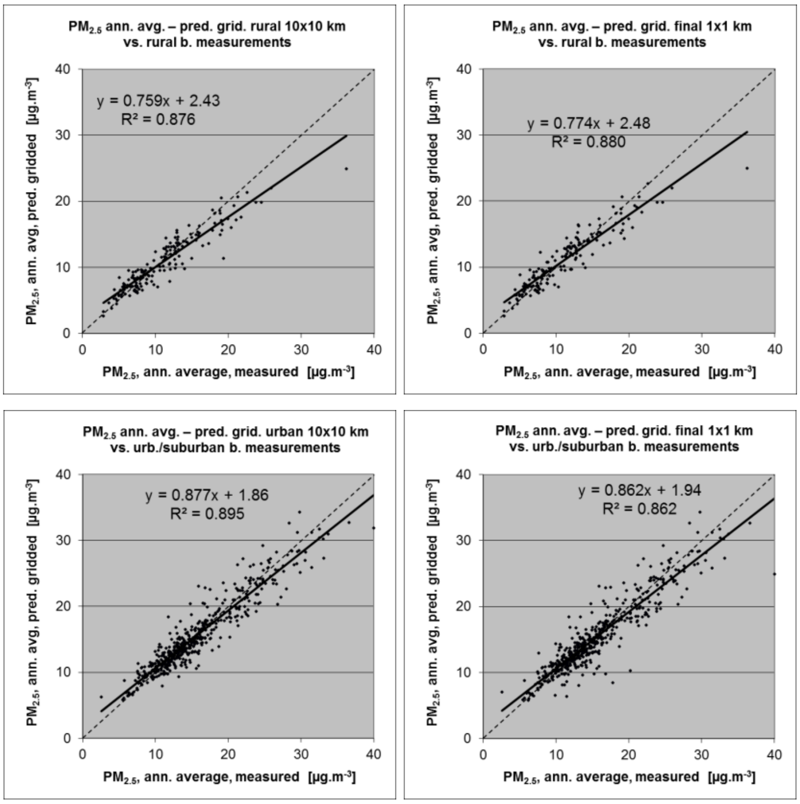

Like in the case of PM_{10}, Table A3.5 shows a better correlated relation with the station measurements (i.e. lower RMSE, higher R^2, smaller intercept and slope closer to 1) for the simply interpolated gridded values than for the point cross-validation predictions, at both rural and urban background map areas. That is because the simple comparison shows the uncertainty at the actual station locations, while the cross-validation prediction simulates the behaviour of the interpolation (within the area covered by measurements) at point positions assuming no actual measurements would exist at these points.

Table A3.5 Statistical indicators from the scatter plots for the predicted point values based on cross-validation and the predicted grid values from separate (rural resp. urban) 10x10 km and final combined 1x1 km versus the measurement point values for rural (left) and urban (right) background stations for $PM_{2.5}$ annual average 2014

$PM_{2.5}$	rural backgr. stations				urban/suburban backgr. stations			
	RMSE	bias	R^2	lin. r. equation	RMSE	bias	R^2	lin r. equation
cross-valid. prediction, separate (r or ub) map	2.5	0.0	0.777	y = 0.707x + 3.25	2.6	0.1	0.810	y = 0.841x + 2.59
grid prediction, 10x10 km separate (r or ub) map	2.0	-0.3	0.876	y = 0.759x + 2.43	1.9	-0.1	0.895	y = 0.877x + 1.86
grid prediction, 1x1 km final combined map	1.9	0.0	0.880	y = 0.774x + 2.48	2.2	-0.2	0.862	y = 0.862x + 1.94

The uncertainty at measurement locations is caused partly by the smoothing effect of the interpolation and partly by the spatial averaging of the values in the 10x10 km grid cells. For example, in urban areas the predicted interpolation gridded value in the separate urban background map will be about 28 $\mu g.m^{-3}$ at the corresponding station point with the measurement value of 30 $\mu g.m^{-3}$, about 6 % too low.

Probability of Target Value exceedance

The probability of target value exceedance map was created for the $PM_{2.5}$ indicator in similar fashion as the PoE maps for PM_{10} indicators. This map at 1x1 km resolution is presented in Map A3.3, with the Target Value (TV) of 25 µg.m^{-3}.

Map A3.3 Map with the probability of the target value exceedance, $PM_{2.5}$ annual average, 2014

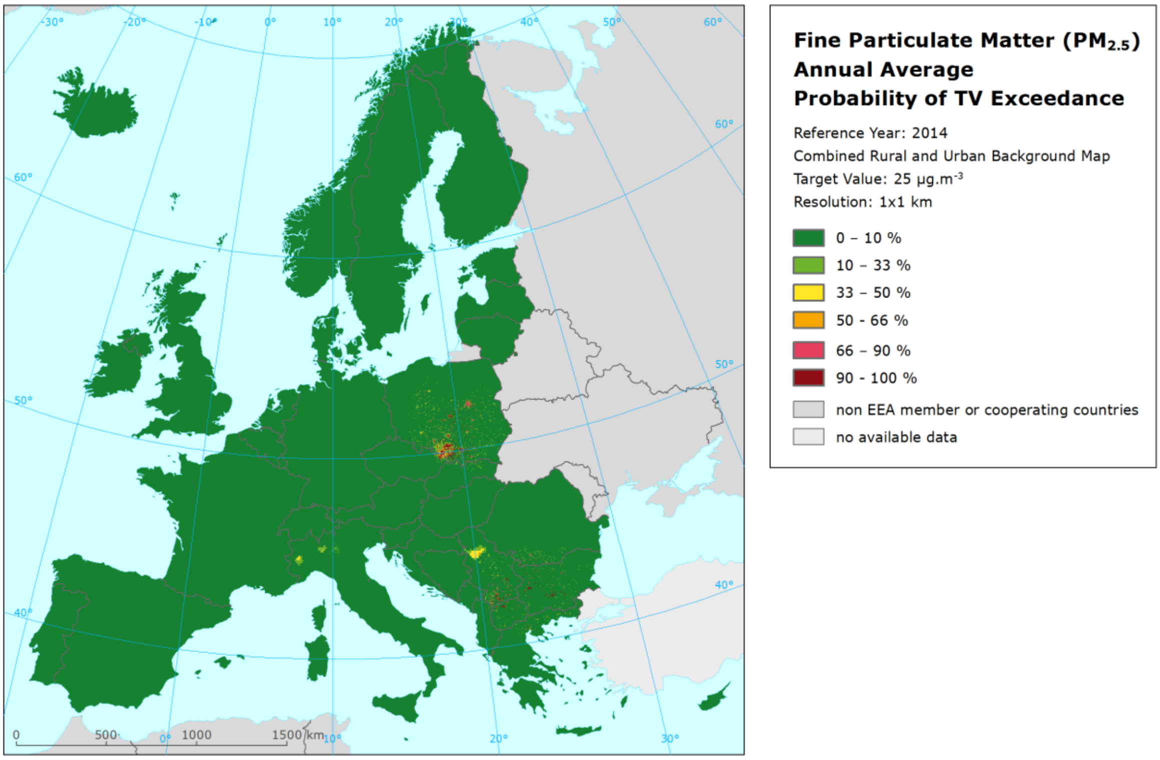

Note: Interpolation uncertainty is considered only, no other sources of uncertainty.

The areas with the highest probability of TV exceedance include the region of southern Poland – north-eastern Czech Republic with the industrial zones of Krakow, Katowice and Ostrava, and the cities in the central part of Poland. Next to this, increased PoE do occur in south-eastern Europe at the larger cities of FYR of Macedonia, Serbia, Bulgaria and in Romania, where only a rather limited set of measurement stations is located. They occur mostly in some urban areas or larger agglomerations such as Bucharest and Craiova with rather high traffic density and heavy industry. Next to this, modest PoE occur in the surroundings of Turin in the northern Italy.

In the other parts of Europe, there is little to no likelihood of TV exceedance, at the level of 10x10 km grids.

One should bear in mind that the map is based on rural and urban/suburban *background* station data only. As such the map reflects rural and urban background situations only. Therefore, this type of map will not resolve the exceedances of limit values that may occur at the many *hotspot* and traffic locations throughout Europe.

A3.3 Ozone

In this section, we present the technical details and the uncertainty estimates for the maps of ozone health-related indicators 93.2 percentile of maximum daily 8-hour means and SOMO35 (i.e. for Maps 4.1 and 4.2), as well as for the maps of ozone vegetation-related indicators AOT40 for vegetation and AOT40 for forests (i.e. for Maps 4.3 and 4.4).

Technical details on the interpolation model

Table A3.6 presents the estimated parameters of the linear regression models and of the residual kriging, including the statistical indicators of both the regression and the kriging.

The adjusted R^2 and standard error show the quality of the regression relation fit. The 93.2 percentile of daily 8-hour maximums shows weaker adjusted R^2 (0.48 resp. 0.38) compared to other indicators, both for rural and for urban areas. In the rural areas, the other three indicators show quite similar values of the adjusted R^2, i.e. 0.55 – 0.57. In the urban areas, the adjusted R^2 for SOMO35 is 0.50. For the vegetation-related indicators the urban maps are not constructed.

Table A3.6 Parameters and statistics of linear regression model and ordinary kriging for ozone indicators 93.2 percentile of maximum daily 8-hourly means and SOMO35 in rural and urban areas for the final combined map and for O_3 indicators AOT40 for vegetation and for forests in rural areas for 2014

		93.2 perc. of dmax 8h		SOMO35		AOT40v	AOT40f
		Rur. areas	Urb. areas	Rur. areas	Urb.areas	Rur. areas	Rur. areas
Linear regression model (LRM, Eq. A1.3)	c (constant)	16.1	48.8	-1629	-1061	-5221	-8912
	a1 (EMEP model)	0.74	0.50	0.50	0.42	0.72	0.54
	a2 (altitude GTOPO)	0.0065		1.54		3.22	5.83
	a3 (wind speed)		-2.91		-132.01		
	a4 (s. solar radiation)	1.41	1.39	322.7	291.26	1047.4	1601.1
	Adjusted R^2	**0.48**	**0.38**	**0.57**	**0.50**	**0.56**	**0.55**
	Stand. Err. [μg.m^{-3}.x]*	**9.0**	**10.4**	**1480**	**1300**	**5242**	**8023**
Ord. krig. (OK) of LRM	nugget	37	38	1.7E+06	9.0E+05	1.3E+07	3.6E+07
	sill	78	39	2.1E+06	1.3E+06	2.4E+07	5.3E+07
	range [km]	900	580	140	250	220	200
LRM + OK of its residuals	**RMSE [μg.m^{-3}.x]***	**7.4**	**7.9**	**1414**	**1133**	**4518**	**7354**
	Relative RMSE [%]	**6.7**	**7.4**	**29.2**	**29.3**	**30.5**	**33.8**
	Bias (MPE) [μg.m^{-3}.x]*	**0.0**	**0.0**	**29**	**5**	**115**	**131**

*) Units for 93.2 percentile of daily 8-h maximums: [μg.m^{-3}], SOMO35: [μg.m^{-3}.d], AOT40c and AOT40f: [μg.m^{-3}.h].

RMSE and bias – highlighted by orange – are the cross-validation indicators, showing the quality of the resulting map. Further in this section, more detailed uncertainty analysis is presented.

Uncertainty estimated by cross-validation

The basic uncertainty analysis is provided by cross-validation. Table A3.6 shows both absolute and relative mean uncertainty, expressed by RMSE and Relative RMSE. The relative mean uncertainty of the 2014 ozone map is about 7 % for both rural and urban areas at the 93.2 percentile of daily 8-h maximums, 29 % for both rural and urban areas at the SOMO35, 31 % at AOT40 for vegetation and 34 % at AOT40 for forests. The small level of the relative uncertainty for the 93.2 percentile of maximum daily 8-h means is given by the concentration level of this indicator. Annex 4 (and specifically Table A4.9) summarises both the absolute and relative uncertainties of different years.

Figure A3.5 shows the cross-validation scatter plots for both the rural and urban areas of the 2014 map for the two health-related ozone indicators.

Figure A3.5 Correlation between cross-validated predicted (y-axis) and measurement values for ozone indicators 93.2 percentile of max. daily 8-hourly means (top) and SOMO35 (bottom) for 2014 for rural (left) and urban (right) areas

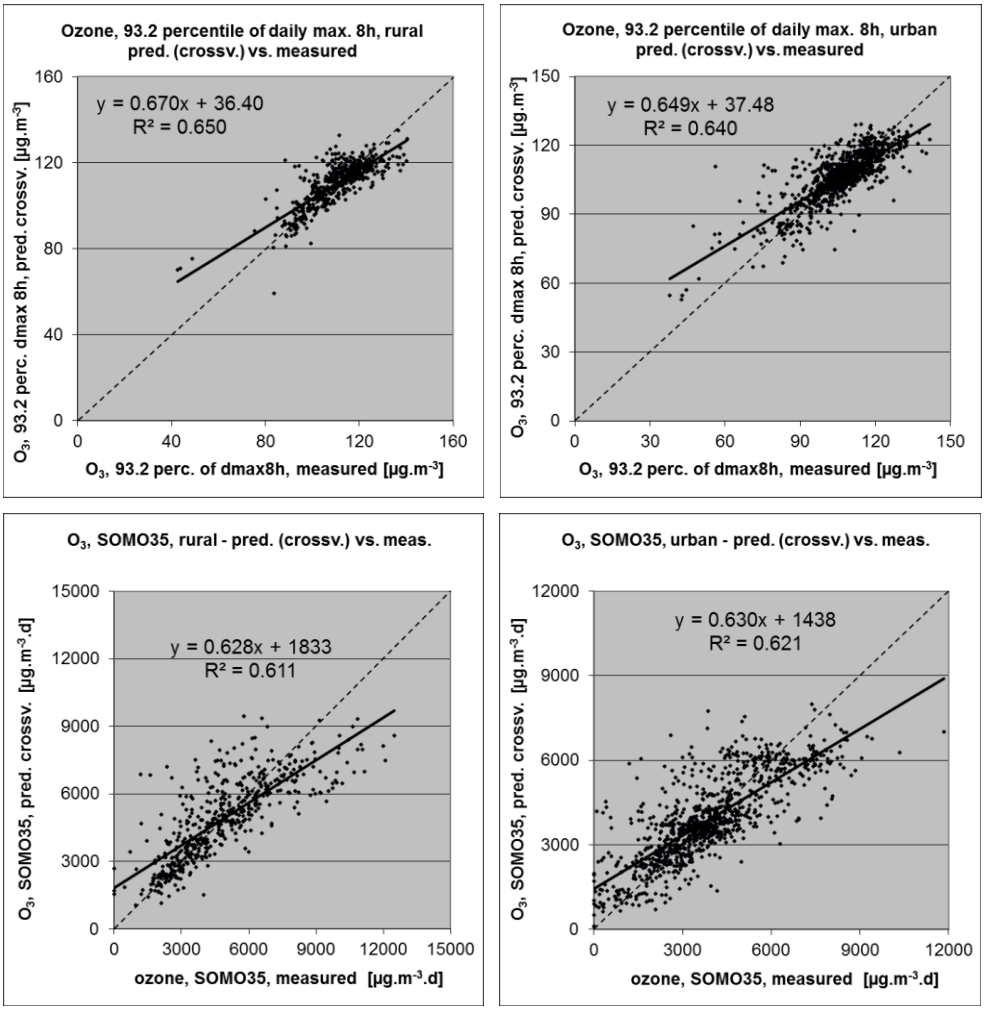

The R^2, an indicator for the interpolation correlation with the observations, shows that about 65 % is attributable to the interpolation in the case of the 93.2 percentile of daily 8-h maximums, while for SOMO35 it is about 62 %. Quite similar fit is found in the previous years (see Table A4.9).

The scatter plots indicate that the higher values are underestimated and the lower values somewhat overestimated by the interpolation method; a typical smoothing effect inherent to the interpolation method with the linear regression and its residuals kriging. For example, in the case of the 93.2 percentile of daily 8-h maximums, in rural areas (Figure A.3.5, left upper panel) an observed value of 135 $\mu g.m^{-3}$ is estimated in the interpolation as 127 $\mu g.m^{-3}$, which is 6 % lower. Or, in the case of SOMO35, in urban areas (right bottom panel of Figure A.3.5) an observed value of 7500 $\mu g.m^{-3}.d$ is estimated in the interpolation as about 6200 $\mu g.m^{-3}.d$, which is 18 % lower.

Figure A3.6 shows the cross-validation scatter plots of the AOT40 for both vegetation and forests. R^2 indicates that about 67 % (in the case of AOT40 for vegetation) resp. 62 % (in the case of AOT40 for forests) of the variability is attributable to the interpolation.

The cross-validation scatter plots show again that in areas with higher accumulated ozone concentrations the interpolation methods tend to deliver underestimated predicted values. For example, in agricultural areas (Figure A3.6, left panel) an observed value of 25 000 $\mu g.m^{-3}.h$ is estimated in the interpolation as about 22 000 µg.m^{-3}.h, i.e. an underestimation of about 12 %. In addition, an overestimation at the lower end of predicted values occurred. One could reduce this under- and overestimation by extending the number of measurement stations and by optimising the spatial distribution of those stations, specifically in areas with elevated values.

Figure A3.6 Correlation between cross-validated predicted (y-axis) and measurement values for ozone indicators AOT40 for vegetation (left) and AOT40 for forests (right) for 2014 for rural areas

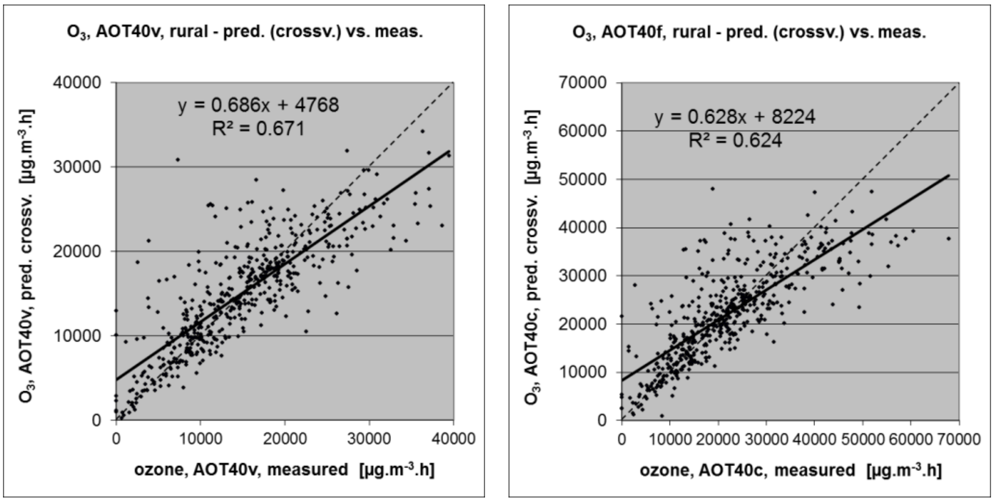

Comparison of point measurement values with the predicted grid value

In addition to the above point observation – point prediction cross-validation, a simple comparison was made between the point observation values and interpolated predicted grid values.

For health related indicators, the comparison has been made primarily for the separate rural and separate urban background maps at 10x10 km resolution. (One can directly relate this comparison result to the cross-validation of the previous section.) Next to this, the comparison has been done also for the final combined maps at 1x1 km resolution.

Figure A3.7 shows the scatterplots for these comparisons, for ozone indicator 93.2 percentile of maximum daily 8-hour means only, as an illustration.

The results of the point observation – point prediction cross-validation of Figure A3.6 and those of the point-grid validation for the separate rural and the separate urban background map, and for the final combined maps at both resolutions are summarised in Table A3.7.

By comparing the scatterplots and the statistical indicators for the separate rural and separate urban background map with the final combined maps, one can evaluate the level of representation of the rural resp. urban background areas in the final combined maps. Both the rural and the urban air quality is fairly well represented in the 1x1 km final combined map.

The uncertainty of the rural and urban background maps at measurement locations is caused partly by the smoothing effect of interpolation and partly by the spatial averaging of the values in the 10x10 km grid cells. The level of smoothing, which leads to underestimation in areas with high values, is weaker in areas where measurements exist than in areas where a measurement point is not available. For example, in the case of the SOMO35, in urban areas an observed value of 7500 µg.m^{-3}.d is estimated in the interpolation as 6400 µg.m^{-3}.d, which is 15 % lower. It is less than the cross-validation underestimation of 18 % at the same point location, when leaving out this one actual measurement point and the interpolation without this station is done (see the previous subsection).

Figure A3.7 Correlation between predicted grid values from rural 10x10 km (upper left), urban 10x10 km (bottom left) and final combined 1x1 km (both right) map (y-axis) versus measurements from rural (top), resp. urban/suburban (bottom) background stations (x-axis) for ozone indicator 93.2 percentile of daily max. 8-hourly means for 2014

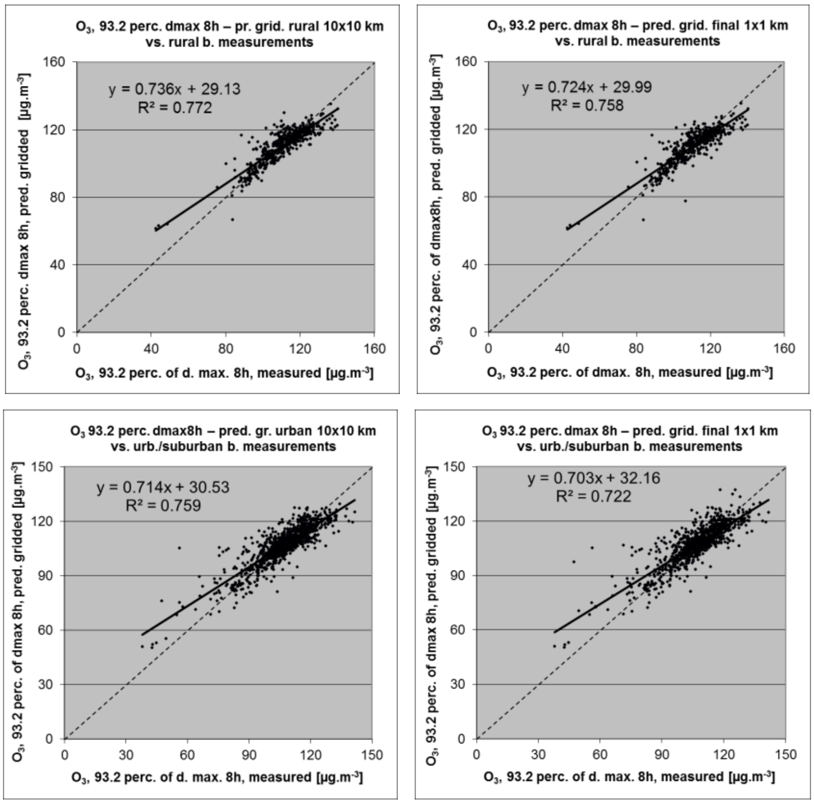

Table A3.7 Statistical indicators from the scatter plots for the predicted point values based on cross-validation and the predicted grid values from separate (rural resp. urban) 10x10 km and final combined 1x1 km map versus the measurement point values for rural (left) and urban (right) background stations for ozone indicators 93.2 percentile of daily max 8h means (top) and SOMO35 (bottom) for 2014

	rural backgr. stations				urban/suburban backgr. stations			
	RMSE	bias	R^2	lin. r. equation	RMSE	bias	R^2	lin r. equation
93.2 percentile of daily max. 8-hour means								
cross-valid. prediction, separate (r or ub) map	3.5	0.1	0.650	y = 0.670x + 36.4	7.9	0.0	0.640	y = 0.649x + 37.5
grid prediction, 10x10 km separate (r or ub) map	6.0	0.0	0.772	y = 0.736x + 29.1	6.5	0.0	0.759	y = 0.714x + 30.5
grid prediction, 1x1 km final merged map	6.2	-0.5	0.758	y = 0.724x + 30.0	7.0	0.5	0.722	y = 0.703x + 32.2
SOMO35								
cross-valid. prediction, separate (r or ub) map	1414	29	0.611	y = 0.628x + 1833	1133	5	0.621	y = 0.630x + 1438
grid prediction, 10x10 km separate (r or ub) map	1160	22	0.741	y = 0.697x + 1493	949	2	0.737	y = 0.691x + 1199
grid prediction, 1x1 km final merged map	1166	-120	0.744	y = 0.680x + 1432	1010	119	0.703	y = 0.717x + 1216

Table A3.8 presents the results of the point observation – point prediction cross-validation of Figure A3.6 and those of the point-grid validation for the rural map, for vegetation related indicators AOT40 for vegetation and AOT40 for forests. Again, one can see for both indicators a better correlation between the station measurements and the averaged interpolated predicted values of the corresponding grid cells, than at the point cross-validation predictions, of Figure A3.6.

Table A3.8 Statistical indicators from the scatter plots for predicted point values based on cross-validation and predicted grid values from rural 2x2 km map versus measurement point values for rural background stations for O_3 indicators AOT40 for vegetation (top) and for forests (bottom) for 2014

	rural backgr. stations			
	RMSE	bias	R^2	linear regression equation
AOT40 for vegetation				
cross-valid. prediction, rural map	4518	115	0.671	y = 0.686x + 4768
grid prediction, 2x2 km rural map	3034	64	0.856	y = 0.792x + 3140
AOT40 for forests				
cross-valid. prediction, rural map	7354	131	0.624	y = 0.628x + 8224
grid prediction, 2x2 km rural map	5424	97	0.802	y = 0.728x + 6012

Probability of Target Value exceedance

Map A3.4 presents a gridded map of 1x1 km resolution showing the probability of target value exceedance for the 93.2 percentile of maximum daily 8-hour means. It was constructed on the basis of the 1x1 km gridded concentration map (Map 4.1), the 1x1 km gridded uncertainty map and the target value (TV) of 120 µg.m^{-3}. Table A1.1 explains the significance of the colour classes in the map.

Map A3.4 Map with the probability of the target value exceedance, ozone indicator 93.2 percentile of maximum daily 8-hour means, 2014

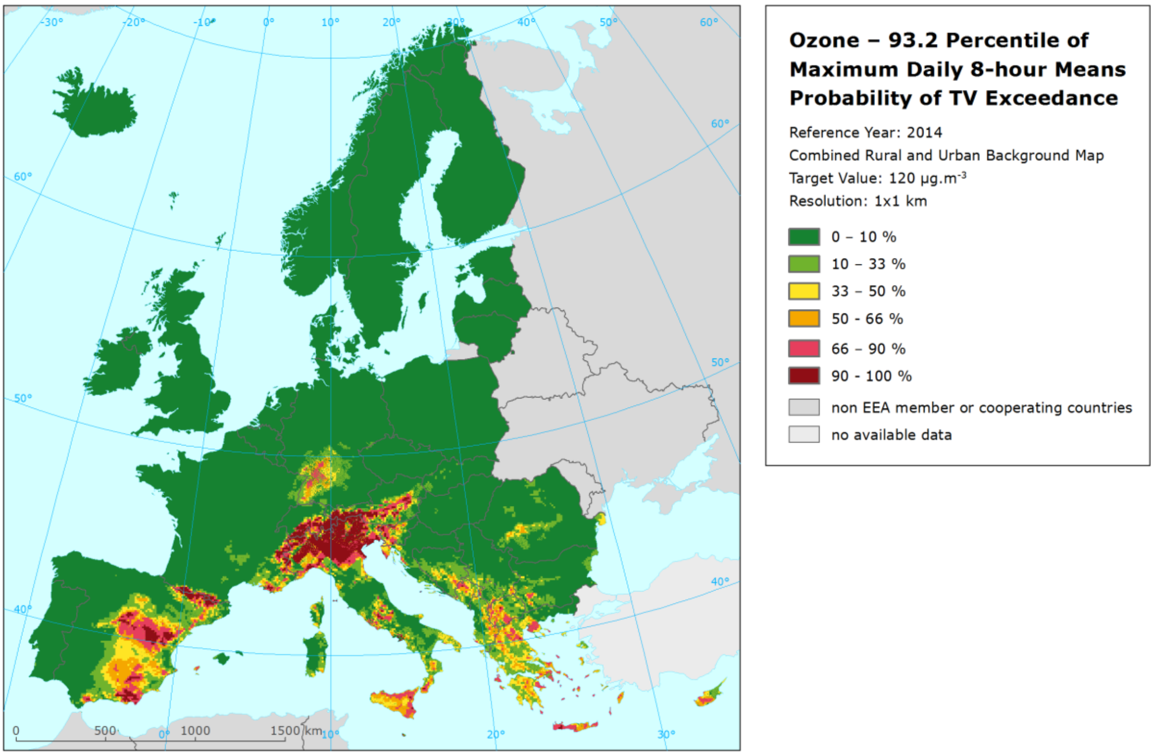

Note: Interpolation uncertainty is considered only, no other sources of uncertainty.

The PoE map for 2014 demonstrates the red or dark red areas (high or large PoE) in the Alpine region, northern, central and southern Italy, southern France, central and southern Spain, the Pyrenees, south-western Germany, Cyprus, Greece, west Bulgaria, and in the west Balkan countries.

No Limit Value or Target Value is set for the WHO recommended ozone health indicator SOMO35, therefore no probability of exceedance map has been prepared.

A3.4 NO_2 and NO_x

In this section, the technical details and the uncertainty estimates for the maps of NO_2 annual average and NO_x annual average, for Maps 5.1 and 5.2, are presented.

Technical details on the interpolation model

In agreement with Horálek et al. (2007) and Annex 1, the NO_x measurements are supplemented by the so-called *pseudo* NO_x stations. The pseudo NO_x data are calculated based on the NO_2 data, using quadratic regression Eq. A1.2. The regression coefficients were estimated based on the rural background stations with both NO_x and NO_2 measurements (see Section 2.1.1). The number of such type of stations is 293. The estimated coefficients of Eq. A1.2 are: $a = 0.0197$, $b = 1.073$, $c = 0.53$.

Table A3.9 presents the estimated parameters of the linear regression models and of the residual kriging and includes the statistical indicators of both the regression and the kriging.

Only stations with measurement data of the relevant pollutant (i.e. not the pseudo stations) are used for calculating of the cross-validation parameters RMSE and bias.

Table A3.9 Parameters and statistics of linear regression model and ordinary kriging of NO_2 annual average for 2014 in rural and urban areas for the final combined map (left) and NO_x annual average for 2014 in rural areas (right)

		NO_2 Annual average		NO_x Annual average
		Rural areas	Urban areas	Rural areas
Linear regresion model (LRM, Eq. A1.3)	c (constant)	10.4	19.34	23.7
	a1 (EMEP model)	0.788	0.53	0.935
	a2 (altitude GTOPO)	-0.0046		-0.0090
	a3 (wind speed)	-1.40	-1.59	-4.32
	a4 (population*1000)		0.015	
	Adjusted R^2	**0.53**	**0.44**	**0.50**
	Standard Error [μg.m^{-3}]	**4.0**	**5.7**	**7.6**
Ordinary kriging (OK) of LRM residuals	nugget	18	21	60
	sill	18	28	67
	range [km]	190	330	560
LRM + OK of its residuals	**RMSE [μg.m^{-3}]**	**4.0**	**5.2**	**5.7**
	Relative RMSE [%]	**43.9**	**25.9**	**47.0**
	Bias (MPE) [μg.m^{-3}]	**0.0**	**0.0**	**0.3**

Uncertainty estimated by cross-validation

Table A3.9 shows both absolute and relative mean uncertainty, expressed by RMSE and Relative RMSE. The absolute mean uncertainty of the final combined map of NO_2 annual average expressed as RMSE is 4 μg.m^{-3} for the rural areas and 5.2 μg.m^{-3} for the urban areas. For the NO_x rural map it is 5.7 μg.m^{-3}.

The relative mean uncertainty of the NO_2 annual average map is 44 % for rural and 26 % for urban areas. The NO_x annual average rural map has a relative mean uncertainty of 47 %.

Figure A3.8 shows the cross-validation scatter plots for NO_2 annual average. The R^2 indicates that about 53 % of the variability is attributable to the interpolation for both the rural and urban areas.

Figure A3.8 Correlation between cross-validated predicted and measurement values for NO_2 annual average 2014 for rural (left) and urban (right) areas

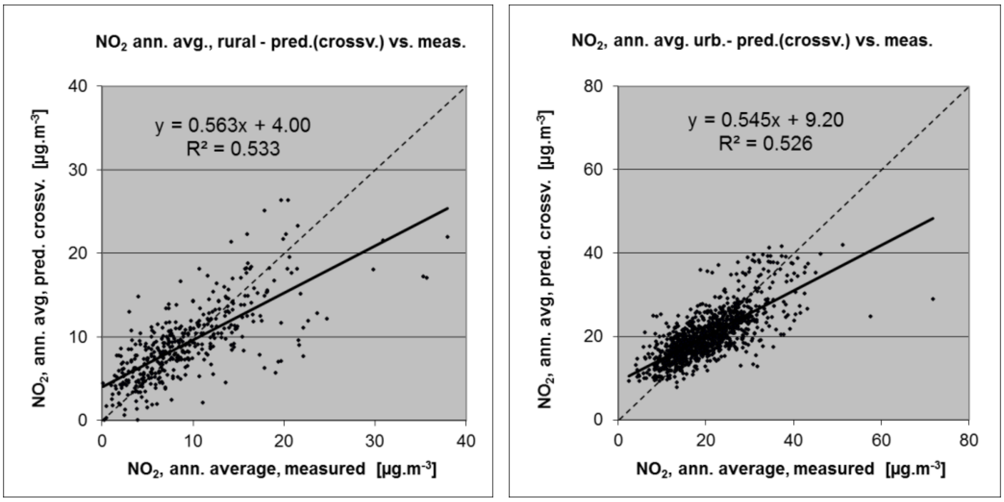

Like in the case of other pollutants, the cross-validation scatter plots indicate the underestimation of high concentrations in the places with no measurements. For example, in urban areas an observed value of 40 µg.m^{-3} is estimated in the interpolations to be about 31 µg.m^{-3}, about 22 % too low.

Figure A3.9 shows the cross-validation scatter plot for NO_x annual average rural map. The R^2 indicates that about 52 % of the variability is attributable to the interpolation.

Figure A3.9 Correlation between cross-validated predicted and measurement values for NO_x annual average 2014 for rural areas

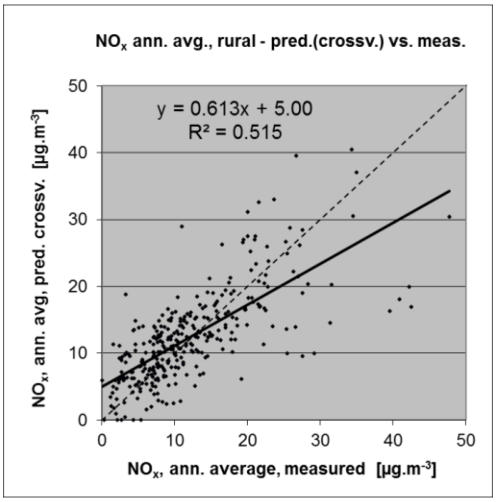

It can be stated that the cross-validation gives poorer results for NO_2 and NO_x maps, compared to PM_{10}, $PM_{2.5}$ and ozone maps. The main reason is the poorer spatial correlation between the predicted and measurement values of NO_2 and NO_x compared to other the pollutants. Therefore, methodological improvement on NO_2 and NO_x mapping is recommended.

Comparison of point measurement values with the predicted grid value

Next to the above presented cross-validation, a simple comparison was made between the point observation values and interpolated predicted grid values.

For NO_2 annual average, the comparison has been made primarily for the separate rural and separate urban background maps at 10x10 km resolution. Beside this, the comparison has been done also for the final combined maps at 1x1 km resolution.

Table A3.10 presents the results of this comparison, together with the results of cross-validation prediction of Figure A3.8.

Table A3.10 Statistical indicators from the scatter plots for the predicted point values based on cross-validation and the predicted grid values from separate (rural resp. urban) 10x10 km and final combined 1x1 km map versus the measurement point values for rural (left) and urban (right) background stations for NO_2 annual average 2014

	rural backgr. stations				urban/suburban backgr. stations			
	RMSE	bias	R^2	lin. r. equation	RMSE	bias	R^2	lin r. equation
cross-valid. prediction, separate (r or ub) map	3.5	4.0	0.533	y = 0.563x + 4.00	5.2	0.0	0.526	y = 0.545x + 9.20
grid prediction, 10x10 km separate (r or ub) map	3.8	0.0	0.568	y = 0.581x + 3.83	4.6	0.0	0.633	y = 0.601x + 8.06
grid prediction, 1x1 km final merged map	4.0	1.3	0.610	y = 0.732x + 3.72	5.0	-0.8	0.590	y = 0.633x + 6.627

Table A3.11 presents the cross-validation results of Figure A3.9 and those of the point-grid simple validation for the rural map of NO_x annual average.

Table A3.11 Statistical indicators from the scatter plots for predicted point values based on cross-validation and predicted grid values from rural 2x2 km map versus measurement point values for rural background stations for NO_x annual average 2014

	rural background stations			
	RMSE	bias	R^2	linear regression equation
cross-valid. prediction, rural map	5.7	0.3	0.515	y = 0.613x + 5.00
grid prediction, 2x2 km rural map	5.5	0.3	0.536	y = 0.623x + 4.87

Annex 4 Inter annual changes

A4.1 PM_{10}

Air concentrations

Map A4.1 presents the inter-annual difference between 2014 and 2013 for annual average PM_{10}. Red areas show an increase of PM_{10} concentration in 2014, while blue areas show a decrease. The highest increases are observed at the eastern areas of Slovakia and Hungary bordering Ukraine and the South-East coastal area of Spain. Other increases are at areas of Poland, Lithuania, Germany and Denmark around the most southern part of the Baltic Sea. More local increases are observed at part of Greece, Bulgaria, the Balkan and Cyprus. Contrary to that, high decreases occur in north-western France and Île de France, and in the Po Valley. Overall, the pattern of the 2014-2013 difference map seems to be rather the opposite of that of the 2013-2012 difference in Horálek et al (2016b). The fluctuations over years seem to be mostly related to the annual meteorological variability. Besides the actual changes in the concentrations, the variability of the linear regression model and variogram parameters may cause minor differences in the concentration levels estimated.

Map A4.1 Difference of PM_{10} annual average concentrations between 2013 and 2014

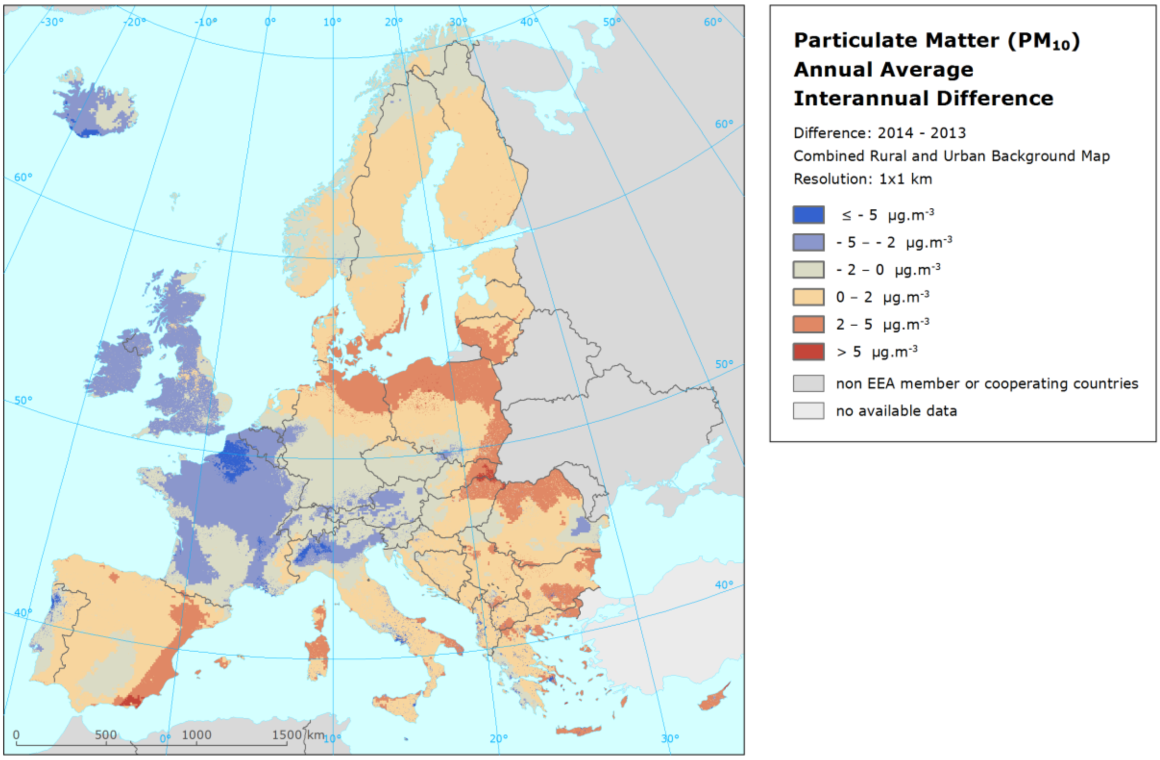

Map A4.2 presents the inter-annual difference between 2014 and 2013 for the 90.4 percentile of the daily mean PM_{10} concentrations. The highest increases are observed in northern Germany, eastern Slovakia/ Hungary and locally on the Balkans. Around the Baltic Sea, large parts of surrounding countries, as well as Denmark and the north-eastern part of The Netherlands, the eastern part of Slovakia and Hungary, part of Bulgaria, the northern Balkan area, the eastern part of Spain and South Italy show increases. The most prominent decreases occur in north-western France and Île de France, and in the Po Valley. Furthermore, decreases are observed in the centre of France in southern Germany, western Austria, Switzerland, Ireland and large rural parts of the UK.

Map A4.2 Difference 90.4 percentile of daily means PM_{10} concentration between 2013 and 2014

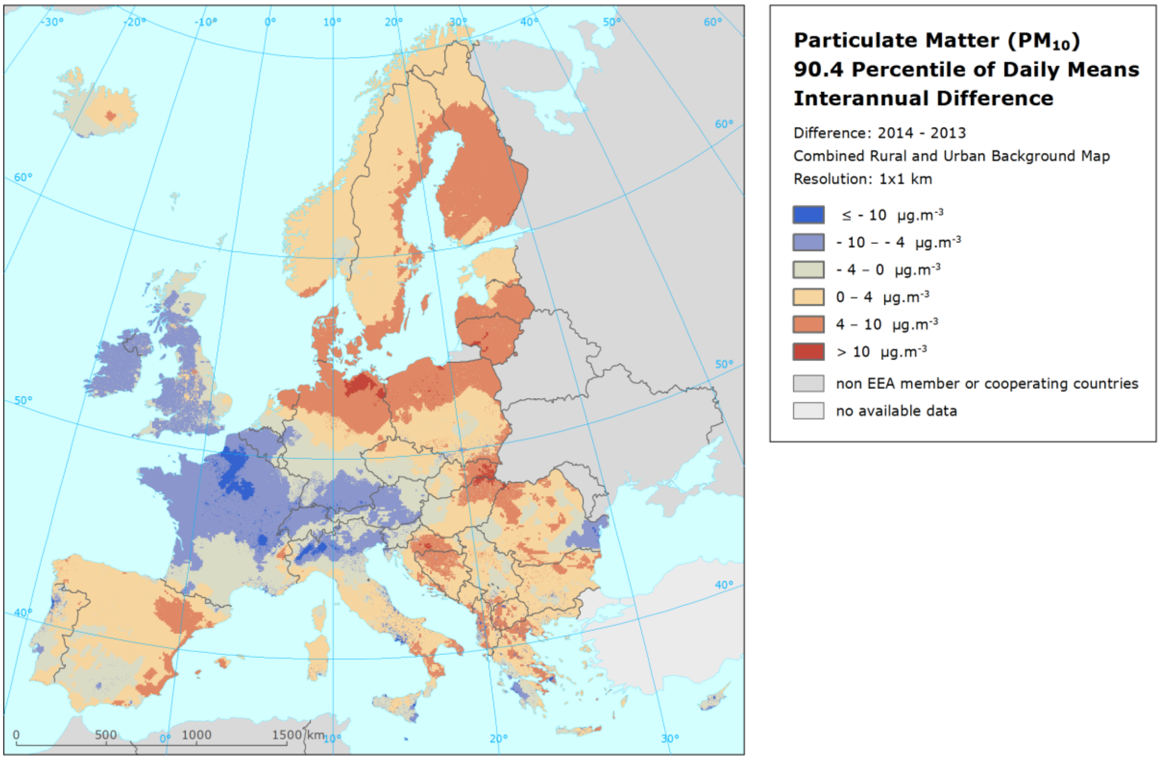

Population exposure

Table A4.1 provides the inter-annual variation in population exposure for PM_{10} annual average over 2005 – 2014 for individual countries and for Europe as a whole, based on the results presented in Chapter 2.1 and in Horálek et al. (2016b and references cited therein). Next to this, the table shows the inter-annual difference between 2013 and 2014. Also, the result of the trend analysis (as described in Section A1.2 of Annex 1) for the ten-year period 2005 – 2014 is presented. The table shows the significance of a linear trend and – if the trend is significant – the slope of this trend.

In 2014, the overall average population-weighted annual mean PM_{10} concentration for the whole of Europe was 21.1 $\mu g.m^{-3}$. This is of more than 1 $\mu g.m^{-3}$ less than in the previous year and the lowest in the whole ten-year period. One may observe a steady reduction of the population-weighted concentration over the period of time 2005 – 2011, with perhaps some flattening effect in 2011 – 2013 and further reduction in 2014. The steepest decrease of population-weighted concentration per country compared to 2013 took place in Greece, Malta, Albania, FYR of Macedonia, France and Cyprus. The highest increase was detected in Denmark, Finland, Lithuania and Estonia.

For most of the countries, significant downward trend is detected. It is detected for almost all countries of northern and western Europe (i.e. apart from France, Luxemburg, Ireland and Iceland), for the most of the southern Europe (e.g. for Portugal, Spain and Italy) and the most of the Balkan countries. Contrary to this, no significant trend is detected e.g. for Poland, Czech Republic, Slovakia, Baltic countries, Greece and Cyprus.

The overall picture of the population-weighted concentration for the totals of 40 European countries demonstrates a downward trend for the years 2005 – 2014. This trend is statistically significant, the slope is about -0.8 $\mu g.m^{-3}$ per year, which means the mean decrease of 0.8 $\mu g.m^{-3}$ per year. For the EU-28, the slope is about -0.7 $\mu g.m^{-3}$ per year.

Table A4.1 Evolution and trend in 2005–2014 and difference between 2014 and 2013 for population-weighted concentration, PM_{10} annual average. Trend estimates are only given when a significant trend is observed (p >0.1).

Country		Population-weighted conc. [μg.m^{-3}]											Trend of pop.-weighted conc. 2005–2014	
		2005	2006	2007	2008	2009	2010	2011	2012	2013	2014	Differ. '14 - '13	Signific.	Slope [μg.m^{-3}.year^{-1}]
Albania	AL	36.3	31.8	31.6	33.3	35.3	45.5	26.5	32.0	32.5	25.7	-6.8		
Andorra	AD	19.5	22.5	20.5	18.7	17.7	17.9	18.0	33.2	25.0	21.3	-3.7		
Austria	AT	25.4	26.0	22.1	21.3	21.6	22.7	20.8	20.0	20.2	17.8	-2.3	**	-0.8
Belgium	BE	29.2	31.3	24.8	23.9	26.5	25.7	24.8	23.2	23.6	20.2	-3.4	**	-0.9
Bosnia-Herzegovina	BA	34.3	33.1	32.4	29.3	37.2	30.8	22.3	27.2	23.1	22.1	-1.0	**	-1.4
Bulgaria	BG	42.6	41.6	40.2	44.2	39.8	38.0	27.3	36.6	36.7	36.2	-0.5	**	-0.7
Croatia	HR	33.6	31.5	30.0	28.1	29.0	27.3	25.0	24.7	23.5	21.7	-1.8	***	-1.3
Cyprus	CY	38.9	35.4	33.9	76.1	41.0	50.2	31.1	42.9	35.8	32.1	-3.7		
Czech Republic	CZ	32.9	33.5	25.6	24.2	25.3	28.3	23.7	25.4	25.6	25.5	-0.1		
Denmark	DK	21.3	23.5	20.8	18.8	16.3	15.7	18.4	16.3	16.3	18.5	2.3	*	-0.6
Estonia	EE	17.7	19.7	15.7	12.9	13.4	14.1	9.8	12.1	13.5	14.8	1.3		
Finland	FI	14.2	17.0	13.7	12.5	11.7	12.2	9.5	10.2	10.5	12.0	1.4	*	-0.6
France	FR	19.3	20.4	24.6	22.6	24.0	23.0	21.8	21.4	20.7	16.7	-4.0		
Germany	DE	23.0	24.2	20.7	19.6	20.7	21.2	19.6	18.4	19.0	18.7	-0.4	**	-0.5
Greece	GR	38.0	33.6	33.5	39.7	35.3	37.3	24.6	30.3	34.6	27.4	-7.2		
Hungary	HU	34.8	32.9	28.7	26.8	27.6	28.1	29.1	26.1	25.3	25.4	0.1	*	-0.8
Iceland	IS	13.8	17.4	12.2	15.2	9.0	10.7	9.3	9.6	11.8	12.7	0.9		
Ireland	IE	12.7	14.9	14.7	15.4	12.8	13.7	12.8	12.4	15.1	13.7	-1.4		
Italy	IT	34.9	33.9	33.2	30.1	28.7	26.4	27.7	27.0	27.0	24.0	-3.0	**	-1.1
Latvia	LV	19.8	21.9	17.8	19.1	18.8	21.5	14.6	18.0	19.5	20.3	0.8		
Liechtenstein	LI	23.4	24.9	20.7	20.6	18.3	17.3	11.3	14.3	15.5	13.1	-2.4	**	-1.3
Lithuania	LT	20.7	22.5	18.5	17.3	19.0	22.0	14.8	18.1	20.4	21.7	1.3		
Luxembourg	LU	18.7	20.8	19.5	18.2	21.0	19.4	16.4	17.2	18.8	17.4	-1.4		
Macedonia, FYR of	MK	46.2	39.3	38.5	41.6	45.4	43.9	23.0	42.3	44.5	39.3	-5.1		
Malta	MT	37.1	29.4	27.0	27.5	27.2	32.5	27.8	25.4	35.7	28.9	-6.8		
Monaco	MC		36.7	34.5	29.5	26.8	24.0	22.8	28.0	22.7	22.3	-0.4	+	-1.3
Montenegro	ME	35.1	33.1	33.1	33.6	35.0	32.8	21.5	28.3	27.0	24.6	-2.4	*	-1.1
Netherlands	NL	29.2	29.1	25.8	24.0	24.3	24.3	25.1	21.1	20.7	20.2	-0.5	**	-0.9
Norway	NO	18.1	19.6	15.6	15.7	14.1	14.7	9.3	12.2	13.8	12.6	-1.2	*	-0.7
Poland	PL	32.7	37.0	28.8	28.3	30.8	35.2	27.2	32.4	30.4	31.5	1.1		
Portugal	PT	30.9	28.4	27.0	21.8	22.9	21.7	20.8	19.9	20.3	16.9	-3.4	***	-1.4
Romania	RO	42.7	39.1	35.0	30.8	28.9	25.2	27.2	28.9	26.0	25.9	0.0	**	-1.8
San Marino	SM	31.7	33.9	31.2	29.6	26.0	25.0	20.9	25.8	22.1	21.2	-1.0	**	-1.4
Serbia (incl. Kosovo*)	RS	44.2	41.8	39.4	40.1	39.5	33.1	30.1	34.9	31.8	32.1	0.3	**	-1.4
Slovakia	SK	34.3	33.8	29.1	26.7	26.9	30.2	27.4	27.9	26.8	27.2	0.4		
Slovenia	SI	30.8	29.0	27.2	25.0	25.2	26.0	25.4	24.3	22.7	20.3	-2.4	**	-1.0
Spain	ES	29.6	31.4	29.6	25.2	23.7	21.4	18.8	20.9	19.1	19.7	0.6	**	-1.5
Sweden	SE	16.9	19.0	15.7	16.3	13.8	12.8	12.3	12.4	13.2	13.8	0.6	*	-0.6
Switzerland	CH	21.3	23.2	21.4	20.5	21.0	19.8	17.7	17.6	18.3	16.5	-1.8	**	-0.7
United Kingdom	UK	21.4	23.2	21.6	19.5	18.4	18.2	17.5	16.5	17.0	16.6	-0.4	**	-0.7
Total		**28.0**	**28.5**	**26.2**	**24.8**	**24.6**	**24.3**	**22.1**	**22.7**	**22.2**	**21.1**	**-1.2**	*******	**-0.8**
EU-28		**27.6**	**28.3**	**26.0**	**24.4**	**24.2**	**24.0**	**22.1**	**22.4**	**22.1**	**20.9**	**-1.2**	*******	**-0.7**

*) under the UN Security Council Resolution 1244/99

EEA (2016b) estimates for the EU-28 for the period 2000 – 2014 an average slope of -0.7 μg.m^{-3} per year measured at the urban/suburban background stations, which one may consider as representative for the most populated areas, and -0.4 μg.m^{-3} per year measured at the rural background stations. The differences in the slope estimates by EEA (2016b) and our paper have their origin in a number of causes, as described further. *Different concentration entity:* EEA (2016b) estimates the trends in the measured 'air pollutant concentrations' at the stations, whereas this paper estimates trends in 'population weighted concentrations'. *Different geographical distribution entity:* EEA (2016b) considers trends at a number of measurement stations ('points') with a certain scatter of spatial distribution and spatial density characteristics varying over Europe, whereas this paper accounts for a complete coverage of the European mapping domain with a set of 'grid cells' as geographical characteristic. *Different 'sample set'*: the set of station point used at EEA (2016b) differs somewhat in its number, its allocation and its spatial distribution/occurrence over Europe, from that of the interpolated mapping in this paper. *Different trend period:* EEA (2016b) estimates the trends at measurement stations over a period of 2000 – 2014, whereas this paper considers in most cases a period of 2005 – 2014. These differences will lead to differences in the average trend levels derived in EEA 2016b and in this paper, such that they need to be compared with the necessary care and reserve.

Table A4.2 shows the evolution of the annual population exposure in the period 2005-2014, the inter-annual difference between 2013 and 2014, and the results of the trend analysis in relation to the PM10 daily limit value. For the period 2005 – 2011, the results of the 36th highest daily mean are presented, while the results of the 90.4 percentile of daily means are given for the period 2012 – 2014. Both statistics are related with the PM_{10} daily limit value according to the AQ Directive (EU, 2008), however the 36th highest daily mean results are somewhat underestimated due to the incompleteness in time series of the measurement data. The level of the underestimation of the population exposure for the whole Europe is almost 1 $\mu g.m^{-3}$ (see Table 6.1), and can explain the most of the increase in 2012 with respect to 2011.

The European-wide population-weighted 90.4 percentile of the daily mean concentrations is estimated for 2014 at 37.1 $\mu g.m^{-3}$, 2.3 $\mu g.m^{-3}$ lower compared to 2013 and the lowest in the period of 2005 – 2014 (even if, as said, until 2011 the underestimated 36th highest daily mean was used).

The overall picture of the population-weighted concentration of both the overall European totals (i.e. totals of 40 European countries) and the EU-28 demonstrates a downward trend of -1.0 $\mu g.m^{-3}$ per year for the years 2005 – 2014, which is statistically significant and means an average decrease of 1.0 $\mu g.m^{-3}$ per year. Due to the underestimation of the values for the 36th highest daily mean, one may conclude the slope is in fact slightly steeper. EEA (2016b) estimates for the EU-28 for the period 2000 – 2014 an average slope of -0.9 $\mu g.m^{-3}$ per year measured at the urban/suburban background stations and -0.7 $\mu g.m^{-3}$ per year measured at the rural background stations. As stated above, the differences between the slope estimates of EEA (2016b) and of this paper have their cause in the differences in the compared entity (i.e. concentration vs. population weighted concentration), in the number and spatial distribution of the stations considered, in the spatial interpolation, and in the different periods of time the trends are accounted for.

The steepest decrease of population-weighted concentration per country compared to 2013 took place in Malta, Greece, Albania, FYR of Macedonia, and Cyprus. The highest increase was detected in Denmark, Lithuania, Finland and Estonia. The results are similar to those obtained for the annual mean.

A significant downward trend is detected for about half of the countries; for the rest no significant trend is detected. However, without the underestimation of the values for the 36th highest daily mean, probably the downward trend would be detected at more countries. This trend is detected for almost the same countries as for the annual average. Across Europe a similar pattern as for the annual average is observed here.

Next to the population-weighted concentration, another trend indicator is the evolution of the percentage of population living in areas with concentrations above the limit value. However, the percentage of population living above the limit value is not a very robust statistical parameter: small changes in concentration might result in large changes in exposed population. The evolution of this statistics for Europe as a whole is presented in Table 6.1. In comparison with the previous nine years, the percentage of population living in areas above the LV is the lowest in 2014. The table showing the evolution of the percentage population in exceedance for individual countries is presented as a supplementary material at the web page http://acm.eionet.europa.eu/reports/ETCACM_TP_2016_6_AQMaps2014, i.e. at the web page of this paper.

Table A4.2 Evolution and trend in 2005–2014 and difference between 2014 and 2013 for population-weighted concentration, PM_{10} indicator 36th highest daily mean / 90.4 percentile of daily means. Trend estimates are only given when a significant trend is observed (p >0.1).

Country		Population-weighted conc. [µg.m^{-3}]											Trend of pop.-weighted conc. 2005–2014	
		36th highest daily mean							90.4 perc. of daily means					
		2005	2006	2007	2008	2009	2010	2011	2012	2013	2014	diff. '14 - '13	Signific.	Slope [µg.m^{-3}.year^{-1}]
Albania	AL	59.8	54.0	53.3	55.7	51.3	69.5	42.8	57.2	61.4	47.4	-14.0		
Andorra	AD	31.1	35.7	32.1	29.3	29.4	28.5	29.2	78.4	47.6	41.9	-5.7		
Austria	AT	45.7	47.1	39.9	36.9	36.7	42.8	38.7	36.1	37.0	32.4	-4.6	*	-1.2
Belgium	BE	46.9	51.3	43.5	38.4	45.8	42.7	45.1	43.9	41.2	35.0	-6.2	*	-1.1
Bosnia-Herzegovina	BA	57.3	57.4	52.7	50.6	57.8	53.7	40.8	52.8	44.2	44.2	0.0		
Bulgaria	BG	73.3	74.2	67.5	78.2	70.3	69.2	46.6	66.9	67.9	68.4	0.5		
Croatia	HR	57.6	53.7	49.6	48.6	46.9	50.5	46.6	45.5	44.6	42.1	-2.5	***	-1.4
Cyprus	CY	63.7	58.2	54.4	130.7	68.6	74.5	46.2	62.0	56.9	47.4	-9.4		
Czech Republic	CZ	60.2	57.5	46.2	42.5	43.6	53.7	46.2	47.6	46.9	47.3	0.4		
Denmark	DK	34.5	37.0	32.5	29.0	26.0	25.5	31.6	26.3	26.7	32.6	5.9		
Estonia	EE	31.7	34.1	28.0	22.4	22.4	25.8	17.6	21.6	22.6	26.4	3.8		
Finland	FI	24.2	29.5	23.9	21.9	19.4	22.7	16.9	18.3	18.0	22.4	4.4	*	-0.8
France	FR	29.8	32.9	41.0	36.3	39.2	37.1	36.6	38.1	36.9	28.2	-8.7		
Germany	DE	38.6	41.3	35.7	31.7	34.4	37.2	35.7	32.8	32.9	33.0	0.1		
Greece	GR	59.9	54.3	53.0	64.9	54.7	64.8	37.6	47.8	61.2	46.4	-14.8		
Hungary	HU	61.6	58.5	48.5	47.5	46.4	52.3	55.4	47.2	44.6	45.3	0.7	*	-1.2
Iceland	IS	19.0	27.2	21.4	25.4	15.8	16.8	15.8	17.6	20.1	22.3	2.2		
Ireland	IE	17.8	24.1	24.8	25.8	21.7	23.2	23.2	21.8	26.3	23.6	-2.7		
Italy	IT	60.2	58.6	57.4	51.7	48.6	45.2	48.6	48.0	49.7	42.1	-7.6	**	-1.8
Latvia	LV	35.9	40.0	31.9	32.7	33.4	37.8	26.7	33.7	33.0	36.1	3.1		
Liechtenstein	LI	40.2	47.5	39.3	38.5	31.5	33.6	21.3	27.7	32.4	23.6	-8.8	**	-2.2
Lithuania	LT	37.7	39.7	33.2	29.5	32.7	39.5	26.6	33.9	34.1	38.8	4.7		
Luxembourg	LU	31.2	35.9	32.5	29.1	34.3	31.9	29.4	30.6	31.5	29.6	-1.9		
Macedonia, FYR of	MK	77.5	69.9	57.8	71.5	75.6	80.1	37.9	80.4	93.1	80.9	-12.2	+	1.6
Malta	MT	62.7	44.8	42.6	40.3	38.7	49.4	39.7	37.8	62.2	42.4	-19.8		
Monaco	MC		59.7	46.2	46.0	41.5	36.1	37.0	46.0	39.0	34.8	-4.2		
Montenegro	ME	58.7	57.9	53.6	56.7	51.8	54.0	36.2	55.9	53.6	49.2	-4.5	*	-0.8
Netherlands	NL	47.5	46.1	41.9	37.7	39.0	40.2	44.0	35.8	34.2	34.5	0.2	*	-1.4
Norway	NO	29.3	31.9	26.3	26.1	24.0	25.7	16.3	21.9	23.7	22.4	-1.3	**	-0.9
Poland	PL	58.6	64.0	50.8	48.6	55.4	65.7	51.4	62.7	55.4	58.0	2.7		
Portugal	PT	52.0	48.3	45.0	35.5	38.5	35.6	35.4	35.8	34.5	29.9	-4.6	**	-2.2
Romania	RO	73.4	65.4	57.7	53.1	49.0	45.2	48.1	50.0	45.4	45.4	0.0	**	-2.6
San Marino	SM	51.7	57.4	54.1	48.9	40.6	44.0	35.9	44.3	40.2	38.5	-1.7	*	-2.2
Serbia (incl. Kosovo*)	RS	73.1	73.1	61.8	68.6	67.6	60.1	54.6	65.9	61.3	63.3	1.9	*	-1.2
Slovakia	SK	60.9	58.5	50.5	47.5	46.2	56.0	51.5	51.6	47.5	48.7	1.2		
Slovenia	SI	53.7	49.2	46.1	42.7	41.9	47.2	48.1	44.0	42.2	37.3	-4.9	*	-1.3
Spain	ES	46.7	49.3	46.9	40.1	38.0	33.4	30.5	34.2	30.7	32.0	1.2	**	-2.2
Sweden	SE	27.7	32.0	25.8	26.4	23.3	22.1	21.1	21.2	22.5	24.3	1.8	*	-0.9
Switzerland	CH	36.0	43.9	39.9	36.5	37.1	36.3	33.0	32.8	36.5	28.3	-8.3	*	-1.2
United Kingdom	UK	32.5	35.5	34.7	32.1	30.1	28.8	30.3	29.6	29.0	28.7	-0.3	**	-0.6
Total		**46.8**	**47.8**	**44.1**	**41.3**	**41.2**	**41.9**	**39.0**	**40.6**	**39.4**	**37.1**	**-2.3**	**	**-1.0**
EU-28		**46.1**	**47.2**	**43.8**	**40.5**	**40.5**	**41.3**	**39.0**	**40.0**	**38.8**	**36.6**	**-2.2**	**	**-1.0**

*) under the UN Security Council Resolution 1244/99

Uncertainties

Table A4.3 summarises the ten-year evolution of the absolute and relative mean interpolation uncertainties, and also R^2 from cross-validation scatterplots, for the rural and maps, for both PM_{10} indicators.

In the year 2014, both the absolute uncertainty results show similar or slightly worse levels compared to 2013 and lower levels compared to all previous years 2005 – 2012, for both PM_{10} indicators. The low uncertainty levels in the urban areas in 2013 – 2014 are influenced by a lack of Turkish urban background stations in these years. Turkish urban stations show high concentrations and uncertainty statistics are sensitive to such values. The results from the Turkish urban background stations were reported since 2008 to 2012, but not in 2013 and 2014.

The results for R^2 from cross-validation scatterplots show quite similar levels to the previous four years.

Table A4.3 Absolute and relative mean uncertainty and R^2 from cross-validation scatterplot for the total European rural and urban areas, PM_{10} indicators annual average and 90.4 percentile of daily means, years 2005 – 2014

PM10			2005	2006	2007	2008	2009	2010	2011	2012	2013	2014
Annual average												
rural areas	abs. mean uncertainty	RMSE [μg.m^{-3}]	5.5	5.8	4.6	5.0	4.6	4.5	4.1	3.8	3.4	3.5
	rel. mean uncertainty	RRMSE [%]	*25.9*	*26.6*	*23.5*	*27.2*	*23.9*	*22.7*	*21.1*	*21.4*	*19.6*	*20.7*
	coeff. of determinatio	R^2	*0.52*	*0.52*	*0.59*	*0.48*	*0.54*	*0.62*	*0.68*	*0.67*	*0.70*	*0.68*
urban areas	abs. mean uncertainty	RMSE [μg.m^{-3}]	5.5	6.1	5.0	6.3	6.7	6.6	6.1	6.1	4.3	4.2
	rel. mean uncertainty	RRMSE [%]	*20.0*	*20.9*	*18.4*	*22.4*	*23.0*	*22.5*	*20.7*	*22.1*	*17.3*	*17.7*
	coeff. of determinatio	R^2	*0.71*	*0.69*	*0.66*	*0.82*	*0.73*	*0.75*	*0.77*	*0.76*	*0.74*	*0.76*
36th max. daily mean (2005 - 2011) / 90.4 percentile of daily means (2012 - 2014)												
rural areas	abs. mean uncertainty	RMSE [μg.m^{-3}]	9.7	9.9	8.0	8.8	8.0	8.6	8.4	7.8	6.5	6.5
	rel. mean uncertainty	RRMSE [%]	*26.3*	*26.6*	*23.5*	*28.2*	*24.1*	*24.4*	*23.5*	*24.3*	*21.0*	*21.5*
	coeff. of determinatio	R^2	*0.55*	*0.56*	*0.60*	*0.52*	*0.56*	*0.64*	*0.66*	*0.64*	*0.69*	*0.69*
urban areas	abs. mean uncertainty	RMSE [μg.m^{-3}]	9.9	11.7	9.1	12.7	13.2	12.2	13.0	12.1	8.6	8.6
	rel. mean uncertainty	RRMSE [%]	*21.4*	*23.5*	*19.6*	*24.4*	*26.7*	*23.7*	*24.3*	*25.0*	*19.5*	*20.4*
	coeff. of determinatio	R^2	*0.75*	*0.65*	*0.65*	*0.79*	*0.72*	*0.77*	*0.75*	*0.75*	*0.75*	*0.76*

A4.2 $PM_{2.5}$

Air concentrations

Map A4.3 presents the inter-annual difference between 2014 and 2013 for annual average $PM_{2.5}$.

The highest increases are seen in northern Germany near the Baltic Sea. Smaller increases are observed in central Finland, Lithuania, Denmark, northern Germany, northern Poland and south-eastern Sweden, eastern Slovakia and in the central Balkan region. The steepest decrease is observed in a large part of France, in Romania, the Po valley, Switzerland and western Austria. The area ranging from France, southern Germany, Switzerland, Austria and Slovenia shows decreased concentrations in 2014 compared to 2013.

Map A4.3 Difference $PM_{2.5}$ annual average concentrations between 2014 and 2013

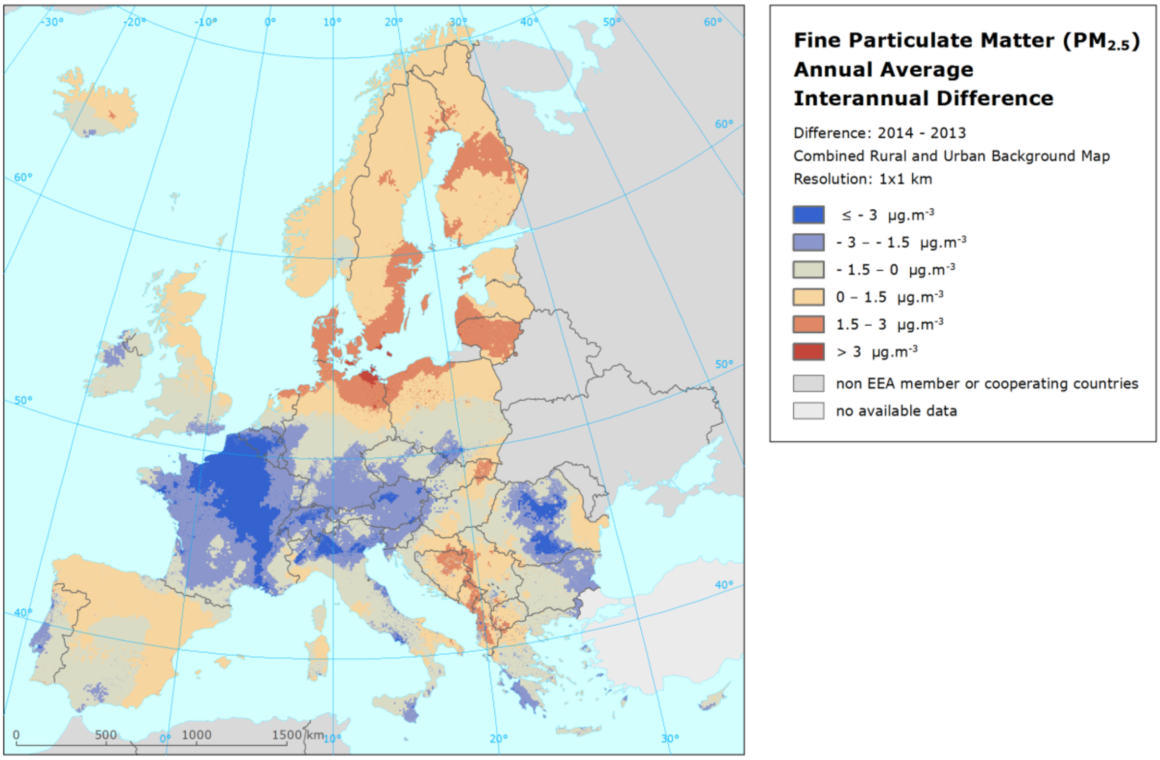

Population exposure

Table A4.4 shows the evolution of the population exposure for the years 2007 – 2014, with missing calculations for 2009, based on the results presented in Chapter 3.1 and in Horálek et al. (2016b) resp. references cited therein. Next to this, the inter-annual difference between 2013 and 2014, and the results of the trend analysis for 2007 – 2014 are presented in this table. It should be noted that this period for the trend analysis is shorter than for PM_{10} and ozone, leading to less robust results.

Considering Europe as a whole, Table A4.4 shows that the overall population-weighted annual mean $PM_{2.5}$ concentration in 2014 was 14.1 $\mu g.m^{-3}$. This is of about 1 $\mu g.m^{-3}$ less than in the previous years and the smallest for all the years presented.

One may observe similar levels in the population-weighted concentration across Europe as a whole in 2007 – 2008, an increase in 2010 and slightly continuous reduction for the period 2010 – 2014. For the whole period 2007 – 2014, a slight downward trend is detected. The estimated slope is about -0.3 $\mu g.m^{-3}$ per year for both Europe as a whole and the EU-28, which means a mean decrease of 0.3 $\mu g.m^{-3}$ per year. EEA (2016b) estimates for the EU-28, for the period 2006 – 2014 an average slope of -0.3 $\mu g.m^{-3}$ per year measured at urban/suburban background stations and of the same -0.3 $\mu g.m^{-3}$ per year measured at rural background stations. The differences between the slope estimates of EEA (2016b) and of this paper have their cause in the compared entity (i.e. concentration vs. population weighted concentration), in the differences in the number and spatial distribution of the stations considered, in the spatial interpolation, and in the different periods of time the trends are accounted for..

The steepest decrease of population-weighted concentration per country compared to 2013 took place in Albania, France, FYR of Macedonia and Greece. The highest increase was detected in Denmark, Lithuania, Finland and Sweden.

Table A4.4 Evolution and trend in 2007–2014 and difference between 2014 and 2013 for population-weighted concentration, $PM_{2.5}$ annual average. Trend estimates are only given when a significant trend is observed (p >0.1).

Country		Population-weighted conc. [µg.m^{-3}]									Trend of pop.-weighted conc. 2007–2014	
		2007	2008	2009	2010	2011	2012	2013	2014	Differ. '14 - '13	Signific.	Slope [µg.m^{-3}.year^{-1}]
Albania	AL	20.8	19.6		25.1	17.2	21.1	20.3	16.5	-3.8		
Andorra	AD	11.5	11.3		12.4	13.7	15.9	11.9	10.0	-1.9		
Austria	AT	16.3	16.4		17.7	16.3	14.8	15.7	12.9	-2.8	+	-0.4
Belgium	BE	16.6	17.1		18.8	17.3	15.8	16.6	13.7	-3.0		
Bosnia-Herzegovina	BA	21.7	20.3		22.2	17.2	18.5	16.0	15.3	-0.7	*	-0.9
Bulgaria	BG	28.8	28.4		24.5	18.3	24.9	24.1	24.0	0.0	+	-0.7
Croatia	HR	19.5	18.5		20.0	19.6	16.8	16.8	15.6	-1.2		
Cyprus	CY	25.0	25.3		21.8	21.0	25.0	17.0	17.0	-0.1	+	-1.2
Czech Republic	CZ	17.5	17.7		21.5	18.8	18.8	19.6	18.7	-1.0		
Denmark	DK	11.5	11.1		11.4	12.5	10.0	9.6	11.6	1.9		
Estonia	EE	8.8	8.9		8.9	8.0	7.9	7.8	8.7	0.8		
Finland	FI	7.7	7.4		7.8	7.4	7.1	5.9	7.4	1.5		
France	FR	14.9	14.7		16.2	15.3	14.7	14.5	11.0	-3.4	+	-0.4
Germany	DE	14.0	14.1		16.3	14.8	13.3	14.2	13.4	-0.8		
Greece	GR	22.0	21.7		20.0	16.8	19.2	19.7	17.0	-2.7	+	-0.6
Hungary	HU	19.3	19.4		20.3	23.1	18.9	18.2	17.3	-0.9		
Iceland	IS	7.1	7.1		6.9	4.6	4.7	6.5	6.6	0.2		
Ireland	IE	8.5	9.6		10.3	7.9	8.1	9.2	9.0	-0.3		
Italy	IT	19.0	19.1		17.5	19.8	18.9	18.2	15.8	-2.3		
Latvia	LV	15.3	16.4	not mapped	14.7	11.1	12.4	12.8	14.1	1.3		
Liechtenstein	LI	15.5	15.5		15.3	8.5	10.2	11.4	9.0	-2.4		
Lithuania	LT	13.8	15.5		15.6	12.7	12.9	13.9	15.5	1.6		
Luxembourg	LU	13.9	14.5		15.8	13.3	12.6	14.3	11.9	-2.5		
Macedonia, FYR of	MK	24.4	23.6		27.5	15.8	29.2	30.4	27.4	-3.0		
Malta	MT	14.9	14.9		13.8	15.6	12.4	12.5	12.0	-0.5		
Monaco	MC	16.5	16.5		14.9	16.4	18.2	13.8	12.9	-0.9		
Montenegro	ME	21.4	19.9		24.6	15.1	18.7	17.1	15.6	-1.5		
Netherlands	NL	16.9	17.0		17.6	17.1	13.7	14.3	13.8	-0.5		
Norway	NO	8.6	8.2		8.8	6.3	7.2	7.1	7.2	0.1		
Poland	PL	20.8	21.1		26.4	21.8	23.9	22.8	22.9	0.2		
Portugal	PT	11.5	10.9		10.5	10.5	9.9	10.0	8.7	-1.4	*	-0.3
Romania	RO	22.4	21.8		17.0	20.5	20.8	18.5	17.5	-1.0		
San Marino	SM	18.2	18.2		16.3	14.7	16.7	15.1	13.5	-1.6	+	-0.6
Serbia (incl. Kosovo*)	RS	26.6	25.4		22.7	21.2	24.3	22.5	22.4	-0.1	+	-0.6
Slovakia	SK	20.2	20.6		21.3	21.8	20.5	20.1	19.2	-0.9		
Slovenia	SI	18.5	18.0		19.0	19.4	17.7	17.4	15.1	-2.3		
Spain	ES	14.1	13.6		11.8	11.1	11.9	11.0	10.7	-0.2	*	-0.5
Sweden	SE	9.2	8.8		8.1	8.1	7.2	6.0	7.6	1.6	*	-0.4
Switzerland	CH	14.9	14.8		15.5	12.6	12.6	13.9	11.6	-2.3		
United Kingdom	UK	12.2	12.5		13.0	12.4	11.9	11.8	11.6	-0.2	+	-0.1
Total		**16.3**	**16.3**		**16.8**	**15.9**	**15.6**	**15.3**	**14.1**	**-1.1**	*	**-0.3**
EU-28		**16.1**	**16.1**		**16.7**	**15.9**	**15.5**	**15.1**	**14.0**	**-1.1**	*	**-0.3**

*) under the UN Security Council Resolution 1244/99

For four countries, significant decreasing trend is detected at the significance level 0.95, and for additional eight countries at the significance level 0.90. For most of the countries, no significant trend is detected. However, the examined period consists of seven years only, so the results of the trend analysis are less robust than for PM_{10} and ozone.

The evolution of the percentage population living in areas with concentrations above the $PM_{2.5}$ target value in Europe as a whole is presented in Table 6.2. In 2014, the lowest percentage is observed, while in the previous years, fluctuations do occur. However, as stated earlier, the percentage population living in areas with concentrations above the target value is not statistically a very robust parameter.

The table showing the evolution of the percentage population in exceedance for individual countries is presented as a supplementary material at the web page of this paper, see http://acm.eionet.europa.eu/reports/ETCACM_TP_2016_6_AQMaps2014.

Uncertainties

Table A4.5 presents the uncertainty results for $PM_{2.5}$ maps for the years 2007 – 2014 (excluding the 'not-mapped' year 2009). Both absolute and relative uncertainties show for 2014 similar or slightly better results than in 2013. In the case of the absolute uncertainties, the 2014 results are the lowest, compared to all the previous years; this is related to the lowest concentration (see e.g. Table 6.2). In the case of the relative uncertainties, the 2014 results are among the better results throughout the years.

The results for R^2 from cross-validation scatterplots show quite similar levels to the previous years.

Table A4.5 Absolute and relative mean uncertainty and R^2 from cross-validation scatterplot for the total European rural and urban areas, $PM_{2.5}$ annual average, years 2007 – 2014

PM2.5			2007	2008	2009	2010	2011	2012	2013	2014
Annual average										
rural areas	abs. mean uncertainty	RMSE [μg.m^{-3}]	3.3	3.5	not mapped	3.4	2.8	3.0	2.7	2.5
	rel. mean uncertainty	RRMSE [%]	*27.4*	*29.8*		*25.0*	*16.8*	*24.9*	*22.1*	*22.4*
	coeff. of determination	R^2				*0.74*	*0.82*	*0.78*	*0.78*	*0.78*
urban areas	abs. mean uncertainty	RMSE [μg.m^{-3}]	4.1	3.6	not mapped	3.1	3.2	3.3	2.9	2.6
	rel. mean uncertainty	RRMSE [%]	*23.7*	*20.0*		*16.8*	*16.7*	*18.7*	*17.5*	*16.4*
	coeff. of determination	R^2				*0.81*	*0.80*	*0.78*	*0.78*	*0.81*

A4.3 Ozone

Air concentrations

Map A4.4 presents the inter-annual difference between 2014 and 2013 for health related ozone indicators, i.e. for 93.2 percentile of maximum daily 8-hour means and for SOMO35. Map A4.5 presents the inter-annual difference between 2014 and 2013 for vegetation related ozone indicators, i.e. for AOT40 for vegetation and AOT40 for forests. In all the maps, red areas show an increase of ozone concentrations, while blue areas show a decrease.

The most of the European area shows a decrease for 93.2 percentile of maximum daily 8-hour means. The steepest decrease can be seen in northern Italy, Switzerland, Slovenia, Croatia, Portugal, Ireland, and Iceland. Somewhat smaller decreases occur at southern Scandinavia, Estonia, Latvia, the UK, most of France, western and northern Spain, Austria, Hungary, Slovakia, south-eastern part of Poland, and northern Greece. Increases are visible in the central and south-eastern parts of Romania, central Italy and eastern Spain. The increases occur mostly in the areas where the '2013 - 2012' difference map showed the steepest decrease.

For SOMO35, a strong decrease is observed in Portugal and south-western Spain. Decreases can also be seen in Norway, southern Sweden and southern Finland, Iceland, central and western Spain, Switzerland, northern Italy, Austria, Slovakia, rural south-eastern Poland, Hungary, west Balkan, Greece and Cyprus.

Map A4.4 Difference concentrations between 2013 and 2014 for ozone indicators 93.2 percentile of daily 8-hour maximums (top) and SOMO35 (bottom)

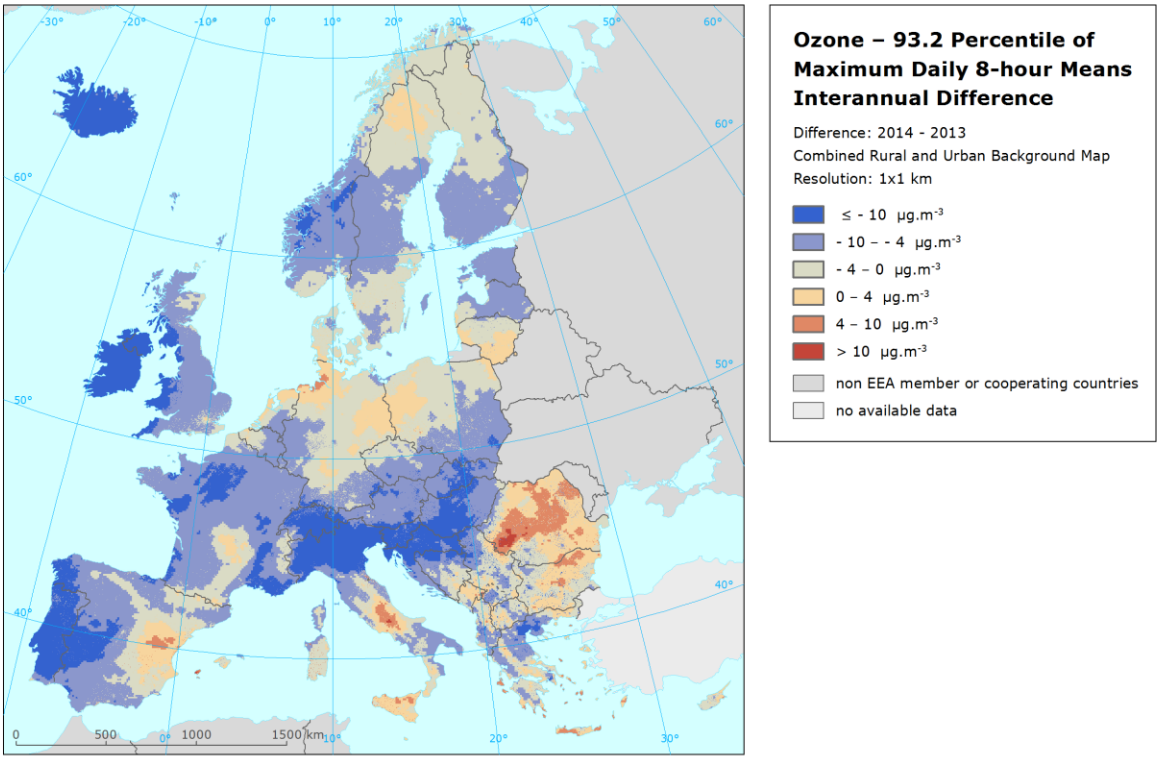

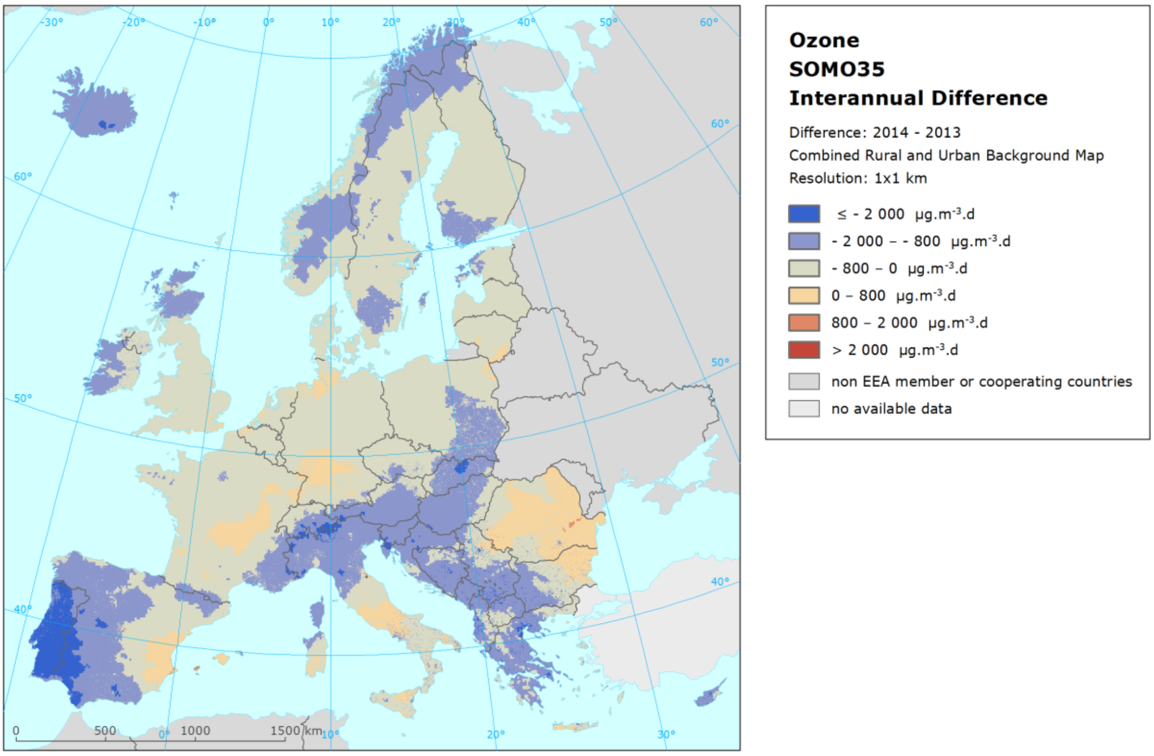

Map A4.5 **Difference concentrations between 2013 and 2014 for ozone indicator AOT40 for vegetation (top) and AOT40 for forests (bottom)**

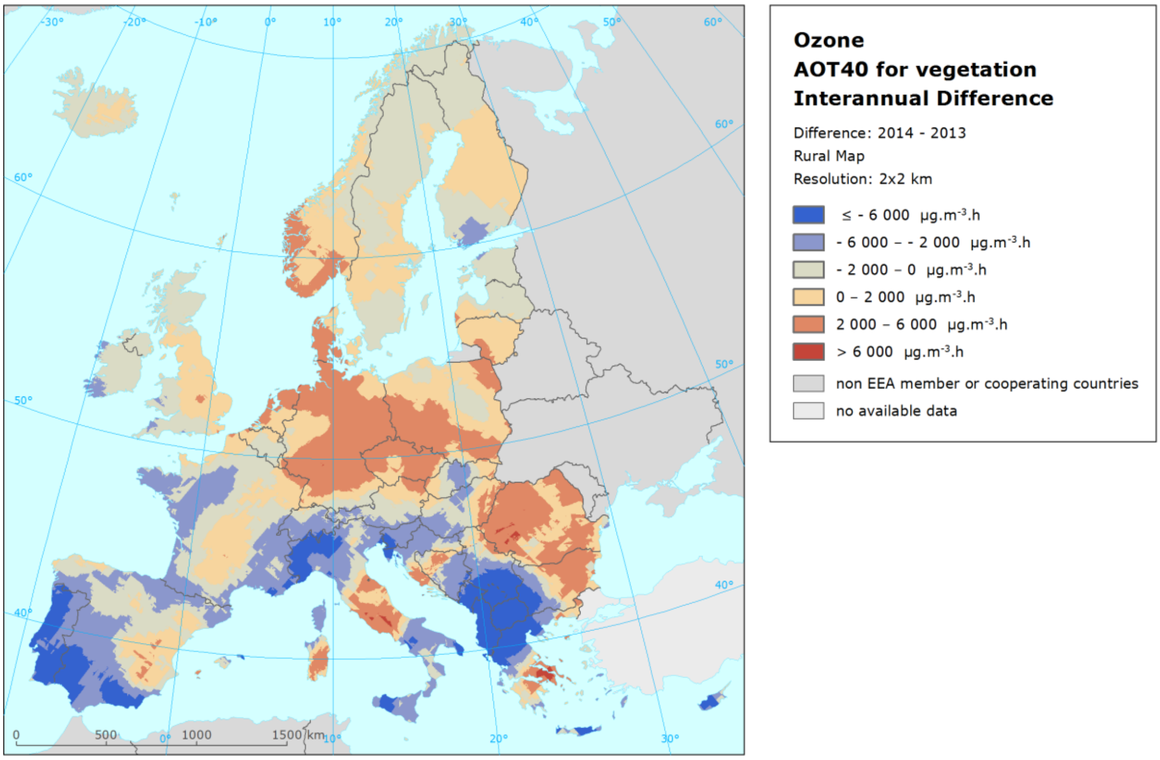

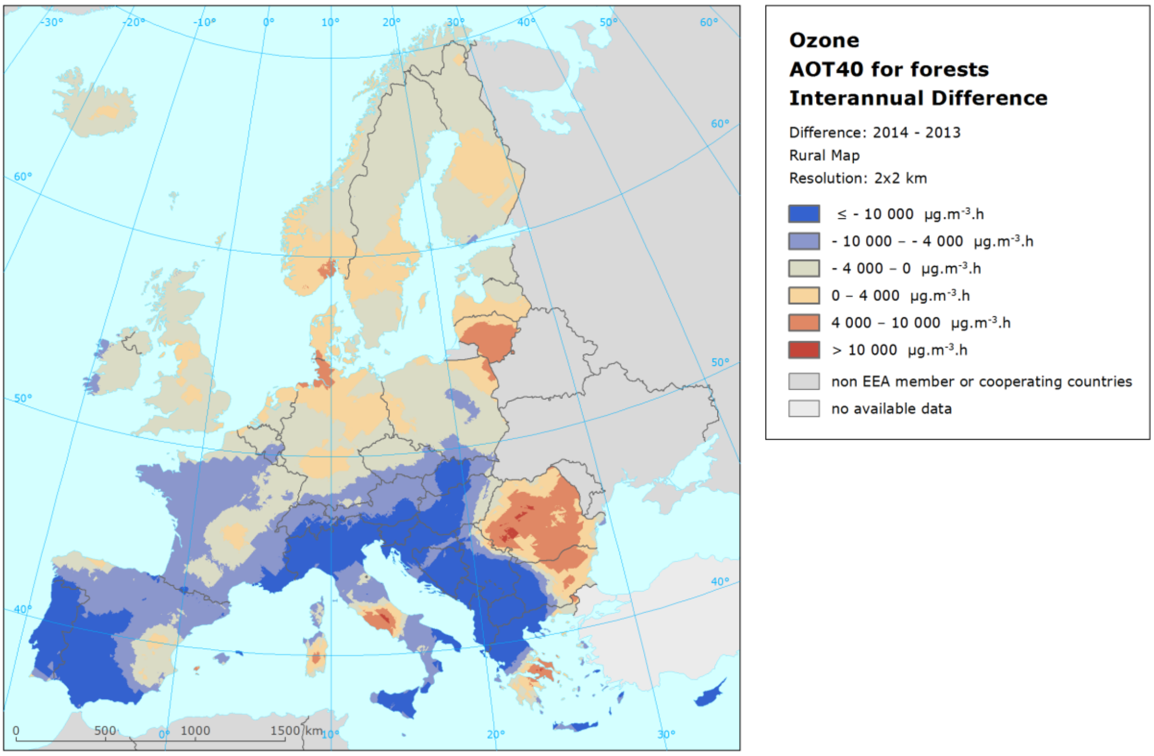

In the case of AOT40 for vegetation, increases are observed in Germany, Denmark, Czech Republic and southern Poland, Romania, eastern Bulgaria, central Italy and southern Greece. Contrary to that, considerable decreases are visible in Portugal and south-eastern Spain, northern Italy and FYR of Macedonia and Albania. Decreases are also observed in western and south-eastern France, Switzerland, Slovenia, Slovakia, Cyprus and the west Balkans. However, it should be noted that the observed decrease in the west Balkans is strongly influenced by just one Macedonian station with extremely high concentrations in 2013, which did not have enough data in 2014 and thus was not used in the mapping. (In the case of the health related ozone indicators, this station did not have enough data also in 2013.)

In the case of AOT40 for forests, the main decrease is visible in Portugal and south-eastern Spain, northern Italy, Slovenia, Croatia, Hungary, Slovakia, Cyprus and the west Balkans (where the steep decrease is influenced by the same Macedonian station as in the case of AOT40 for vegetation). Decreases can be also seen in Switzerland, Austria, western and south-eastern France, central and northern Spain and in southern Italy. Increases are observed especially in Romania, Lithuania and central Italy.

Population exposure

Table A4.6 provides the evolution of the annual population exposure in the period 2005–2014, the inter-annual difference between 2013 and 2014, and the results of the trend analysis. For the period 2005 – 2011, the results of the 26th highest maximum daily 8-hour mean are presented, while the results of the 93.2 percentile of maximum daily 8-hour means are given for the period 2012 – 2014. Both statistics are related to the ozone target value threshold for the protection of health according to the AQ Directive (EU, 2008), however the 26th highest maximum daily 8-hour mean results are somewhat underestimated due to the incomplete time series of the measurement data. The level of the underestimation of the population exposure for the whole Europe is about 0.6 $\mu g.m^{-3}$ (see Table 6.3).

In 2014 the overall population-weighted concentration for ozone indicator 93.2 percentile of maximum daily 8-hour means for whole of Europe was 102.9 $\mu g.m^{-3}$. This is almost 6 $\mu g.m^{-3}$ less than in previous year and the smallest in the whole ten years period. Examining the time series 2005 – 2014, one could conclude that 2006 was an exceptional year with highly elevated ozone, which was followed by the decrease of concentration levels in 2007 – 2010 and some increase and flattening in 2011 – 2013 and further reduction in 2014.

The overall picture of the population-weighted concentration for the totals of 40 European countries shows a slightly downward trend for the years 2005 – 2014. This trend is statistically significant, the slope is about -1 $\mu g.m^{-3}$ per year for both Europe as a whole and the EU-28, which means an average decrease of about 1 $\mu g.m^{-3}$ per year. Due to the underestimation of the 26th highest maximum daily 8-hour mean values, one may suppose the slope is in fact slightly steeper. EEA (2016b) estimates for the EU-28, for a period 2000 – 2014, an average slope of the 93.2 percentile of the maximum daily 8-hour O_3 concentration trend of -0.7 $\mu g.m^{-3}$ per year measured at urban/suburban background stations and -0.9 $\mu g.m^{-3}$ per year measured at rural background stations, for EU-28, for the period 2000 – 2014. The differences between the slope estimates of EEA (2016b) and of this paper have their cause in the compared entity (i.e. concentration vs. population weighted concentration), in the differences in the number and spatial distribution of the stations considered, in the spatial interpolation and in the different periods of time the trends are accounted for.

The steepest decrease of population-weighted concentration per country compared to 2013 is seen in Ireland, Iceland, FYR of Macedonia and Serbia. (However, it should be noted the lack of ozone stations in Iceland.) The only countries with increase are San Marino (with large inter-annual fluctuations), Malta and Sweden.

Table A4.6 Evolution and trend in 2005–2014 and difference between 2014 and 2013 for population-weighted concentration, ozone indicator 26th highest maximum daily 8-hour mean / 93.2 percentile of maximum daily 8-hour means. Trend estimates are only given when a significant trend is observed (p >0.1).

Country		Population-weighted conc. [μg.m^{-3}]											Trend of pop.-weighted conc. 2005–2014	
		26th highest daily maximum 8-hour mean							93.2 perc. of d. max. 8-h m.					
		2005	2006	2007	2008	2009	2010	2011	2012	2013	2014	Differ. '14 - '13	Signific.	Slope [μg.m^{-3}.year^{-1}]
Albania	AL	122.7	117.9	126.9	115.3	114.7	109.5	121.1	134.4	117.8	107.4	-10.4		
Andorra	AD	127.2	119.1	118.6	122.0	115.6	122.4	120.6	122.5	122.4	117.4	-5.1		
Austria	AT	120.6	124.9	122.8	114.8	116.4	118.4	118.6	118.7	121.4	112.0	-9.5		
Belgium	BE	104.0	126.0	98.9	103.6	101.5	97.7	104.4	94.7	102.5	99.0	-3.5		
Bosnia-Herzegovina	BA	119.9	118.1	122.5	113.7	114.5	107.4	109.9	126.3	116.2	105.6	-10.6		
Bulgaria	BG	109.9	105.0	115.7	114.4	112.0	103.8	105.1	116.5	103.5	94.6	-8.9		
Croatia	HR	122.8	124.8	124.7	115.5	115.6	114.3	118.3	125.7	119.4	109.5	-10.0		
Cyprus	CY	114.5	102.1	116.9	115.2	120.8	109.8	112.0	116.2	110.9	104.6	-6.3		
Czech Republic	CZ	121.6	126.5	121.0	114.6	113.5	114.1	114.8	116.7	113.9	109.6	-4.2	*	-1.2
Denmark	DK	95.0	104.9	95.2	102.6	95.5	91.4	96.9	95.7	96.7	96.6	0.0		
Estonia	EE	94.2	105.1	94.1	96.3	90.8	97.2	94.8	93.3	97.6	92.8	-4.8		
Finland	FI	92.9	100.7	89.0	94.3	90.6	92.2	93.0	88.8	92.6	89.1	-3.5		
France	FR	113.8	122.0	109.0	107.3	107.3	111.6	112.8	104.7	113.2	105.6	-7.6		
Germany	DE	113.8	125.8	113.3	113.5	108.8	112.8	111.5	107.1	110.2	107.9	-2.4	**	-0.8
Greece	GR	125.4	115.8	126.5	131.1	122.8	119.4	126.5	133.1	123.5	112.2	-11.3		
Hungary	HU	119.7	121.7	125.0	117.5	124.2	110.9	117.1	122.3	113.9	103.2	-10.7		
Iceland	IS	85.2	93.3	81.1	90.8	81.4	78.3	83.6	81.1	87.8	69.0	-18.8		
Ireland	IE	86.5	90.2	84.2	92.1	84.9	85.6	84.4	87.1	91.6	58.1	-33.5		
Italy	IT	131.1	135.1	129.5	123.2	125.8	124.3	127.7	130.5	126.1	116.2	-9.9		
Latvia	LV	91.3	104.5	95.8	94.9	91.9	93.2	96.3	99.0	98.0	91.8	-6.1		
Liechtenstein	LI	106.9	127.3	119.9	119.4	118.9	123.3	116.4	118.0	124.8	113.4	-11.5		
Lithuania	LT	103.0	110.1	98.1	102.0	95.8	96.9	101.4	101.4	98.8	96.5	-2.3		
Luxembourg	LU	119.9	130.0	111.7	112.1	108.6	111.4	110.4	99.0	109.5	105.5	-4.0	**	-1.6
Macedonia, FYR of	MK	117.5	110.3	121.1	121.0	111.3	109.0	117.4	136.3	118.1	102.0	-16.1		
Malta	MT	105.9	115.6	109.1	108.4	107.7	109.4	112.6	116.7	112.0	115.8	3.7	+	0.9
Monaco	MC		142.4	127.3	123.1	127.2	124.0	126.6	118.9	122.5	116.3	-6.2		
Montenegro	ME	120.8	114.3	122.3	118.1	111.7	108.6	115.1	127.1	113.2	105.6	-7.6		
Netherlands	NL	93.7	116.1	94.1	98.4	94.7	90.7	98.6	94.1	99.5	97.5	-1.9		
Norway	NO	98.1	101.7	91.3	99.0	94.0	88.8	93.7	90.9	94.5	88.7	-5.7	+	-1.0
Poland	PL	113.6	120.4	112.9	109.7	107.8	106.6	109.5	112.0	109.4	107.2	-2.2	*	-0.8
Portugal	PT	119.0	119.4	111.0	102.7	112.4	112.0	108.4	106.0	113.5	101.0	-12.5		
Romania	RO	112.1	105.7	116.9	110.1	108.8	94.0	91.1	103.1	86.5	83.3	-3.2	**	-2.9
San Marino	SM	130.8	120.8	130.4	119.0	118.1	116.1	117.9	121.2	110.7	118.4	7.6	*	-1.4
Serbia (incl. Kosovo*)	RS	115.6	108.5	122.5	117.3	115.8	102.5	112.0	124.1	110.5	95.6	-14.8		
Slovakia	SK	121.3	122.2	122.2	116.4	122.7	112.8	118.5	121.2	117.4	110.2	-7.2		
Slovenia	SI	122.6	132.6	126.6	116.9	119.7	122.1	125.5	125.8	125.5	115.0	-10.5		
Spain	ES	117.7	116.2	115.4	110.7	113.1	115.4	112.1	112.7	114.9	112.2	-2.6		
Sweden	SE	97.6	104.5	93.5	97.6	94.2	91.2	96.1	94.0	94.8	95.4	0.6		
Switzerland	CH	122.6	132.6	120.1	116.8	117.3	124.7	120.8	117.3	124.2	113.8	-10.5		
United Kingdom	UK	87.2	98.0	83.3	93.1	86.8	81.6	87.8	84.0	89.7	84.1	-5.6		
Total		**112.1**	**118.2**	**110.7**	**109.8**	**108.1**	**106.8**	**108.9**	**108.5**	**108.9**	**102.9**	**-5.9**	*	**-1.0**
EU-28		**111.8**	**118.3**	**110.2**	**109.5**	**107.8**	**106.8**	**108.7**	**107.7**	**108.6**	**103.0**	**-5.6**	**	**-1.0**

*) under the UN Security Council Resolution 1244/99

For six countries, significant decreasing trend is detected at the significance level 0.95. For most of the countries, no significant trend is detected. This is influenced by quite large inter-annual fluctuations of the ozone concentrations caused by the different meteorological conditions.

Table A4.7 provides the evolution of the annual population exposure in the period 2005–2014, the inter-annual difference between 2013 and 2014, and the results of the trend analysis, for the ozone indicator SOMO35, based on the results presented in Chapter 4.2 and in Horálek et al. (2016b) resp. references cited therein.

Table A4.7 Evolution and trend in 2005–2014 and difference between 2014 and 2013 for population-weighted concentration, ozone indicator SOMO35. Trend estimates are only given when a significant trend is observed (p >0.1).

Country		Population-weighted conc. [$\mu g.m^{-3}.d$]											Trend of pop.-weighted conc. 2005–2014	
		2005	2006	2007	2008	2009	2010	2011	2012	2013	2014	Differ. '14 - '13	Signific.	Slope [$\mu g.m^{-3}.d.year^{-1}$]
Albania	AL	7 911	7 193	7 817	7 668	6 754	5 617	7 769	8 760	7 179	4 376	-2 803		
Andorra	AD	7 520	6 587	7 121	6 319	7 186	7 282	7 891	8 058	7 303	6 692	-612		
Austria	AT	5 946	6 237	5 874	5 099	5 050	4 969	5 452	5 419	5 389	4 423	-966	*	-106
Belgium	BE	2 775	4 017	2 235	2 520	2 599	2 401	2 714	2 050	2 520	2 297	-223		
Bosnia-Herzegovina	BA	6 714	6 571	6 938	5 972	5 536	4 879	5 702	7 322	5 670	3 852	-1 817		
Bulgaria	BG	5 311	4 896	6 064	5 797	5 686	4 377	5 215	5 960	4 082	2 519	-1 562		
Croatia	HR	6 324	6 928	6 756	5 899	5 491	5 419	6 470	7 143	5 989	4 503	-1 486		
Cyprus	CY	7 155	5 759	7 739	8 027	8 788	7 374	8 773	8 369	7 909	5 426	-2 483		
Czech Republic	CZ	5 845	6 097	5 123	4 576	4 487	4 160	4 743	4 806	4 266	3 822	-444	*	-208
Denmark	DK	2 519	3 578	2 440	3 080	2 440	2 245	2 752	2 662	2 749	2 611	-139		
Estonia	EE	2 437	3 594	2 061	2 363	1 762	2 646	2 516	2 310	2 545	1 991	-554		
Finland	FI	2 275	3 141	1 332	1 938	1 623	1 925	2 052	1 650	2 011	1 615	-396		
France	FR	4 591	4 972	3 686	3 563	4 025	4 139	4 439	3 635	4 098	3 786	-312		
Germany	DE	3 940	4 860	3 648	3 822	3 507	3 652	3 668	3 357	3 506	3 287	-220	*	-71
Greece	GR	8 321	6 657	8 330	8 969	8 330	7 483	9 182	9 378	8 532	5 926	-2 606		
Hungary	HU	5 751	5 738	6 547	5 751	6 631	4 408	5 828	6 342	4 604	3 620	-984		
Iceland	IS	1 329	2 265	1 168	2 224	833	775	1 094	1 242	1 473	218	-1 255		
Ireland	IE	1 701	2 453	1 412	2 096	1 487	1 419	1 353	1 479	2 043	868	-1 175		
Italy	IT	7 634	8 205	7 506	6 386	6 986	6 302	7 532	7 328	6 576	5 569	-1 007	*	-162
Latvia	LV	2 391	3 734	2 262	2 347	1 837	2 304	2 708	3 103	2 614	2 213	-401		
Liechtenstein	LI	5 233	6 258	4 826	4 930	5 271	5 244	5 128	5 132	5 221	4 360	-861		
Lithuania	LT	3 671	4 535	2 744	3 059	2 291	2 608	3 131	3 358	2 703	2 457	-246		
Luxembourg	LU	4 769	5 090	3 424	3 557	3 500	3 505	3 527	2 561	3 167	2 872	-295	*	-180
Macedonia, FYR of	MK	7 069	6 297	6 690	7 133	6 229	5 081	7 110	8 472	6 326	3 215	-3 111		
Malta	MT	6 971	7 797	7 209	6 582	6 634	6 722	7 127	8 022	7 403	6 946	-457		
Monaco	MC		8 903	8 381	7 246	8 325	8 028	8 354	6 979	7 795	7 112	-683		
Montenegro	ME	7 608	6 554	7 379	7 120	6 237	5 653	6 970	8 584	6 674	4 012	-2 662		
Netherlands	NL	1 901	3 245	1 816	2 104	1 922	1 916	2 283	1 949	2 410	2 244	-167		
Norway	NO	2 580	3 496	1 705	2 514	2 000	1 803	2 395	2 128	2 443	2 113	-330		
Poland	PL	4 784	5 416	4 179	3 951	3 747	3 278	4 065	4 045	3 792	3 425	-367	*	-151
Portugal	PT	5 510	5 257	4 863	3 851	5 003	5 133	4 552	4 240	5 091	3 519	-1 572	+	-141
Romania	RO	5 238	4 798	5 882	5 039	5 044	3 033	3 276	3 967	2 221	1 842	-379	*	-379
San Marino	SM	7 540	6 321	7 296	5 863	5 860	5 331	6 220	6 048	5 067	5 949	881	*	-177
Serbia (incl. Kosovo*)	RS	5 947	5 239	6 768	6 378	6 118	4 001	5 793	6 844	4 738	2 762	-1 976		
Slovakia	SK	6 141	6 261	6 098	5 455	6 348	4 748	6 051	6 103	5 116	4 344	-771	+	-148
Slovenia	SI	6 242	7 480	6 671	5 761	5 775	5 998	7 062	7 092	6 540	5 086	-1 454		
Spain	ES	6 139	5 813	5 992	5 110	5 983	6 088	5 858	5 850	5 895	5 436	-460		
Sweden	SE	2 682	3 635	1 795	2 387	2 100	2 025	2 628	2 233	2 317	2 318	1		
Switzerland	CH	5 740	6 321	5 114	4 619	5 139	5 127	5 435	4 990	4 919	4 417	-502	*	-103
United Kingdom	UK	1 551	2 676	1 174	2 044	1 433	1 072	1 471	1 183	1 606	1 337	-269		
Total		**4 706**	**5 167**	**4 411**	**4 275**	**4 275**	**3 917**	**4 414**	**4 279**	**4 089**	**3 500**	**-590**	*****	**-134**
EU28		**4 613**	**5 128**	**4 319**	**4 178**	**4 208**	**3 888**	**4 339**	**4 154**	**4 040**	**3 506**	**-534**	*****	**-116**

*) under the UN Security Council Resolution 1244/99

In 2014 the overall population-weighted value of ozone indicator SOMO35 for whole of Europe was 3500 µg.m^{-3}.d. This is of about 590 µg.m^{-3}.d less than in previous year and the smallest in the whole ten years period. Examining the time series 2005 – 2014, one can see quite similar development as in the case of the 93.2 percentile of maximum daily 8-hour means. The overall evolution of the population-weighted concentration for the totals of 40 European countries shows a slightly downward trend for the years 2005 – 2014. This trend is statistically significant; the slope is about -134, which means an average decrease of about 134 µg.m^{-3}·d per year. For the EU-28, the slope is about -116 µg.m^{-3}·d per year. EEA (2016b) estimates for the EU-28 the slope of -65 µg/m^{3}·d per year measured at urban/suburban background stations and -117 µg/m^{3}·d per year measured at rural background stations, for the period 2000 – 2014. The differences between the slope estimates of EEA (2016b) and of this paper have their cause in the differences in the compared entity (i.e. concentration vs. population weighted concentration), in the number and spatial distribution of the stations considered, in the spatial interpolation, and in the different periods of time the trends are accounted for.

The steepest decrease of population-weighted concentration per country compared to 2013 took place in FYR of Macedonia, Albania, Montenegro, Greece and Cyprus. No increase was detected in any country, apart from San Marino.

For nine countries, significant decreasing trend is detected at the significance level 0.95. The most of these countries are located in the central Europe. For most of the countries, no significant trend is detected. This is influenced by quite large inter-annual fluctuations of the ozone concentrations caused by the different meteorological conditions.

Next to the population weighted concentration evolution, the evolution of the percentage European population living in areas with concentrations above the ozone target value for the 93.2 percentile of maximum daily 8-hour means resp. above a level of 6 000 µg.m^{-3}.d for SOMO35 is presented in Table 6.4. In 2014, the lowest percentage population in areas with concentrations in exceedance is observed for both indicators. Concerning the previous years, the population exposed to ozone level above the target value threshold is in the period 2008 – 2014 lower than in the preceding period of 2005 – 2007, while fluctuations do occur for SOMO35. However, as stated earlier, the percentage population living in areas with concentrations above the target value threshold is not statistically a very robust parameter.

The table showing the evolution of the percentage population in exceedance (resp. above the specific SOMO35 threshold) for individual countries is presented as a supplementary material at the web page of this paper, see http://acm.eionet.europa.eu/reports/ETCACM_TP_2016_6_AQMaps2014.

Vegetation exposure

The evolution of the agricultural land (*crops*) exposed to accumulated ozone concentrations (AOT40 for vegetation) exceeding the target value (TV) threshold and the long-term objective (LTO) for Europe as a whole in the ten years period 2005 – 2014 is presented in Table 6.5. The same table also shows the evolution of the *forest* land exposed to accumulated ozone concentrations (AOT40 for forests) exceeding the level of 20 000 µg.m^{-3}.h (earlier used Reporting Value, RV) and Critical Level (CL) for Europe as a whole. The results are discussed in Chapter 6.

The table showing the evolution of the percentage land in exceedance for individual countries, for both AOT40 indicators, is presented as supplementary material at the web page of this paper, see http://acm.eionet.europa.eu/reports/ETCACM_TP_2016_6_AQMaps2014.

Uncertainties

Table A4.9 shows the evolution of the absolute and relative mean interpolation uncertainties and also R^2 from cross-validation scatterplots for the maps for all four ozone indicators, in the ten years period 2005 – 2014.

The absolute mean interpolation uncertainty results of 2014 show the lowest levels for all the ten years period, which is influenced by the lowest levels of the ozone concentration values in this year.

For the relative uncertainties and R^2 from cross-validation scatterplots, the uncertainty results of 2014 maps fit within the fluctuation of the previous years.

Table A4.9 Absolute and relative mean uncertainty and R^2 from cross-validation scatterplot for the total European areas, ozone indicators 93.2 percentile of maximum daily 8-hour means, SOMO35, AOT40 for vegetation and AOT40 for forests, years 2005 – 2014

Ozone			2005	2006	2007	2008	2009	2010	2011	2012	2013	2014
26th highest daily max. 8-hr mean (2005 - 2011) / 93.2 percentile of daily max. 8-hr means (2012 - 2014)												
rural areas	abs. mean uncertainty	RMSE [$\mu g.m^{-3}$]	12.3	11.2	8.8	8.7	8.2	8.9	8.4	8.5	8.5	7.4
	rel. mean uncertainty	RRMSE [%]	*10.3*	*8.9*	*7.5*	*7.6*	*7.2*	*7.7*	*7.2*	*7.4*	*7.3*	*6.7*
	coeff. of determinatio	R^2	*0.51*	*0.49*	*0.71*	*0.56*	*0.69*	*0.68*	*0.67*	*0.71*	*0.72*	*0.65*
urban areas	abs. mean uncertainty	RMSE [$\mu g.m^{-3}$]	10.0	10.2	8.9	8.8	9.3	9.2	9.1	9.1	9.1	7.9
	rel. mean uncertainty	RRMSE [%]	*8.9*	*8.4*	*7.9*	*7.9*	*8.4*	*8.2*	*8.1*	*8.3*	*8.1*	*7.4*
	coeff. of determinatio	R^2	*0.50*	*0.53*	*0.66*	*0.61*	*0.64*	*0.71*	*0.66*	*0.68*	*0.70*	*0.64*
SOMO35												
rural areas	abs. mean uncertainty	RMSE [$\mu g.m^{-3}.d$]	2 173	2 077	1 801	1 609	1 635	1 608	1 747	1 633	1 596	1 414
	rel. mean uncertainty	RRMSE [%]	*35.5*	*31.6*	*33.3*	*30.7*	*29.7*	*29.6*	*29.6*	*29.2*	*29.2*	*29.2*
	coeff. of determinatio	R^2	*0.55*	*0.47*	*0.63*	*0.63*	*0.63*	*0.62*	*0.63*	*0.68*	*0.61*	*0.61*
urban areas	abs. mean uncertainty	RMSE [$\mu g.m^{-3}.d$]	1 459	1 472	1 260	1 293	1 475	1 278	1 374	1 362	1 194	1 133
	rel. mean uncertainty	RRMSE [%]	*32.0*	*29.2*	*29.5*	*31.3*	*33.1*	*29.6*	*29.7*	*31.7*	*28.1*	*29.3*
	coeff. of determinatio	R^2	*0.58*	*0.49*	*0.67*	*0.54*	*0.62*	*0.65*	*0.66*	*0.67*	*0.66*	*0.62*
AOT40 for vegetation												
rural areas	abs. mean uncertainty	RMSE [$\mu g.m^{-3}.h$]	7 677	7 674	5 876	5 283	5 138	5 198	5 263	5 062	5 179	4 518
	rel. mean uncertainty	RRMSE [%]	*40.7*	*29.6*	*39.6*	*31.3*	*37.7*	*30.8*	*34.9*	*32.9*	*34.6*	*30.5*
	coeff. of determinatio	R^2	*0.58*	*0.53*	*0.63*	*0.53*	*0.69*	*0.67*	*0.62*	*0.70*	*0.68*	*0.67*
AOT40 for forests												
rural areas	abs. mean uncertainty	RMSE [$\mu g.m^{-3}.h$]	12 474	11 990	10 190	8 750	9 304	8 384	9 341	8 847	9 257	7 354
	rel. mean uncertainty	RRMSE [%]	*41.5*	*33.6*	*37.1*	*34.0*	*33.9*	*31.4*	*32.7*	*32.8*	*34.7*	*33.8*
	coeff. of determinatio	R^2	*0.55*	*0.49*	*0.67*	*0.56*	*0.68*	*0.69*	*0.67*	*0.70*	*0.68*	*0.62*

Neither NO_2 nor NO_x maps were presented in the last years' reports, so no inter annual differences and no annual variations are presented for these pollutants.

Annex 5 Concentration maps including station points

Throughout the report, the concentration maps presented do not include station points, contrary to the previous reports (e.g. Horálek et al., 2015, 2016b). The reason is to better visualise the health related indicators with their distinct concentration levels at the more fragmented and smaller urban areas in predominant rural areas. The allocation of these smaller 'patches' is better discriminated now that the map is presented in a 1x1 km grid resolution, as the smoothing effect of the formerly used 10x10 km grid resolution does not play a role any longer.

As presented in Annex 3, the kriging interpolation methodology somewhat smooths the concentration field. Therefore, it is valuable to present in this Annex 5 the indicator maps *including* the concentration values resulting from the measurement data at the station points. These points provide important additional visual information on the smoothing effect caused by the interpolation. For instance, maps A5.1 and A5.2 present PM_{10} indicators annual average and 90.4 percentile of daily means and include the stations points used in the interpolation. They correspond to Maps 2.1 and 2.2 of the main report, but without station points. Table A5.1 provides an overview on the maps of the main report and the corresponding maps including stations point values as presented in this annex.

Both the rural and the urban/suburban background stations are included in the maps of the health related indicators, while the rural stations only are shown in the maps of vegetation related indicators. For $PM_{2.5}$ and NO_x, only the stations with relevant measured data (i.e. not the pseudo stations) are presented.

Table A5.1 Overview of maps presented in this Annex 5 and their relation with the maps presented in the main report

Air pollutant	Indicator	Map including station points	Map without station points
PM_{10}	Annual average	A5.1	2.1
	90.4 percentile of daily means	A5.2	2.2
$PM_{2.5}$	Annual average	A5.3	3.1
Ozone	93.2 percentile of maximum daily 8-hour means	A5.4	4.1
	SOMO35	A5.5	4.2
	AOT40 for vegetation ([a])	A5.6	4.3
	AOT40 for forests ([a])	A5.7	4.4
NO_2	Annual average	A5.8	5.1
NO_x	Annual average ([a])	A5.9	5.2

([a]) Rural map, applicable for rural areas only.

Map A5.1 Concentration map of PM_{10} annual average including station points, 2014

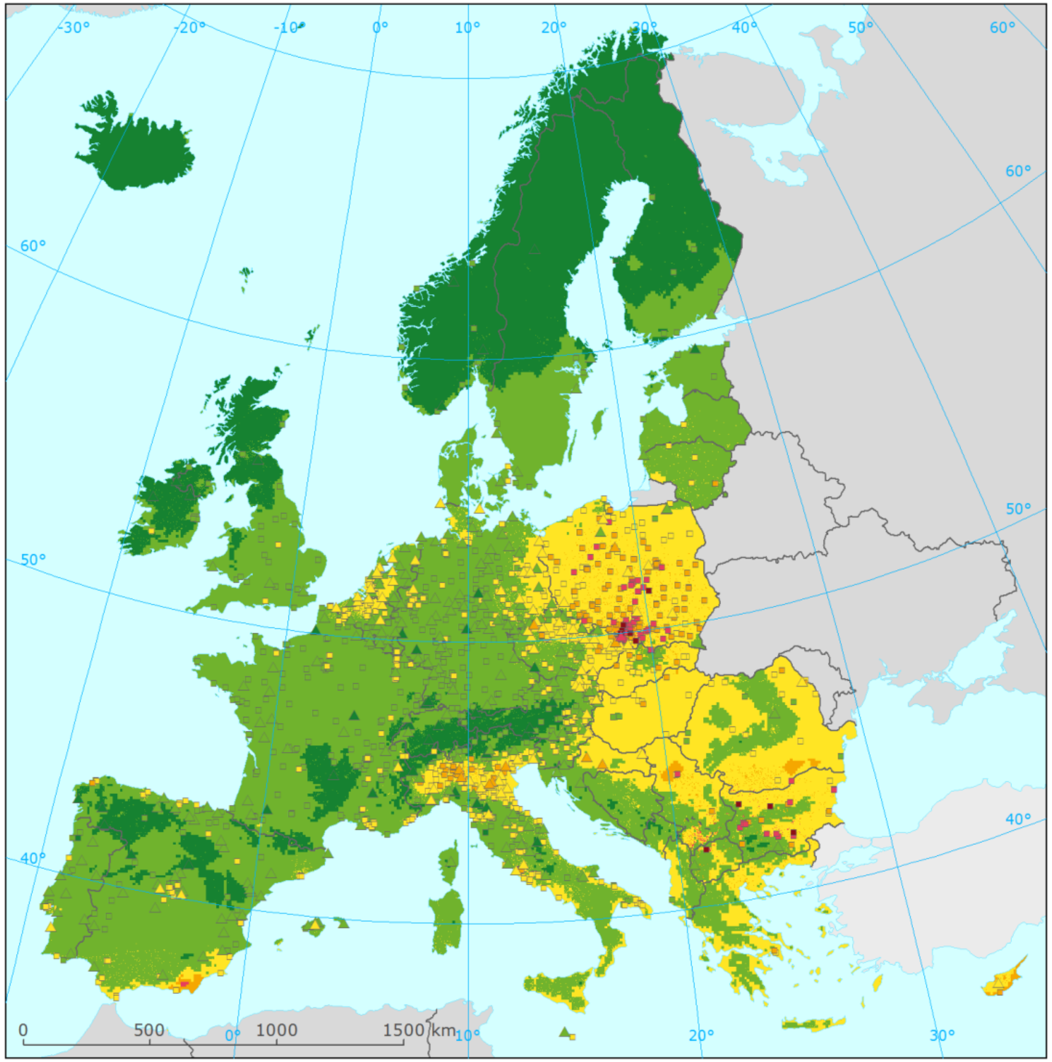

Particulate Matter (PM_{10}) Annual Average

Reference Year: 2014
Combined Rural and Urban Background Map
Resolution: 1x1 km

- ≤ 10 $\mu g.m^{-3}$
- 10 - 20 $\mu g.m^{-3}$
- 20 - 30 $\mu g.m^{-3}$ (20 = WHO AQ Guideline)
- 30 - 40 $\mu g.m^{-3}$
- 40 - 50 $\mu g.m^{-3}$ (40 = LV)
- > 50 $\mu g.m^{-3}$
- non EEA member or cooperating countries
- no available data
- △ rural background station
- □ urban/suburban background station

Map A5.2 Concentration map of PM_{10} indicator 90.4 percentile of daily means including station points, 2014

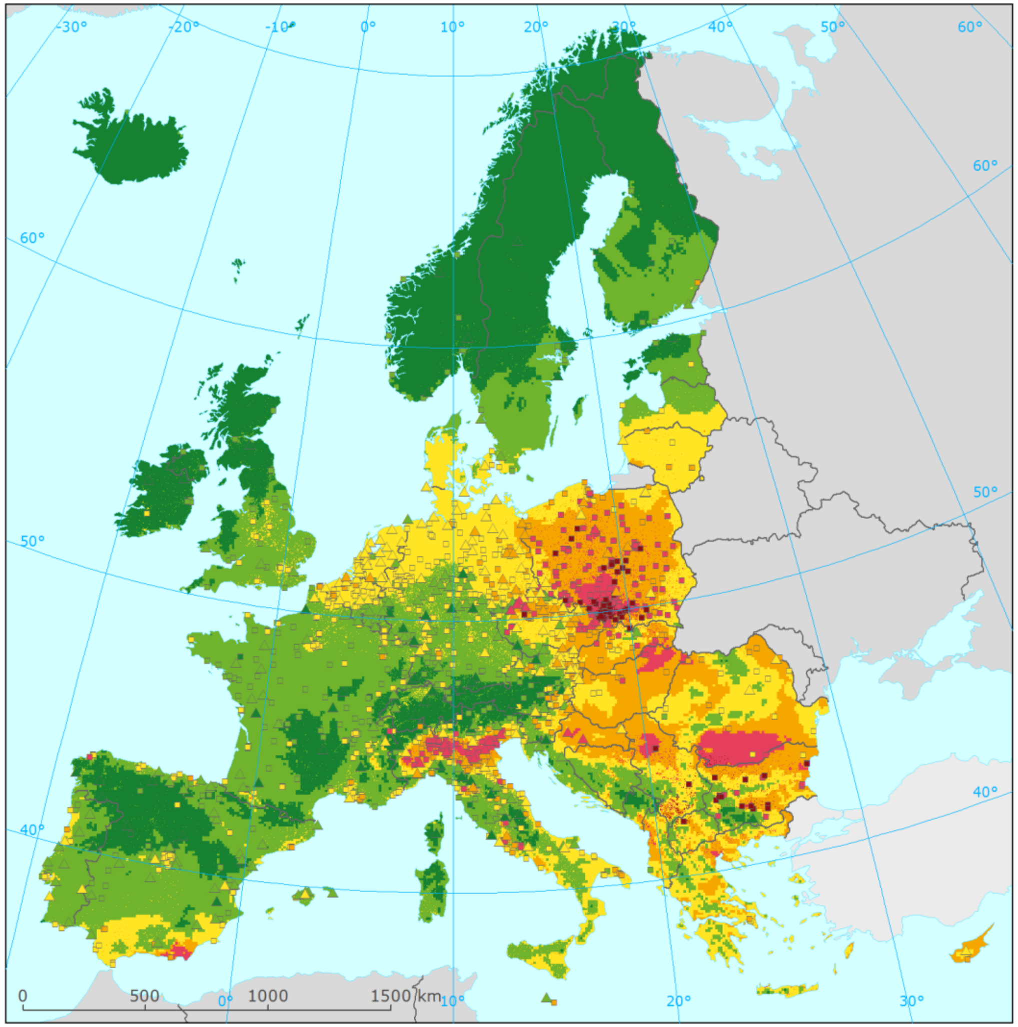

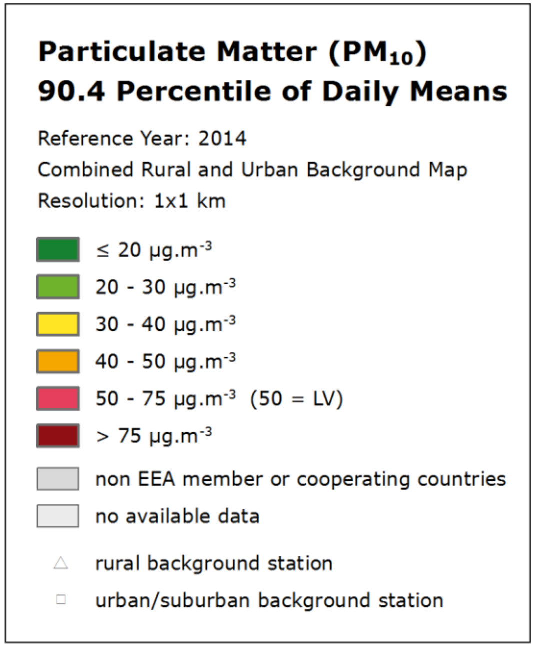

Map A5.3 Concentration map of $PM_{2.5}$ annual average including station points, 2014

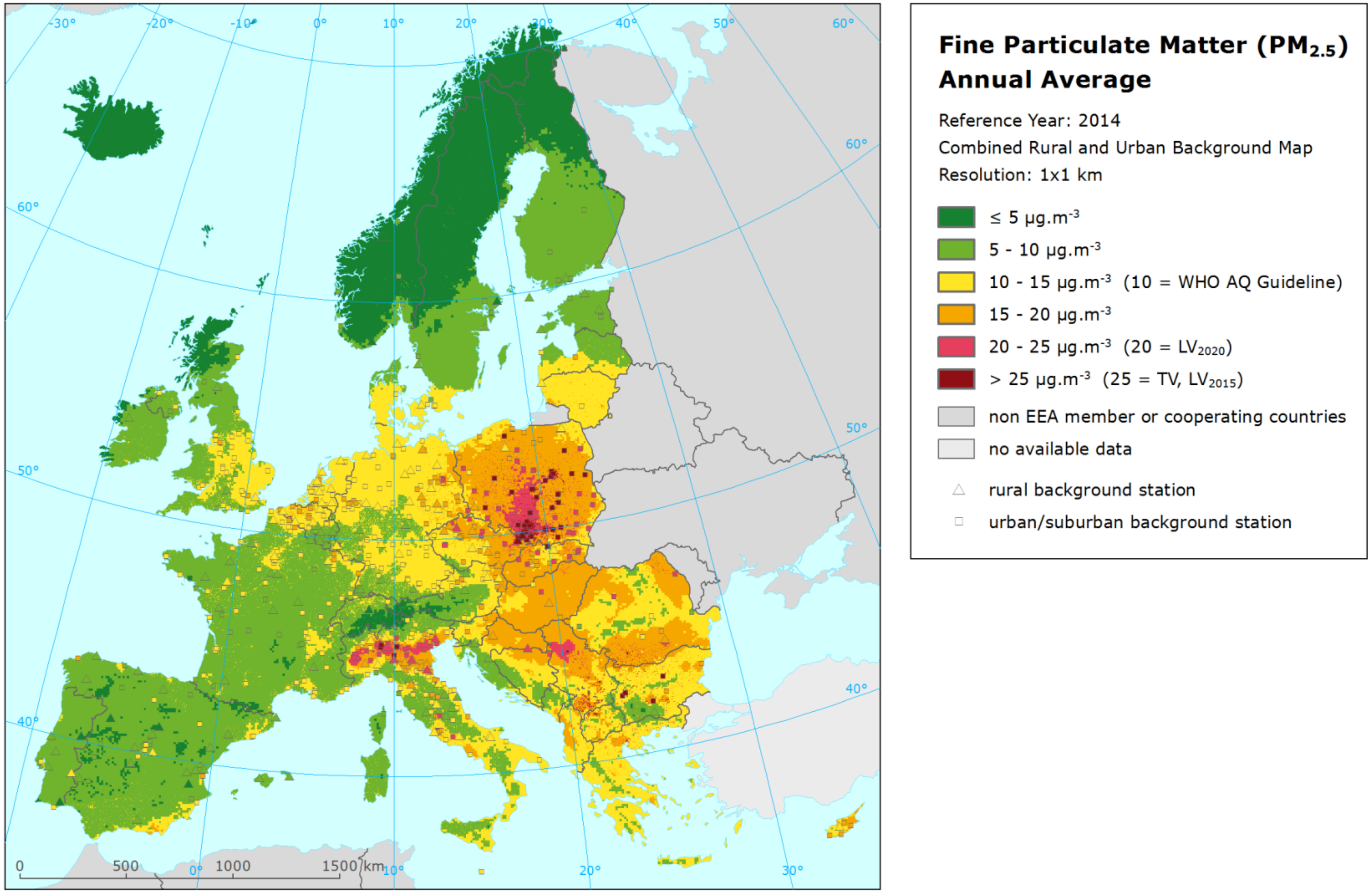

Map A5.2 Concentration map of ozone indicator 93.2 percentile of maximum daily 8-hour means including station points, 2014

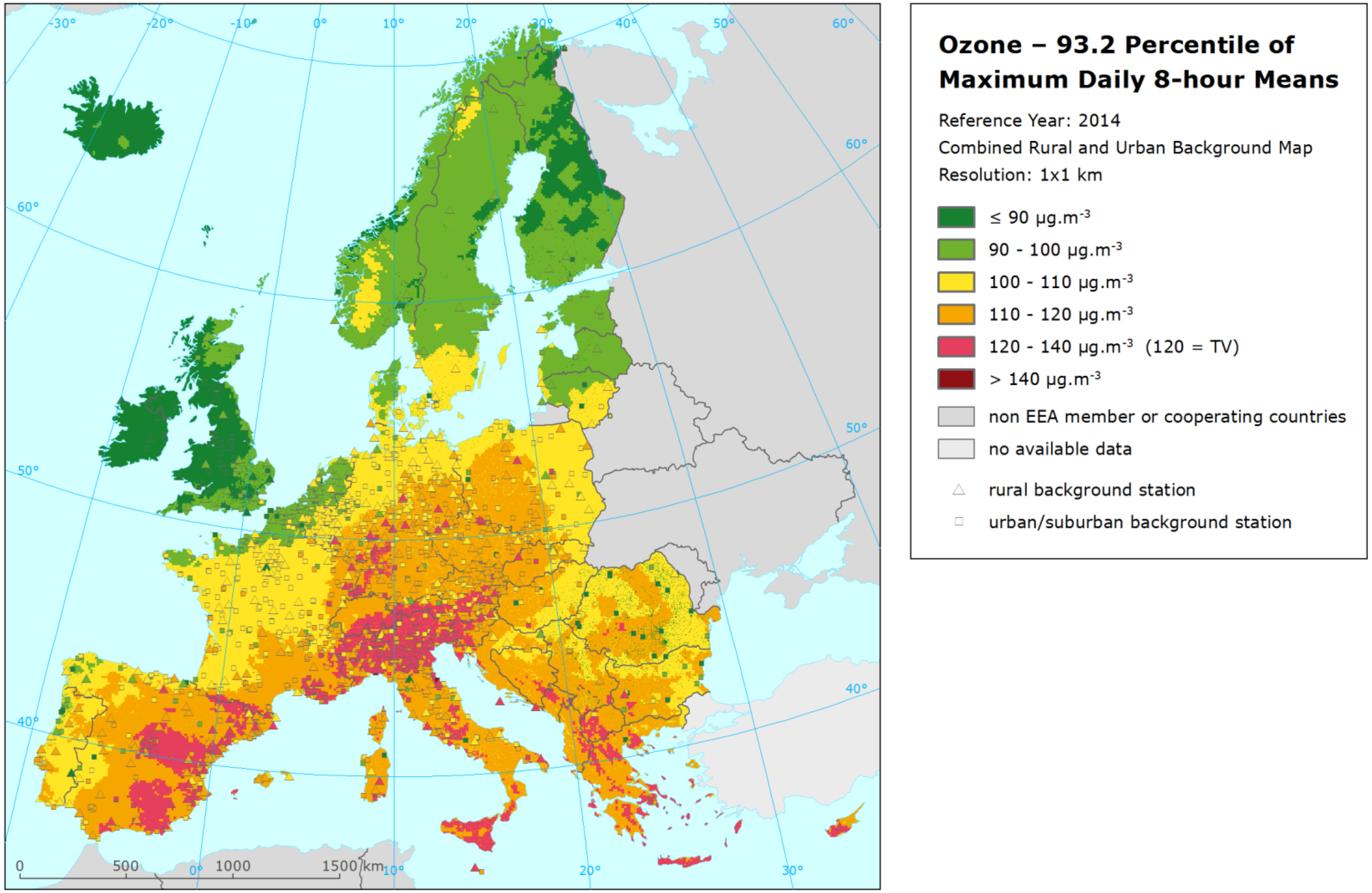

Map A5.5 Concentration map of ozone indicator SOMO35 including station points, 2014

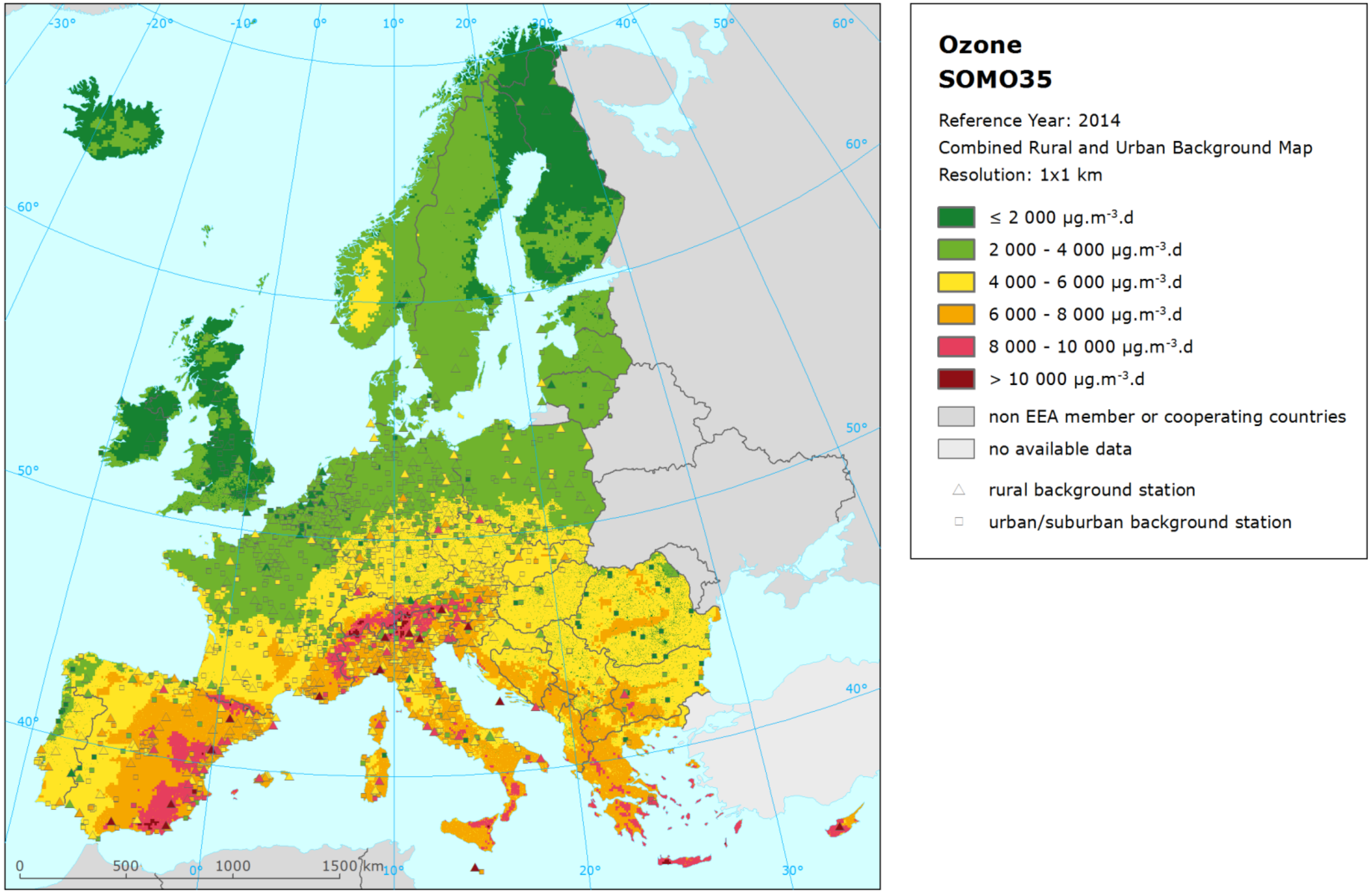

Map A5.6 Concentration map of ozone indicator AOT40 for vegetation including station points, rural air quality, 2014

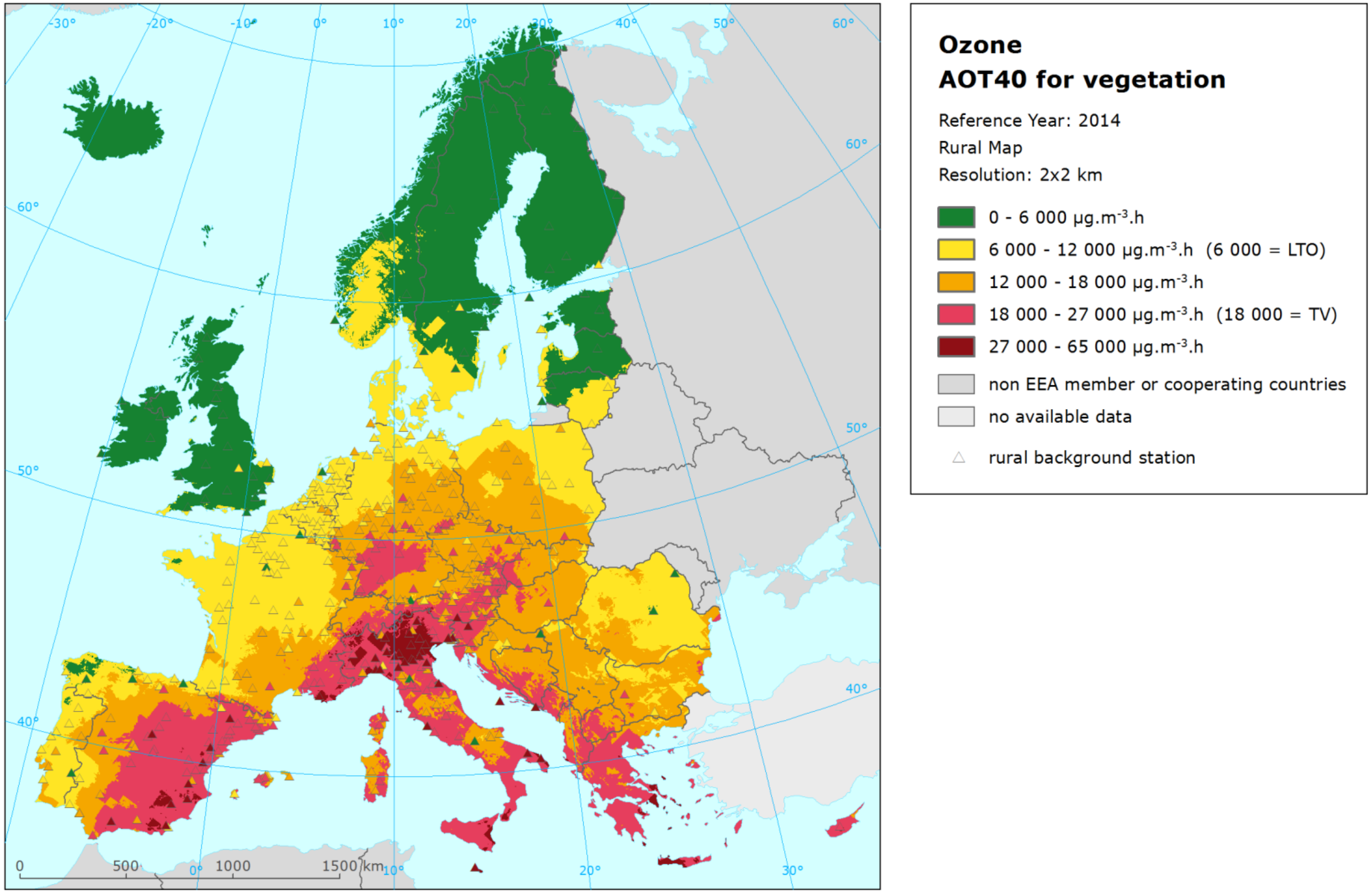

Map A5.7 Concentration map of ozone indicator AOT40 for forests including station points, rural air quality, 2014

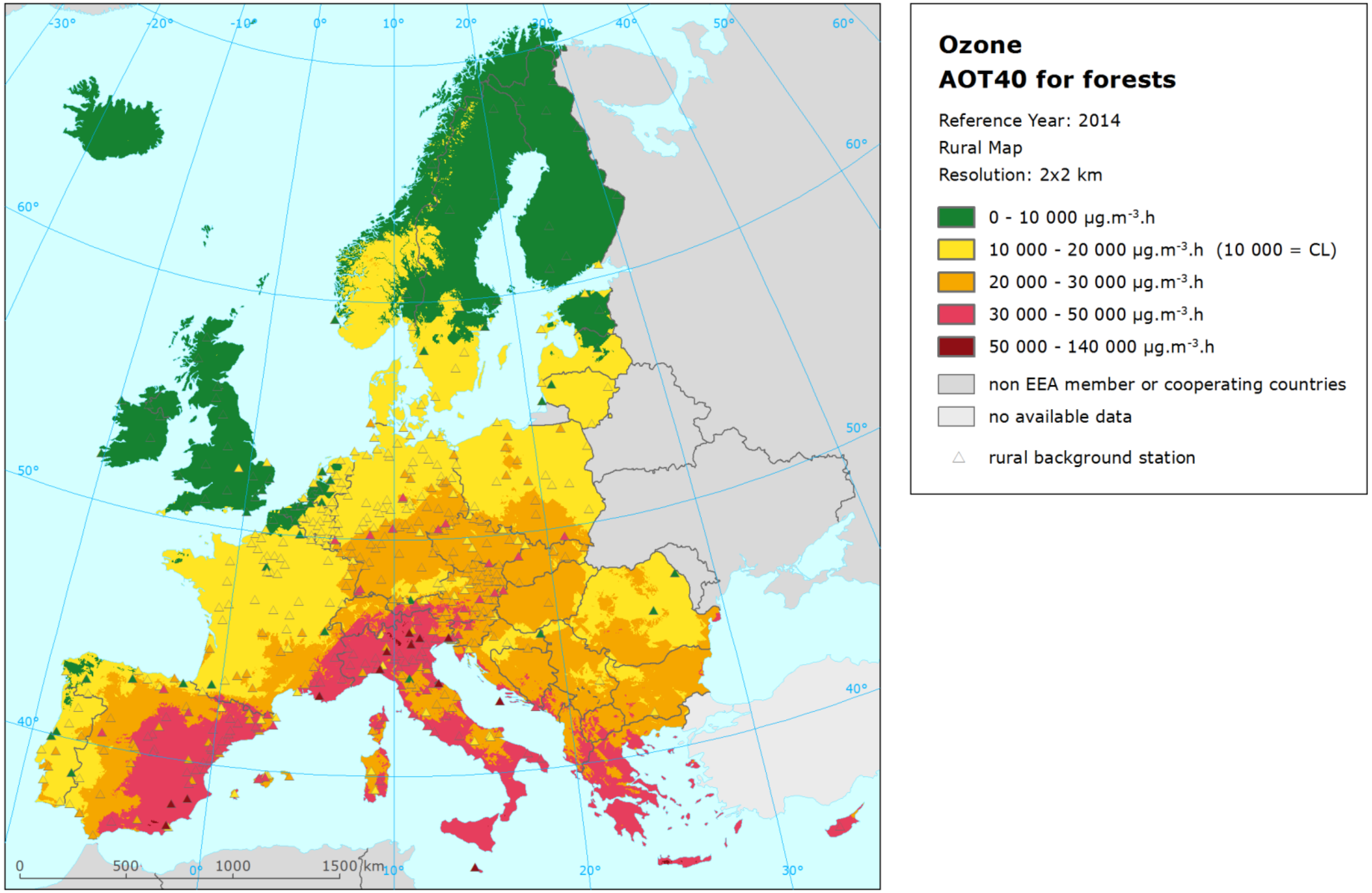

Map A5.8 Concentration map of NO_2 annual average including station points, 2014

Nitrogen Dioxide (NO_2)
Annual Average

Reference Year: 2014
Combined Rural and Urban Background Map
Resolution: 1x1 km

- ≤ 10 $\mu g.m^{-3}$
- 10 - 20 $\mu g.m^{-3}$
- 20 - 30 $\mu g.m^{-3}$
- 30 - 40 $\mu g.m^{-3}$
- 40 - 45 $\mu g.m^{-3}$ (40 = LV)
- > 45 $\mu g.m^{-3}$
- non EEA member or cooperating countries
- no available data
- △ rural background station
- □ urban/suburban background station

Map A5.9 Concentration map of NO_x annual average including station points, rural air quality, 2014